

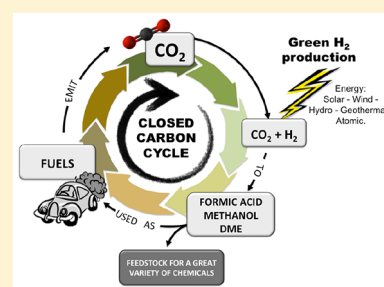
## Challenges in the Greener Production of Formates/Formic Acid, Methanol, and DME by Heterogeneously Catalyzed CO<sub>2</sub> Hydrogenation Processes

Andrea Álvarez,<sup>†</sup> Atul Bansode,<sup>†</sup> Atsushi Urakawa,<sup>\*,†</sup> Anastasiya V. Bavykina,<sup>‡</sup> Tim A. Wezendonk,<sup>‡</sup> Michiel Makkee,<sup>‡</sup> Jorge Gascon,<sup>\*,‡</sup> and Freek Kapteijn<sup>\*,‡</sup>

<sup>†</sup>Institute of Chemical Research of Catalonia (ICIQ), The Barcelona Institute of Science and Technology, Avinguda dels Països Catalans 16, 43007 Tarragona, Spain

<sup>‡</sup>Catalysis Engineering, Chemical Engineering Department, Delft University of Technology, Van der Maasweg 9, 2629 HZ Delft, The Netherlands

**ABSTRACT:** The recent advances in the development of heterogeneous catalysts and processes for the direct hydrogenation of CO<sub>2</sub> to formate/formic acid, methanol, and dimethyl ether are thoroughly reviewed, with special emphasis on thermodynamics and catalyst design considerations. After introducing the main motivation for the development of such processes, we first summarize the most important aspects of CO<sub>2</sub> capture and green routes to produce H<sub>2</sub>. Once the scene in terms of feedstocks is introduced, we carefully summarize the state of the art in the development of heterogeneous catalysts for these important hydrogenation reactions. Finally, in an attempt to give an order of magnitude regarding CO<sub>2</sub> valorization, we critically assess economical aspects of the production of methanol and DME and outline future research and development directions.



### CONTENTS

|  |      |
|--|------|
| 1. Introduction  | 9804 |
| 2. Carbon Dioxide Capture  | 9805 |
| 3. Green Routes To Produce H <sub>2</sub>  | 9806 |
| 4. Direct Hydrogenation of CO <sub>2</sub> to Formate/Formic Acid                      | 9807 |
| 4.1. Thermodynamic Considerations  | 9807 |
| 4.2. Catalytic Systems   | 9807 |
| 4.2.1. Supported/Unsupported Metal Catalysts   | 9808 |
| 4.2.2. Heterogenized Molecular Catalysts   | 9810 |
| 4.3. Reaction Mechanism  | 9814 |
| 5. Direct Hydrogenation of CO <sub>2</sub> to Methanol and DME                         | 9815 |
| 5.1. Thermodynamic Considerations  | 9816 |
| 5.2. Catalytic Systems   | 9818 |
| 5.2.1. Catalysts for the Direct Hydrogenation of CO <sub>2</sub> to CH <sub>3</sub> OH | 9818 |
| 5.2.2. Catalysts for the Direct Hydrogenation of CO <sub>2</sub> to DME                | 9822 |
| 5.3. Reaction Mechanism  | 9825 |
| 5.3.1. Reaction Mechanism of CO <sub>2</sub> Hydrogenation to Methanol                 | 9825 |
| 5.3.2. Reaction Mechanism of CO <sub>2</sub> Hydrogenation to DME                      | 9826 |
| 5.4. Process and Economic Aspects  | 9826 |
| 6. Summary and Future Perspectives   | 9828 |
| Author Information   | 9830 |
| Corresponding Authors  | 9830 |
| ORCID  | 9830 |

|                 |      |
|-----------------|------|
| Notes           | 9830 |
| Biographies     | 9831 |
| Acknowledgments | 9831 |
| References      | 9831 |

### 1. INTRODUCTION

Nowadays few people can ignore the strong scientific evidence that demonstrates a clear correlation between emissions of greenhouse gases and global warming. Among these gases, CO<sub>2</sub> is by far the most emitted and, therefore, the main responsible. At the same time, it would be difficult to deny that CO<sub>2</sub> emitting technologies are the engine of our society and that, on a short to medium term, the only path forward to mitigate the consequences of our “way of life” on the environment involves improvements in current technologies and their integration with capture of CO<sub>2</sub> along with the development of non-CO<sub>2</sub> emitting technologies for energy generation and production of chemicals.

The great societal relevance of this issue is highlighted by the large number of international actions from governments and industries established over the past decades. These include the Intergovernmental Panel on Climate Change (IPCC), the United Nations Framework Commission on Climate Change, the Global Climate Change Initiative, the European Strategic Energy Technology Plan (SET-Plan), and the European

**Special Issue:** Carbon Capture and Separation

**Received:** December 7, 2016

**Published:** June 28, 2017

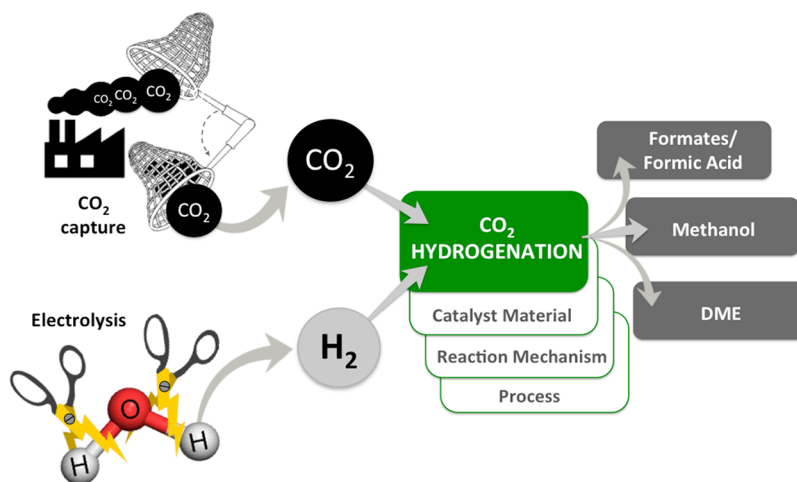


**Figure 1.** Scope and aspects covered in this review.

Technology Platform for Zero Emission Fossil Fuel Power Plants (ZEP).<sup>1–4</sup>

The use of fossil fuels has, however, in addition to the issues presented above, other less evident consequences, the most important one being the fact that, through combustion of hydrocarbons, we are depleting carbon (the element) sources which are equally instrumental to our society. Indeed, the petrochemical industry (the one that transforms oil into goods other than transportation fuels) is another important pillar of our society, and it may, in the long term, run out of its most important feedstock.

In view of these outstanding challenges, it is not surprising that the valorization of CO<sub>2</sub> is gaining interest in the scientific and industrial communities. Indeed, although CO<sub>2</sub> storage after capture has long been seen as a good alternative to tackle global warming, issues related to its safe storage and a paradigm shift in which CO<sub>2</sub> is not seen anymore as a waste but as an alternative carbon feedstock have prompted intense research activities into methods for the transformation of this stable molecule into useful chemicals and energy carriers. The recent advancements in the development of heterogeneous catalysts for this challenging task are summarized in this review. More specifically, we focus on catalytic technologies that deliver with high selectivity a single hydrogenation product, namely, formate/formic acid, methanol, and dimethyl ether. The choice for such processes is based not only on the number of research articles and patents published on these topics but especially on the fact that these are the most likely technologies to be first implemented, since the absence of complex, energy consuming separation units in such processes may facilitate their operation. Furthermore, when considering the envisaged products and the amounts of CO<sub>2</sub> emitted per year, potential technologies for the valorization of CO<sub>2</sub> have to deliver either important chemical intermediates or highly consumed final products, such as energy carriers. For these reasons, in the current review, we first summarize the main technologies for CO<sub>2</sub> capture from point sources and green ways of generating H<sub>2</sub>, with special emphasis on feedstock prices, which together with the catalytic process followed will eventually determine the final price of the hydrogenation products. Subsequently, we analyze in detail recent and old developments in heterogeneous catalysts for the direct hydrogenation of CO<sub>2</sub> to either formates, methanol, or dimethyl ether. We start these analyses from thermodynamic considerations and move to the different types of heterogeneous catalysts proposed in the open and patent

literature. The main components of this review on CO<sub>2</sub> hydrogenation process are schematically summarized in Figure 1. This article is finally wrapped up with our personal opinion about future directions in the development of new generations of catalysts and processes for the efficient hydrogenation of CO<sub>2</sub> to valuable chemicals and energy carriers.

## 2. CARBON DIOXIDE CAPTURE

Although this step is not the main topic of this review, the capture of CO<sub>2</sub> and, more specifically, the price and efficiency of capture methods and the different sources of CO<sub>2</sub> will be the key in valorizing this alternative carbon feedstock. The international Energy Agency reported in 2012 that over 40% of the global CO<sub>2</sub> emissions are related to energy and heat generation. This is due not only to the number of electricity generating plants around the world but especially to the fact that this sector relies heavily on coal, the most carbon containing fossil fuel. Manufacturing and industrial processes (such as paper, food, chemicals, cement, and steel industries) account for additional 20% emissions, while transportation (both of goods and of people) accounts for another 20% of the total emissions. These numbers indicate that capture technologies, if applied at large point sources such as energy generation and industrial sectors, could “easily” reduce current CO<sub>2</sub> emissions by 60%, while at the same time providing huge amounts of carbon dioxide as feedstock for further production processes. When focusing on combustion processes, three lines of capturing technologies exist: postcombustion, precombustion, and oxyfuel combustion.

Postcombustion CO<sub>2</sub> capture involves a treatment of the flue gases produced after the fuel is burned. In this case, the hot combustion gases exiting the boiler consist mainly of nitrogen (from air) along with lower concentrations of water vapor and CO<sub>2</sub> (the concentration of the latter depends on the combustible used). Additional air pollutants, such as sulfur dioxide, nitrogen oxides, particulate matter, and other trace species such as mercury, are removed to meet the emission standards.<sup>5</sup> The main challenge in *postcombustion* CO<sub>2</sub> capture is the low partial pressure of CO<sub>2</sub> and the huge amount of flue gas to process. The CO<sub>2</sub> content (volume basis) can be as low as 4% in a gas turbine plant, around 15% for coal power plants, and more concentrated (~20–30%) for cement and steel production plants. With current commercial technology, the most effective method of CO<sub>2</sub> capture from flue gases is chemical absorption in an aqueous solution of an amine-based organic, such as mono- or

diethanolamine (MEA, DEA). Typically 85 to 90% of the CO<sub>2</sub> is captured with these technologies at a price highly defined by the regeneration energetics of the amine solution.<sup>5</sup> In addition to clear environmental concerns related to amine degradation and in spite of great improvements of this technology through process optimization, bringing the price of CO<sub>2</sub> capture with this technology below 60 \$/ton CO<sub>2</sub> seems rather unrealistic. Alternative technologies, not yet commercially implemented, involve adsorption, CO<sub>2</sub> conversion, chemical looping, and membrane separation. Especially, the latter technology has attracted a great deal of interest and seems to be the most promising alternative, as recently reviewed by several groups. For instance, Merkel et al.,<sup>6</sup> using the MTR's membrane Polaris as the base case (permeance 1000 GPU, CO<sub>2</sub>/N<sub>2</sub> selectivity  $\alpha = 50$ ), found an optimal process configuration (two-step counter-flow/sweep membrane process), with which a 90% CO<sub>2</sub> recovery can be achieved at a price of 18 €/ton CO<sub>2</sub> (including compression), highlighting the large potential of membrane technologies for the capture of CO<sub>2</sub>.

Removal of carbon from fuel prior to combustion is usually done via partial oxidation with pure oxygen or gasification. The result is a gaseous fuel consisting mainly of carbon monoxide and hydrogen, which can be burned to generate electricity in a combined cycle power plant. This approach is known as the integrated gasification combined cycle (IGCC) power generation. After particulate impurities are removed from the syngas, a two-stage water-gas shift reactor converts the carbon monoxide to CO<sub>2</sub>. The result is a mixture of CO<sub>2</sub> and hydrogen (and water). Given the higher partial pressure of CO<sub>2</sub> in this stream, milder solvents, such as the widely used commercial Selexol (which employs a glycol-based solvent) and Rectisol (using refrigerated methanol), can be used for the capture of CO<sub>2</sub>, leaving a stream of nearly pure hydrogen that is burned in a combined cycle power plant to generate electricity.<sup>7</sup> Nonetheless, there is still a significant energy penalty associated with CO<sub>2</sub> capture due to the need for shift reactors and other separation processes. Overall, costs associated with current commercial precombustion capture technologies are around 60 \$/ton CO<sub>2</sub>. In the case of precombustion capture, again membranes could be instrumental in drastically reducing capture costs. Recently, Ku et al.<sup>8</sup> published a detailed study on membrane performance requirements for precombustion CO<sub>2</sub> capture applying a single step high-temperature membrane process. High performance membranes should be able to deliver the desired 90% carbon capture at prices below 20 \$/ton CO<sub>2</sub>.<sup>9</sup>

The last option for CO<sub>2</sub> capture, the oxyfuel process, makes use of pure oxygen for the combustion, resulting in a flue gas containing mainly water vapor and carbon dioxide. Condensation of the water results in a nearly pure carbon dioxide stream. The major energy penalty here is the production of pure oxygen by air separation and on the manufacture of the materials needed to withstand the much higher combustion temperatures.

A recent analysis has shown that the thermodynamic minimum energy demand for capturing 90% of the CO<sub>2</sub> from the flue gas of a typical coal-fired power plant is approximately 3.5% (assuming a flue gas containing 12–15% CO<sub>2</sub> at 40 °C).<sup>10</sup> Although the best commercially available technologies still require an additional 16% energy input (note that this is the case for new natural gas based combined cycles and precombustion capture based on absorption) and the most promising membrane technologies may reduce these to ca. 6%, reaching CO<sub>2</sub> costs below 20 \$/ton CO<sub>2</sub> over the next few decades will be very unlikely. Whether these prices will be sufficiently low for CO<sub>2</sub> to

become a feasible feedstock will most likely depend on the implementation of governmental and industrial driven policies such as the proposed Levelised Cost of Energy (LCOE) proposed in Europe<sup>2,4</sup> that includes capture costs into the final electricity bill. If these regulations and other are finally applied, then the opportunities for the implementation of point source capture technologies and subsequent valorization of CO<sub>2</sub> will be immense.

### 3. GREEN ROUTES TO PRODUCE H<sub>2</sub>

Traditional methods to produce H<sub>2</sub> rely on the use of fossil fuels and, therefore, produce large amounts of CO<sub>2</sub>, obviously undesired for the application at hand. Current industrial production from conventional fossil sources like natural gas reforming or coal gasification is low cost (<1 \$/kg H<sub>2</sub>).<sup>11,12</sup> Steam methane reforming (SMR) is the least expensive and most common method to produce hydrogen, as it requires an external heat source but does not demand pure oxygen. Coal gasification (CG) is a more complex, two-stage process; the feedstock costs are lower than in SMR while the capital costs of a CG plant are higher. Coal is first converted through steam/oxygen gasification/oxidation at high temperature and pressure toward CO<sub>2</sub>-rich syngas, of which the hydrogen content is subsequently enhanced by the water-gas shift (WGS) reaction. Therefore, the hydrogen production costs through CG are slightly higher than for SMR (0.92 \$/kg H<sub>2</sub> vs 0.75 \$/kg H<sub>2</sub>).<sup>13</sup> An alternative method in fossil fuel conversion is plasma arc decomposition (PAD) where the high-temperature pyrolysis of methane produces pure H<sub>2</sub> and solid carbon. In spite of economically attractive estimations, commercial operation was abandoned.<sup>14</sup> Further, the large energy demand for this process is often met by conventional energy supply as well and, thus, results in CO<sub>2</sub> emissions comparable to SMR.<sup>15</sup>

The alternative for hydrogen production up to the megawatt range is alkaline water electrolysis (WE).<sup>16</sup> The costs of electrolysis are higher than those of fossil fuel utilization due to Pt-catalyst used as electrode, to the required water purification before electrolysis, and to the price of electricity: commercially available electrolysis systems produce hydrogen around 2–3 \$/kg H<sub>2</sub> at a 0.05 \$/kWh electricity cost.<sup>17</sup> In this case, the electrical energy necessary for water splitting can easily be supplied by photovoltaic power (PV) plants to close the green cycle of water electrolysis. Other ways toward green water electrolysis are polymer electrolyte membranes (PEM), solid oxide electrolyzers (SOEC), and carbon-assisted water electrolysis (CAWE); however, these technologies are still in the demonstration or research phase.<sup>18,19</sup> For the PEM electrolysis, on the one hand the development of stack concepts is a necessary breakthrough for industrial application, and noble metal loading and long-term stability are still a matter of concern.<sup>20</sup> On the other hand, SOEC can produce hydrogen while achieving 100% Faradaic efficiency, and thus, this technology has a huge potential for industrial application when issues related to durability of the ceramics and steam/hydrogen electrode under these high temperatures are solved. Similar challenges hold for high-temperature electrolysis, where instead of water, steam is dissociated to H<sub>2</sub> and O<sub>2</sub>. Engineering chemically stable materials for use at high temperatures and reducing/oxidizing environments, such as the electrolyte, electrodes, and support materials, is key to efficient hydrogen generation.<sup>21</sup> Current state of the art does not allow a cost-effective operation of high-temperature electrolysis (>4.5 \$/kg H<sub>2</sub>), and although water splitting can also



be performed thermally, the high temperatures to be reached (>2500 K) result in a costly operation as well (>4 \$/kg H<sub>2</sub>).

In addition to the above-described processes, there are not many other megawatt-range technologies that can reach high levels of process efficiency. Yet, biomass conversion can reach energy efficiency levels (defined as useful output over consumed input) over 50%, comparable to fossil fuel conversion and water electrolysis.<sup>22</sup> The main routes for biomass utilization are (steam) gasification and thermochemical conversion, resulting in CO<sub>2</sub>-rich syngas mixtures, which further require hydrogen enrichment through WGS.<sup>23</sup> Still, biomass conversion is roughly twice as expensive as SMR or CG at a price between 1 and 2 \$/kg H<sub>2</sub>.<sup>24</sup> Furthermore, the major downside of biomass utilization is the high acidification potential due to coemission of SO<sub>2</sub> and the potential amounts of inorganics and/or ash. Biomass conversion routes have in common high SO<sub>2</sub> emissions of >10 g/kg H<sub>2</sub>, comparable to SMR.<sup>18</sup> Although it is not common in the literature to assign costs to acidification potential, the sulfur-cleanup associated costs might decrease the economic potential of biomass conversion even further.

The technologies with the lowest efficiency for green hydrogen production are photocatalytic water splitting and associated photovoltaic systems such as PV electrolysis. Nonetheless, photocatalytic hydrogen production from water splitting in the visible-light region has high potential for application as a green route to hydrogen.<sup>25</sup> On one hand the inherent strengths of the above technologies are the near-absent global warming and acidification potential due to negligible CO<sub>2</sub> and SO<sub>2</sub> emissions. The energy efficiencies of the systems are, on the other hand, quite low with a maximum of 11%,<sup>26,27</sup> while the aim is to reach 30%.<sup>28</sup> Keys in catalyst development are maximizing visible-light utilization and improving efficiency of electron–hole separation while avoiding recombination and the stability of the investigated materials.<sup>29–31</sup> Additionally, the coupled system of hydrogen evolution and oxygen evolution in photocatalysis requires efficient electron transfer between the two catalyst particles. Current development in these highly complex photocatalysts allowed pure water splitting with a solar-to-hydrogen energy conversion of 1.1% and apparent quantum yield of over 30% at 419 nm, the highest values obtained to date.<sup>32</sup> Since the technology is still immature, hydrogen production costs are among the highest reported, and rise up to 10 \$/kg H<sub>2</sub>.<sup>13,18</sup>

In summary, from the existing H<sub>2</sub> producing technologies and considering environmental aspects (it would make very little sense to use nongreen hydrogen to hydrogenate CO<sub>2</sub>), alkaline water electrolysis should be at this moment the technology of choice for the prospective valorization of carbon dioxide. Additionally, we would like to stress that local or *in situ* generation on demand would be preferred over off-site H<sub>2</sub> generation and transportation.

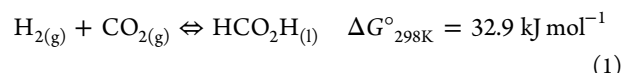
#### 4. DIRECT HYDROGENATION OF CO<sub>2</sub> TO FORMATE/FORMIC ACID

Formic acid, apart from being a valuable chemical commonly used as preservative and antibacterial agent, is an established hydrogen storage component via its decomposition to CO<sub>2</sub> and H<sub>2</sub> with a possible reversible transformation back to regenerate formic acid, thus serving as a platform for chemical energy storage.<sup>33</sup> It contains 53 g L<sup>−1</sup> hydrogen at room temperature and atmospheric pressure. By weight, pure formic acid stores 4.3 wt % hydrogen. Being liquid at ambient conditions, its transportation and storage is more straightforward than that of molecular

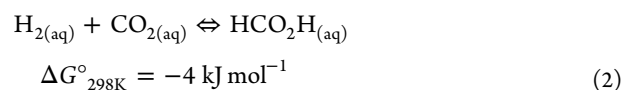
hydrogen. Despite the relatively low gravimetric hydrogen content, all the hydrogen can be recovered from formic acid. The current industrial methods of formic acid production include hydrolysis of methyl formate or formamide and oxidation of biomass.<sup>34</sup> Compared to these traditional synthesis methods, the direct hydrogenation of carbon dioxide into formic acid serves two important, distinguishing purposes, namely, CO<sub>2</sub> utilization and hydrogen storage in a liquid form as mentioned above.

##### 4.1. Thermodynamic Considerations

The conversion of carbon dioxide and hydrogen into formic acid commonly involves a phase change from gaseous reagents into a liquid product. Therefore, the reaction is obviously entropically disfavored, when the gas phase reactants are considered (eq 1):<sup>35</sup>



On the other hand, the presence of solvent alters the thermodynamics of the reaction and the reaction becomes slightly exergonic when operated in the aqueous phase (eq 2):<sup>35</sup>



To make the transformation of carbon dioxide to formic acid (or formates) feasible in practice, the thermodynamic equilibrium has to be disturbed by secondary reaction or molecular interaction. The common strategies are by esterification, e.g., reacting formic acid/formates with methanol to yield methyl formate, reacting them with primary or secondary amines to yield formamides, or simply neutralization with a weak base such as tertiary amines or alkali/alkaline earth bicarbonates.<sup>36,37</sup>

##### 4.2. Catalytic Systems

In 1976 Inoue et al. published for the first time the catalytic synthesis of formic acid from carbon dioxide using a homogeneous catalyst, a Ru complex with phosphine ligands.<sup>38</sup> Since then, much effort has been devoted to this field of catalysis. An enormous number of attempts employing transition metal complexes, mostly Ir- and Ru-based ones, were made, and the outcome is truly fascinating. The recent progress in homogeneous catalytic systems for the synthesis of formic acid and formates has been excellently reviewed by several research teams.<sup>37,39–43</sup> To the best of our knowledge, a record TOF of 1,100,000 h<sup>−1</sup> was achieved by Filonenko et al. using a Ru PNP pincer complex.<sup>44</sup> In spite of the impressive turnover frequencies achieved by several homogeneous catalysts, when this production rate is expressed as the amount of CO<sub>2</sub> hydrogenated per unit time and volume of reactor, the obtained numbers are still far from what would be desired from an industrial standpoint. This is a consequence of the low catalyst concentrations often used in homogeneously catalyzed processes. On the other hand, heterogeneous catalysts, with obvious practical advantages for continuous operation and product separation, are comparatively much less investigated for this reaction, but recently the number of examples is increasing remarkably.<sup>45</sup>

In this section, we summarize the state of the art of the heterogeneous catalysts reported for the synthesis of formic acid/formates. The catalyst types are classified as follows: (1) unsupported and supported bulk/nanometal catalysts and (2) heterogenized molecular catalysts. The most popular catalyst types reported to date and covered in this review are summarized in Figure 2.

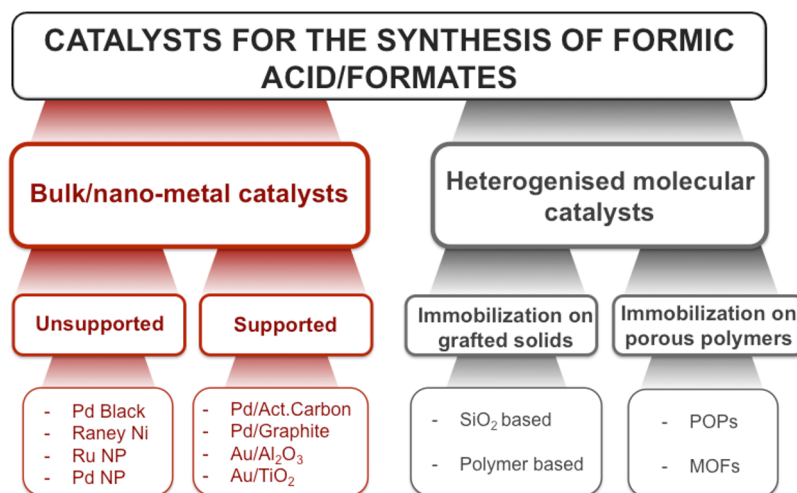


Figure 2. Heterogeneous catalytic systems reported for the CO<sub>2</sub> hydrogenation to formic acid/formates.

**4.2.1. Supported/Unsupported Metal Catalysts.** The initial studies on the reaction using heterogeneous catalysts were reported employing pure metal as an active catalyst element. The first synthesis of formates by hydrogenation reaction dates back to 1914 by Bredig and Carter using a Pd black catalyst under relatively mild conditions (70–95 °C, 30–60 bar of H<sub>2</sub>, 0–30 bar of CO<sub>2</sub>).<sup>46</sup> The synthesis employed alkali/alkaline earth (bi)carbonates as the CO<sub>2</sub> source in the presence of H<sub>2</sub> (in some cases gaseous CO<sub>2</sub> was also added). In 1935 Farlow and Adkins reported the synthesis of formamides over Raney Ni through CO<sub>2</sub> hydrogenation at high pressure (400 bar) in the presence of primary and secondary amines in alcohol as solvent.<sup>47</sup> As evident from the two early examples, the common strategies used nowadays in homogeneous catalysis to shift the reaction equilibrium with alkali/alkaline earth metals and amines (*vide supra*) were routinely employed for heterogeneous catalytic systems. As a pure metal catalyst, recently prominent catalytic activity of Ru nanoparticles has been reported. Srivastava et al.<sup>48</sup> evaluated the activity of Ru nanoparticles generated *in situ* in an ionic liquid ([DAMI][NTf<sub>2</sub>]) (DAMI, 1,3-di(*N,N*-dimethylaminoethyl)-2-methylimidazolium; NTf<sub>2</sub>, bis-(trifluoromethylsulfonyl) imide) which was used as solvent together with water, and they reported a TOF of 376 h<sup>-1</sup> at 100 °C (Table 1, entry 41). In another report, Umegaki et al. performed the reaction with supercritical CO<sub>2</sub> in the presence of trimethylamine (NEt<sub>3</sub>) and water as promoter using Ru nanoparticles prepared in a methanol solution under solvothermal conditions, achieving a high TON of 6351 after 3 h at 80 °C (Table 1, entry 42).<sup>49</sup> It is interesting to note that the presence of water somehow affected positively the catalytic performance using Ru nanoparticles.

In heterogeneous catalysis, support materials are often employed to increase the number of active sites (often metal surfaces) by dispersing active metals in space on the nanometer scale. Besides, they are known to play key roles in catalytic reactions by altering the electronic structure of active metals, creating unique active sites at the perimeter of active metal and support, and/or enhancing the interaction of reaction substrate with the catalyst thus enhancing the reaction rate. Although the number is limited, there are representative examples convincingly describing support effects in the formates/formic acid synthesis using metal catalysts supported on different solid materials.

Stalder et al. studied the effects of active metal and support in the conversion of aqueous sodium bicarbonate to sodium formate. Among Al<sub>2</sub>O<sub>3</sub>-supported Ru, Rh, Pd, and Pt catalysts, Pd/Al<sub>2</sub>O<sub>3</sub> showed the best catalytic performance. The catalyst performed ca. 75 times better in terms of initial TOF than Pd black, although a carbon-supported Pd catalyst was found to be even superior (ca. 6 times more active than Pd/Al<sub>2</sub>O<sub>3</sub>) with a TON of 115 after 24 h (Table 1, entries 3, 4, 22).<sup>50</sup> Similarly, Su et al. investigated the activity of Pd catalysts supported on different materials such as activated carbon, Al<sub>2</sub>O<sub>3</sub>, CaCO<sub>3</sub>, and BaSO<sub>4</sub>, and the activated carbon supported Pd showed superior catalytic performance.<sup>51</sup> Furthermore, positive effects of heteroatom modification to the carbon support have been reported by other researchers. Bi et al. studied supported Pd catalysts for reversible (de)hydrogenation between potassium bicarbonate and formate as a way to (dis)charge hydrogen to the catalyst solution. The use of Pd particles supported on reduced graphite oxide (Pd/r-GO) yielded a TON of 7088 after 32 h at 1 wt % Pd loading for the hydrogenation reaction.<sup>52</sup> They screened several Pd loadings (1, 2, and 5 wt %), and the lowest Pd loading gave the best results, which were explained by larger lattice strain (Table 1, entries 25–27), although the origin of the higher activity is not clear.<sup>52</sup> Lee et al. employed a nitrogen-containing mesoporous graphitic carbon nitride as the support of Pd nanoparticle, and the catalyst exhibited higher activity than a commercial Pd/C. They concluded that the basic sites of the support could stabilize the nanosized Pd (ca. 1.7 nm) as well as facilitate the initial interaction with CO<sub>2</sub> with the support, thus facilitating the synthesis of formic acid.<sup>53</sup>

It is also interesting to note that the hydrogenation of bicarbonates to formates is reported to be more facile than that of carbonates, which was consistently observed for different cations (sodium, potassium, or ammonium) in the salts.<sup>51</sup> The best hydrogenation activity was observed when ammonium bicarbonate was hydrogenated over activated carbon supported Pd, yielding a TON of 782. It was explained by a higher equilibrium concentration of HCO<sub>3</sub><sup>-</sup> over CO<sub>3</sub><sup>2-</sup> than in the case of potassium or sodium salts. The highest yield of 90.4% was obtained after 2 h using ammonium bicarbonate as the source of CO<sub>2</sub> (Table 1, entries 14 vs 5–13, 15).<sup>51</sup> As suggested by Su et al., all similar reactions in aqueous solutions or mixtures of amines/carbonates under CO<sub>2</sub> pressure may, in fact, utilize HCO<sub>3</sub><sup>-</sup> as the actual substrate in the catalytic cycle.<sup>51</sup> This could

Table 1. Summary of the Different Metal Nanoparticle Based Catalysts Reported for the Hydrogenation of CO<sub>2</sub> to Formic Acid/Formates

| entry               | catalyst metal        | support                           | P <sub>H<sub>2</sub></sub> /atm | P <sub>CO<sub>2</sub></sub> /atm | base/additive                                   | T/°C | solvent                       | C <sub>FA</sub> /M | t/h | TON  | TOF/h <sup>-1</sup> |
|---------------------|-----------------------|-----------------------------------|---------------------------------|----------------------------------|---|------|-------------------------------|--------------------|-----|------|---------------------|
| 1 <sup>46</sup>     | Pd bulk               | no                                | 60                              | 0                                | KHCO <sub>3</sub>                               | 70   | H <sub>2</sub> O              | 0.37               | 23  | 5    | 0.22                |
| 2 <sup>46</sup>     | Pd bulk               | no                                | 50                              | 20                               | CaCO <sub>3</sub>                               | 70   | H <sub>2</sub> O              | 0.02               | 4.5 | 0.28 | 0.06                |
| 3 <sup>50</sup>     | Pd bulk               | no                                | 1                               | 0                                | NaHCO <sub>3</sub>                              | 25   | H <sub>2</sub> O              | 0.2                | 53  | 2.1  | 0.02 <sup>a</sup>   |
| 4 <sup>50</sup>     | Pd NP                 | C                                 | 1.7                             | 0                                | NaHCO <sub>3</sub>                              | 25   | H <sub>2</sub> O              | 0.53               | 46  | 115  | 25 <sup>a</sup>     |
| 5 <sup>52</sup>     | Pd NP                 | C                                 | 29.6                            | 0                                | KHCO <sub>3</sub>                               | 100  | H <sub>2</sub> O              | 3.79               | 10  | 1973 | 197                 |
| 5 <sup>51</sup>     | Pd NP                 | AC                                | 27                              | 0                                | NaHCO <sub>3</sub>                              | 20   | H <sub>2</sub> O              | 0.29               | 1   | 527  | 527                 |
| 6 <sup>51</sup>     | Pd NP                 | AC                                | 27                              | 0                                | KHCO <sub>3</sub>                               | 20   | H <sub>2</sub> O              | 0.31               | 1   | 567  | 567                 |
| 7 <sup>51</sup>     | Pd NP                 | AC                                | 27                              | 0                                | NH <sub>4</sub> HCO <sub>3</sub>                | 20   | H <sub>2</sub> O              | 0.43               | 1   | 782  | 782                 |
| 8 <sup>51</sup>     | Pd NP                 | AC                                | 27                              | 0                                | NH <sub>4</sub> HCO <sub>3</sub>                | 20   | H <sub>2</sub> O              | 0.86               | 6   | 1571 | 262                 |
| 9 <sup>51</sup>     | Pd NP                 | AC                                | 27                              | 0                                | NH <sub>4</sub> HCO <sub>3</sub>                | 20   | H <sub>2</sub> O              | 0.97               | 6   | 1769 | 118                 |
| 10 <sup>51</sup>    | Pd NP                 | AC                                | 6.9                             | 0                                | NH <sub>4</sub> HCO <sub>3</sub>                | 20   | H <sub>2</sub> O              | 0.17               | 1   | 312  | 312                 |
| 11 <sup>51</sup>    | Pd NP                 | AC                                | 13.6                            | 0                                | NH <sub>4</sub> HCO <sub>3</sub>                | 20   | H <sub>2</sub> O              | 0.32               | 1   | 579  | 579                 |
| 12 <sup>51</sup>    | Pd NP                 | AC                                | 41.4                            | 0                                | NH <sub>4</sub> HCO <sub>3</sub>                | 20   | H <sub>2</sub> O              | 0.54               | 1   | 982  | 982                 |
| 13 <sup>51</sup>    | Pd NP                 | AC                                | 54.5                            | 0                                | NH <sub>4</sub> HCO <sub>3</sub>                | 20   | H <sub>2</sub> O              | 0.60               | 1   | 1103 | 1103                |
| 14 <sup>51</sup>    | Pd NP                 | AC                                | 54.5                            | 0                                | NH <sub>4</sub> HCO <sub>3</sub>                | 20   | H <sub>2</sub> O              | 0.91               | 2   | 1672 | 836                 |
| 15 <sup>51</sup>    | Pd NP                 | AC                                | 27                              | 0                                | (NH <sub>4</sub> ) <sub>2</sub> CO <sub>3</sub> | 20   | H <sub>2</sub> O              | 0.15               | 1   | 278  | 278                 |
| 16 <sup>55</sup>    | Pd NP                 | AC                                | 27                              | 0                                | NH <sub>2</sub> CO <sub>2</sub> NH <sub>4</sub> | 20   | EtOH                          | 0.2                | 1   | 373  | 373                 |
| 17 <sup>55</sup>    | Pd NP                 | AC                                | 27                              | 0                                | NH <sub>2</sub> CO <sub>2</sub> NH <sub>4</sub> | 20   | EtOH 70%/H <sub>2</sub> O 30% | 0.22               | 1   | 405  | 405                 |
| 18 <sup>55</sup>    | Pd NP                 | AC                                | 27                              | 0                                | NH <sub>2</sub> CO <sub>2</sub> NH <sub>4</sub> | 20   | EtOH 70%/H <sub>2</sub> O 30% | 0.46               | 8   | 845  | 106                 |
| 19 <sup>55</sup>    | Pd NP                 | AC                                | 27                              | 0                                | NH <sub>2</sub> CO <sub>2</sub> NH <sub>4</sub> | 20   | EtOH 30%/H <sub>2</sub> O 70% | 0.09               | 1   | 162  | 162                 |
| 20 <sup>50</sup>    | Pd NP                 | BaSO <sub>4</sub>                 | 1                               | 0                                | NaHCO <sub>3</sub>                              | 25   | H <sub>2</sub> O              | 0.09               | 50  | 19   | 2.1 <sup>a</sup>    |
| 21 <sup>51</sup>    | Pd NP                 | BaSO <sub>4</sub>                 | 27                              | 0                                | NH <sub>4</sub> HCO <sub>3</sub>                | 20   | H <sub>2</sub> O              | 0.03               | 1   | 212  | 212                 |
| 22 <sup>50</sup>    | Pd NP                 | γ-Al <sub>2</sub> O <sub>3</sub>  | 1                               | 0                                | NaHCO <sub>3</sub>                              | 25   | H <sub>2</sub> O              | 0.23               | 53  | 50   | 1.5 <sup>a</sup>    |
| 23 <sup>51</sup>    | Pd NP                 | Al <sub>2</sub> O <sub>3</sub>    | 27                              | 0                                | NH <sub>4</sub> HCO <sub>3</sub>                | 20   | H <sub>2</sub> O              | 0.09               | 1   | 278  | 278                 |
| 24 <sup>51</sup>    | Pd NP                 | CaCO <sub>3</sub>                 | 27                              | 0                                | NH <sub>4</sub> HCO <sub>3</sub>                | 20   | H <sub>2</sub> O              | 0.005              | 1   | 20   | 20                  |
| 25 <sup>52</sup>    | Pd NP (1 wt %)        | r-GO                              | 39.5                            | 0                                | KHCO <sub>3</sub>                               | 100  | H <sub>2</sub> O              | 4.54               | 32  | 7088 | 221                 |
| 26 <sup>52</sup>    | Pd NP (2 wt %)        | r-GO                              | 39.5                            | 0                                | KHCO <sub>3</sub>                               | 100  | H <sub>2</sub> O              | 4.06               | 10  | 2117 | 211.7               |
| 27 <sup>52</sup>    | Pd NP (5 wt %)        | r-GO                              | 39.5                            | 0                                | KHCO <sub>3</sub>                               | 100  | H <sub>2</sub> O              | 3.18               | 10  | 1658 | 166                 |
| 28 <sup>53</sup>    | Pd NP                 | mpg-C <sub>3</sub> N <sub>4</sub> | 26.6                            | 12.8                             | NEt <sub>3</sub>                                | 150  | D <sub>2</sub> O              | 0.37               | 24  | 106  | 4.4                 |
| 29 <sup>60</sup>    | PdNi                  | CNT-GR                            | 24.7                            | 24.7                             | no  | 40   | H <sub>2</sub> O              | 0.02               | 15  | 6.4  | 0.0072              |
| 30 <sup>47</sup>    | Ni Raney <sup>c</sup> | no                                | 40/140                          | 60                               | 1-Ph-2-aminopropanol-1                          | 80   | EtOH                          |                    | 1   |      |                     |
| 31 <sup>61</sup>    | Ni/Fe powder          | no                                |                                 | ≈11 <sup>b</sup>                 | K <sub>2</sub> CO <sub>3</sub>                  | 300  | H <sub>2</sub> O              | 0.07               | 2   | 0.02 | 0.01                |
| 32 <sup>58</sup>    | Au NP                 | no                                | 20                              | 20                               | NEt <sub>3</sub>                                | 70   | EtOH                          | 0.001              | 20  | 0.6  | 0.03                |
| 33 <sup>56–57</sup> | Au (AUROLite)         | TiO <sub>2</sub>                  | 90                              | 90                               | NEt <sub>3</sub>                                | 40   | NEt <sub>3</sub>              |                    | 52  | 855  | 16.4                |
| 34 <sup>58</sup>    | Au NP                 | TiO <sub>2</sub>                  | 20                              | 20                               | NEt <sub>3</sub>                                | 70   | EtOH                          | 0.09               | 20  | 111  | 5.5                 |
| 35 <sup>58</sup>    | Au NP                 | Al <sub>2</sub> O <sub>3</sub>    | 20                              | 20                               | NEt <sub>3</sub>                                | 70   | EtOH                          | 0.2                | 20  | 215  | 10.8                |
| 36 <sup>58</sup>    | Au NP                 | ZnO                               | 20                              | 20                               | NEt <sub>3</sub>                                | 70   | EtOH                          | 0.002              | 20  | 2    | 0.1                 |
| 37 <sup>58</sup>    | Au NP                 | CeO <sub>2</sub>                  | 20                              | 20                               | NEt <sub>3</sub>                                | 70   | EtOH                          | 0.002              | 20  | 8    | 0.4                 |
| 38 <sup>58</sup>    | Au NP                 | MgAl-hydratalcite                 | 20                              | 20                               | NEt <sub>3</sub>                                | 70   | EtOH                          | 0.016              | 20  | 91   | 4.6                 |
| 39 <sup>58</sup>    | Au NP                 | MgCr-hydratalcite                 | 20                              | 20                               | NEt <sub>3</sub>                                | 70   | EtOH                          | 0.007              | 20  | 52   | 2.6                 |
| 40 <sup>58</sup>    | Au NP                 | CuCr <sub>2</sub> O <sub>4</sub>  | 20                              | 20                               | NEt <sub>3</sub>                                | 70   | EtOH                          | 0.002              | 20  | 6    | 0.3                 |
| 41 <sup>48</sup>    | Ru NP                 | no                                | 197                             | 197                              | no  | 100  | [DAMI][NTf <sub>2</sub> ]     |                    | 2.5 | 940  | 376                 |
| 42 <sup>49</sup>    | Ru NP                 | no                                | 49                              | 128                              | NEt <sub>3</sub>                                | 80   | water                         | 27.6               | 3   | 6351 | 2117                |
| 43 <sup>51</sup>    | Ru NP                 | AC                                | 27                              | 0                                | NH <sub>4</sub> HCO <sub>3</sub>                | 20   | H <sub>2</sub> O              | 0.002              | 3   | 1    | 3                   |
| 44 <sup>59</sup>    | Ru                    | AC                                | 49                              | 84                               | NEt <sub>3</sub>                                | 80   | EtOH                          | 0.05               | 1   | 10   | 10                  |
| 45 <sup>59</sup>    | Ru                    | Al <sub>2</sub> O <sub>3</sub>    | 49                              | 84                               | NEt <sub>3</sub>                                | 80   | EtOH                          | 0.455              | 1   | 91   | 91                  |
| 46 <sup>51</sup>    | Rh NP                 | AC                                | 27                              | 0                                | NH <sub>4</sub> HCO <sub>3</sub>                | 20   | H <sub>2</sub> O              | 0.002              | 3   | 1    | 3                   |

<sup>a</sup>Initial rates (reported by authors). <sup>b</sup>6.4 mmol of CO<sub>2</sub>, the pressure was estimated without taking into consideration CO<sub>2</sub> solubility. <sup>c</sup>No reaction volume data, yield 55%.

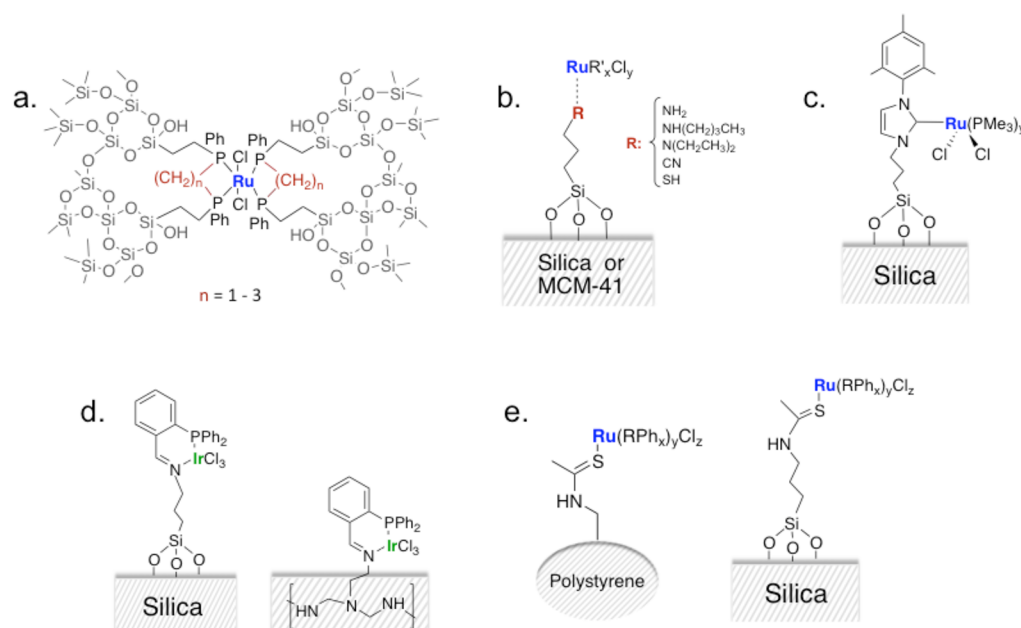


**Figure 3.** Immobilization strategies of molecular complexes on grafted solid support for CO<sub>2</sub> hydrogenation. These “precatalyst” structures are created based on (a) refs 76 ( $n = 1,3$ ), 75 ( $n = 2$ ), and 77 ( $n = 3$ ); (b) refs 78–80; (c) ref 81; (d) refs 82 and 83; and (e) refs 84, 80, and 85.

also explain the beneficial effect of a small amount of H<sub>2</sub>O on CO<sub>2</sub> hydrogenation, often observed in organic solvent systems.<sup>54</sup> Su et al. also showed that the higher reactivity of bicarbonates is conditional and solvent-dependent.<sup>55</sup> Among ammonium salts, carbonates and carbamates were more easily hydrogenated than bicarbonates in ethanol-rich solutions (Table 1, entries 16, 17, 19).

While Pd is the most popular active metal known for the reaction, contrasting results have been reported. With the assumption that an active catalyst promotes both the forward reaction (formic acid synthesis) and the reverse one (formic acid decomposition), Preti et al. investigated H<sub>2</sub> and CO<sub>2</sub> gas evolution arising from the decomposition of HCOOH/NEt<sub>3</sub> in the presence of different metal black catalysts of groups 8–11 (Raney Ni, Co, Cu, Ru, Rh, Pd, Ag, Ir, Pt, and Au).<sup>56</sup> Surprisingly, only Au black was active for the decomposition reaction. Though the catalyst showed a fair activity, the Au black deactivated quickly due to the aggregation of Au particles (thus resulting in less active surface area). For this reason, a dispersed Au catalyst on TiO<sub>2</sub> (1 wt % Au/TiO<sub>2</sub>, AUROLite from Mintek) was tested. The catalyst exhibited high activity and excellent stability, even for 41 days (Table 1, entry 33).<sup>57</sup> Filonenko et al. studied the activity of unsupported and supported Au nanoparticles.<sup>58</sup> In line with previous studies, higher catalytic activities per unit mass of Au were found for supported Au catalysts. They screened a series of supports (TiO<sub>2</sub>, Al<sub>2</sub>O<sub>3</sub>, ZnO, CeO<sub>2</sub>, MgAl-hydrotalcite, MgCr-hydrotalcite, and CuCr<sub>2</sub>O<sub>4</sub>) and observed the highest activity for Au/Al<sub>2</sub>O<sub>3</sub>, which was two times higher than for Au/TiO<sub>2</sub> (TONs of 215 and 111, respectively). They proposed that the basic sites of the Al<sub>2</sub>O<sub>3</sub> support play an important role, acting cooperatively with Au<sup>0</sup> nanoparticles (Table 1, entries 34–40) as discussed later.

In the report of Hao et al., Ru catalysts supported on MgO, activated carbon, and  $\gamma$ -Al<sub>2</sub>O<sub>3</sub> were investigated for the reaction.<sup>59</sup> They suggested that surface hydroxyl groups on the support resulted in synergetic effects with the metal and a positive influence on the reaction. Accordingly, the catalytic performance increased in the following order: Ru/MgO (no

activity) < Ru/activated carbon (TON of 10) < Ru/ $\gamma$ -Al<sub>2</sub>O<sub>3</sub> (TON of 91) (Table 1, entries 44, 45).

Not only monometallic systems but also bimetallic catalytic systems have been reported for the reaction. Nguyen et al. prepared PdNi alloys supported on carbon nanotube-graphene (PdNi/CNT-GR) and performed the hydrogenation of CO<sub>2</sub> in the absence of a base. The composite support was chosen to avoid the common phenomenon of stacking of GR and bundling of CNTs. They both act as spacers, which helps to expose their entire surface areas during catalysis. The supported PdNi material showed a higher activity than the single metals, attributed to synergetic effects. Together with the main product, formate, a small amount of acetic acid was also detected (Table 1, entry 29).<sup>60</sup> As a different approach, Takahashi et al. examined a mixture of Fe and Ni powders for CO<sub>2</sub> hydrogenation without H<sub>2</sub> under a hydrothermal condition using water as the hydrogen source and in the presence of K<sub>2</sub>CO<sub>3</sub>. Encouragingly, 2.5 mmol of formic acid could be synthesized at 300 °C.<sup>61</sup>

According to the literature, Pd and Au are the most verified active metals for the synthesis of formic acid/formates and their catalytic activity can be enhanced with a proper choice of support material. Hydrophobic carbon-based materials seem preferred choices as support for Pd catalysts, whereas more hydrophilic support materials such as Al<sub>2</sub>O<sub>3</sub> and TiO<sub>2</sub> are preferably employed for Au catalysts (the same is also indicated for Ru catalysts). Still, the number of studies on (un)supported metal particle catalysts is small and discrepancies on the fundamental aspects, e.g., which metal is more active for the reaction, remain. Further investigations on this catalytic system for formic acid and formate synthesis are absolutely demanded to establish clearer catalyst structure–activity relationships.

**4.2.2. Heterogenized Molecular Catalysts.** From the comparison of activities and reaction mechanisms reported for homogeneous catalysts<sup>62–69</sup> and those reported for metal nanoparticle based systems, a large difference is obvious. Clearly, molecularly dispersed metal sites offer a more reactive environment for the hydrogenation of CO<sub>2</sub> to formic acid/formates. In this spirit, many researchers have studied in the past few decades



**Table 2.** Summary of the Different Heterogeneous Molecular Catalysts Reported for the Direct Hydrogenation of CO<sub>2</sub> to Formic Acid/Formates

| entry            | catalyst metal  | support          | P <sub>H<sub>2</sub></sub> /atm | P <sub>CO<sub>2</sub></sub> /atm | base/additive                       | T/°C | solvent          | C <sub>FA</sub> /M | t/h | TON  | TOF/h <sup>-1</sup> |
|------------------|-----------------|------------------|---------------------------------|----------------------------------|-------------------------------------|------|------------------|--------------------|-----|------|---------------------|
| 1 <sup>79</sup>  | Ru              | silica           | 39                              | 69                               | NEt <sub>3</sub> /PPh <sub>3</sub>  | 80   | EtOH             | 0.42               | 1   | 656  | 656                 |
| 2 <sup>78</sup>  | Ru              | silica           | 39                              | 69                               | NEt <sub>3</sub> /PPh <sub>3</sub>  | 80   | EtOH             | 1.1                | 1   | 1384 | 1384                |
| 3 <sup>78</sup>  | Ru              | silica           | 39                              | 69                               | NEt <sub>3</sub> /PPh <sub>3</sub>  | 80   | EtOH             | 0.69               | 1   | 868  | 868                 |
| 4 <sup>84</sup>  | Ru              | silica           | 89                              | 89                               | [mammim][TfO]/PPh <sub>3</sub>      | 60   | H <sub>2</sub> O | 47                 | 2   | 206  | 103                 |
| 5 <sup>85</sup>  | Ru <sup>a</sup> | silica           | 89                              | 89                               | [DAMI][TfO]/PPh <sub>3</sub>        | 80   | H <sub>2</sub> O | 188                | 2   | 1840 | 920                 |
| 6 <sup>79</sup>  | Ru              | MCM-41           | 53                              | 92                               | NEt <sub>3</sub> /PPh <sub>3</sub>  | 80   | EtOH             | 0.41               | 1   | 1022 | 1022                |
| 7 <sup>79</sup>  | Ru              | MCM-41           | 53                              | 92                               | NEt <sub>3</sub> /PPh <sub>3</sub>  | 80   | MeOH             | 0.43               | 1   | 1075 | 1075                |
| 8 <sup>79</sup>  | Ru              | MCM-41           | 53                              | 92                               | NEt <sub>3</sub> /PPh <sub>3</sub>  | 80   | PrOH             | 0.17               | 1   | 427  | 427                 |
| 9 <sup>79</sup>  | Ru              | MCM-41           | 53                              | 92                               | NEt <sub>3</sub> /AsPh <sub>3</sub> | 80   | EtOH             | 0.07               | 1   | 171  | 171                 |
| 10 <sup>79</sup> | Ru              | MCM-41           | 53                              | 92                               | NEt <sub>3</sub> /NPh <sub>3</sub>  | 80   | EtOH             | 0.07               | 1   | 179  | 179                 |
| 11 <sup>79</sup> | Ru              | MCM-41           | 53                              | 92                               | NEt <sub>3</sub> /PPh <sub>3</sub>  | 80   | EtOH             | 0.23               | 1   | 723  | 723                 |
| 12 <sup>79</sup> | Ru              | MCM-41           | 53                              | 92                               | NEt <sub>3</sub> /PPh <sub>3</sub>  | 80   | EtOH             | 0.21               | 1   | 537  | 537                 |
| 13 <sup>89</sup> | Ru              | TB-MOP           | 59                              | 59                               | NEt <sub>3</sub> /PPh <sub>3</sub>  | 40   | NEt <sub>3</sub> | 10.8               | 24  | 2254 | 94                  |
| 14 <sup>82</sup> | Ir              | silica           | 19.7                            | 19.7                             | NEt <sub>3</sub>                    | 60   | H <sub>2</sub> O | 0.13               | 2   | 1300 | 650                 |
| 15 <sup>82</sup> | Ir              | silica           | 19.7                            | 19.7                             | NEt <sub>3</sub>                    | 120  | H <sub>2</sub> O | 0.23               | 2   | 2300 | 1150                |
| 16 <sup>83</sup> | Ir              | polyethylenimine | 19.7                            | 19.7                             | NEt <sub>3</sub>                    | 120  | H <sub>2</sub> O | 0.04               | 1   | 284  | 284                 |
| 17 <sup>90</sup> | Ir              | Bpy-CTF          | 19.7                            | 19.7                             | NEt <sub>3</sub>                    | 80   | H <sub>2</sub> O | 0.06               | 2   | 500  | 250                 |
| 18 <sup>90</sup> | Ir              | Bpy-CTF          | 19.7                            | 19.7                             | NEt <sub>3</sub>                    | 120  | H <sub>2</sub> O | 0.4                | 2   | 3320 | 1660                |
| 19 <sup>90</sup> | Ir              | Bpy-CTF          | 19.7                            | 19.7                             | NEt <sub>3</sub>                    | 160  | H <sub>2</sub> O | 0.33               | 2   | 2700 | 1350                |
| 20 <sup>90</sup> | Ir              | Bpy-CTF          | 39.5                            | 39.5                             | NEt <sub>3</sub>                    | 120  | H <sub>2</sub> O | 0.61               | 2   | 5000 | 2500                |
| 21 <sup>91</sup> | Ir              | HBF              | 39.5                            | 39.5                             | NEt <sub>3</sub>                    | 120  | H <sub>2</sub> O | 0.01               | 0.5 | 750  | 1500                |
| 22 <sup>98</sup> | Ir (0.2 w%)     | spheres-CTF      | 9.8                             | 9.8                              | KHCO <sub>3</sub>                   | 90   | H <sub>2</sub> O | 0.004              | 2   | 219  | 110                 |
| 23 <sup>98</sup> | Ir (2 w%)       | spheres-CTF      | 9.8                             | 9.8                              | KHCO <sub>3</sub>                   | 90   | H <sub>2</sub> O | 0.009              | 2   | 54   | 27                  |

<sup>a</sup>Concentration in water, calculated back from TON, the volume of ionic liquid was not taken into consider.

the immobilization of homogeneous systems on different supports, looking for an easier catalyst handling and a higher activity per unit volume. Though Hübner et al.<sup>70</sup> have questioned industrial application of immobilized complexes on, e.g., questionable lower costs, lower rates, and metal leaching, and more attention should indeed be devoted to such critical aspects, these systems can offer the clear advantage of combining the desired properties of tunable, well-defined, highly active catalytic sites of a homogeneous system with a heterogeneous one. This section describes the latest achievements in the field of heterogenized molecular catalysts, which are categorized to those supported on (1) silica- and polymer-based materials and (2) porous organic polymers.

#### 4.2.2.1. Molecular Catalysts Immobilized on Grafted Solids.

Following the reports on the extraordinary reactivity of homogeneous Ru phosphine complexes, mainly with trimethylphosphine ligand by Jessop et al. for CO<sub>2</sub> hydrogenation to formic acid, formates, and derivatives in supercritical CO<sub>2</sub> as solvent and reactant,<sup>71–73</sup> the group of Baiker performed the synthesis of a formic acid derivative, formamide, by the reaction of CO<sub>2</sub> and H<sub>2</sub> with a primary amine under solvent-free conditions. They reported an excellent activity of Ru complexes with alkyl-bridged bidentate phosphine ligands, particularly of dppe (Ph<sub>2</sub>P(CH<sub>2</sub>)<sub>2</sub>PPh<sub>2</sub>) in comparison with dpmm (Ph<sub>2</sub>PCH<sub>2</sub>PPh<sub>2</sub>), dppp (Ph<sub>2</sub>P(CH<sub>2</sub>)<sub>3</sub>PPh<sub>2</sub>), and nonbridged trimethylphosphine (P(CH<sub>3</sub>)<sub>3</sub>) ligands.<sup>74</sup> Soon thereafter, the same group pioneered the immobilization of Ru with multiple coordination by bridged phosphine ligands (Figure 3a, bis[2'-(triethoxysilyl)ethylphenylphosphino]X (X: methane, ethane, and propane; thus called bspm, bspe, and bspp in structural analogy to dpmm, dppe, and dppp ligands, respectively)) in the matrix of SiO<sub>2</sub> aerogel and xerogel for the synthesis of formamides from primary and secondary amines.<sup>75–77</sup> Although good catalytic performance was presented, it was a few to several

times less effective as catalyst than the homogeneous counterparts.

The group of Zheng evaluated the use of surface-grafted silica, including mesoporous MCM-41, containing various functional donor groups such as NR<sub>2</sub>, CN, and SH, to allow the coordination to Ru complexes (Figure 3b), and studied the roles of support and the donor ligand in CO<sub>2</sub> hydrogenation to formic acid and derivatives.<sup>75,78–80</sup> Comparing activities of the “precatalyst” structures (the active system is formed under reaction conditions) based on primary, secondary, and tertiary amine ligands, the secondary amine showed the highest TOF (1384 h<sup>-1</sup>, Table 2, entry 2) in the presence of a base (NEt<sub>3</sub>).<sup>78</sup> Secondary amines are generally known to be better electron donors, which could explain the increase in catalytic activity. Furthermore, among the systems with three different ligand types (amine, nitrile, and thiol terminal groups) anchored to MCM-41, the amine-based precatalyst showed the highest activity. Again, this was attributed to the optimal electron donation effects in comparison with the other linkers. No activity was detected when no PPh<sub>3</sub> was added, something generally reported. Upon catalyst recycling no further addition of this ligand was required, indicating that the formation of the active catalytic species occurred under the reaction conditions in the first run. Although no characterization of the active structure or of the spent catalyst was reported, it was assumed that an octahedral dihydrido Ru complex was formed under reaction conditions. Baffert et al. immobilized a tailored ruthenium–N-heterocyclic carbene (NHC) species in the pores of a mesostructured silica matrix (Figure 3c). The active sites were spectroscopically verified, and the catalytic system displayed promising activities in the hydrogenation of carbon dioxide.<sup>81</sup> However, significant metal leaching (50%) was observed. In general, leaching is observed when the active metal (Ru) was bound through a single coordination to a ligand grafted on



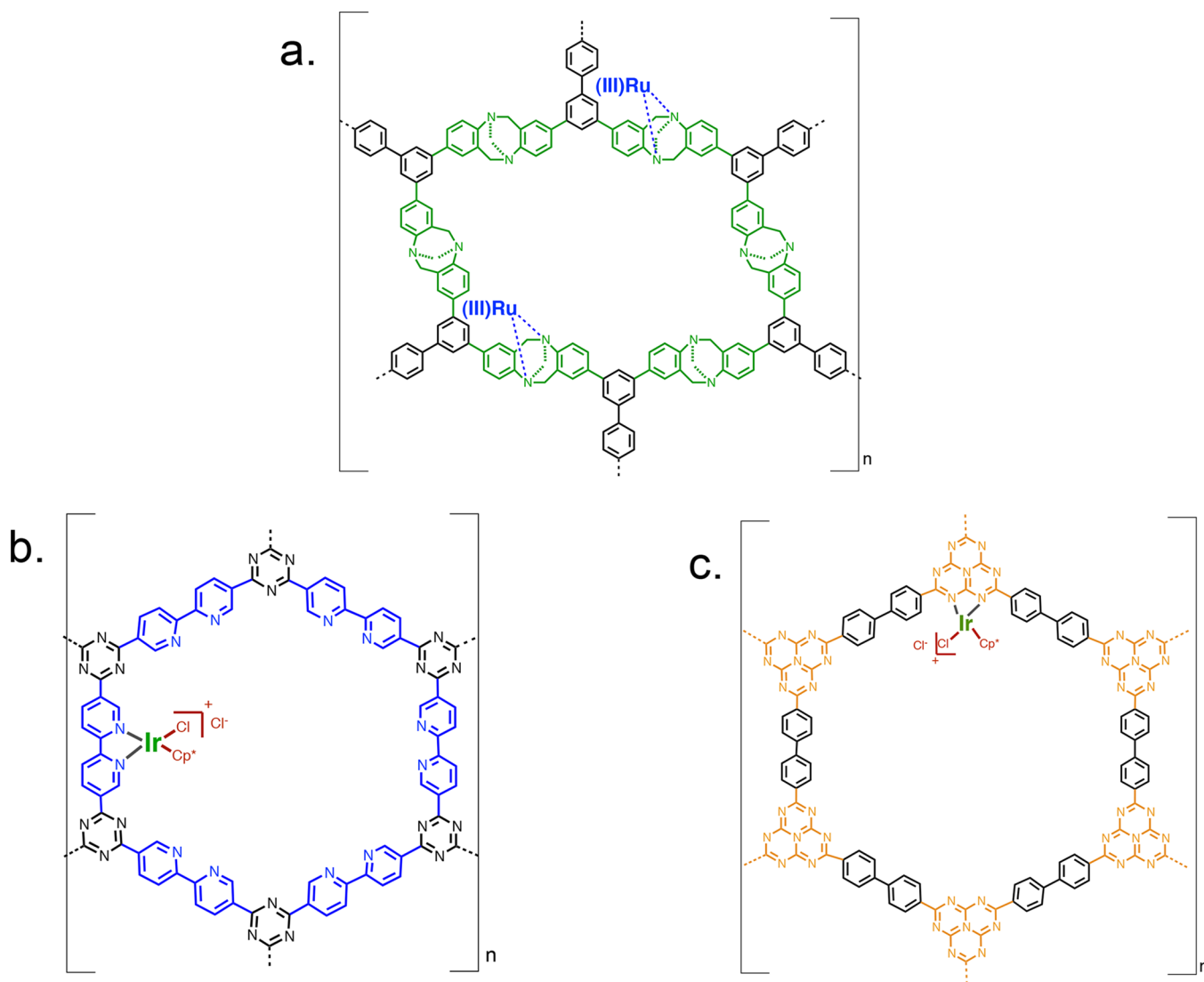


**Figure 4.** Immobilization of Ru/Ir molecular complexes on porous organic polymers. (a) Created after ref 89. (b) Adapted with permission from ref 90. Copyright 2015 Wiley-VCH Verlag GmbH & Co. KGaA. (c) Adapted with permission from ref 91. Copyright 2016 Elsevier.

support material via an alkyl chain, while the degree of metal leaching was dependent on the coordinating terminal group. For example, over the first reaction cycle 8% of active metal leaching was indicated for the amine functionalized silica compared to the one functionalized with thiol (2.5% metal leaching) ascribed to the weaker complexation, but higher activity of the former.<sup>79</sup> Although in this case the Ru–H vibration was detected by FTIR, no characterization was reported for the spent catalyst. Rohr et al. showed that multiple coordination using two bidentate ligands (Figure 3a) could greatly improve the stability of the catalyst by enhancing the binding strength to Ru compared to the cases where the active metal is weakly bound via a single coordination (Figure 3b).<sup>75</sup>

The group of Hicks reported the first immobilization of an iridium catalyst for this reaction. Conventional introduction of amine groups on silica support was followed by a further functionalization by a Schiff base reaction with *o*-(diphenylphosphino)benzaldehyde to form an imine group.<sup>82</sup> Among amine, monodentate phosphine, and imine-phosphines as the grafted ligand, only phosphine-containing catalysts showed activity. The highest obtained TONs after 2 h were 1300 at 60 °C and 2300 at 120 °C (Table 2, entries 14, 15),

respectively. Notably, the imine-phosphine ligand allows bidentate coordination (Figure 3d) and thus improved the stability of the catalyst. The same researchers also explored the use of an amine containing polymer (Figure 3d) as support.<sup>83</sup> The idea behind was to capture carbon dioxide with amine functionalities in order to increase the catalytic activity. Similar to the work using the silica support, the use of the imine-phosphine grafted ligand led to the highest activity. Nevertheless, the catalysts barely showed activity without addition of a base in spite of the presence of amine groups at the surface of the support.

Zhang et al. immobilized a Ru complex in a way similar to the previous examples and obtained a molecular heterogeneous “Si”–(CH<sub>2</sub>)<sub>3</sub>NH(CSCH<sub>3</sub>)–{RuCl<sub>3</sub>–PPh<sub>3</sub>} precatalyst supported on SiO<sub>2</sub> or polystyrene (Figure 3e).<sup>45,84</sup> In their study, an ionic liquid was used as reusable base, which can form a salt with formic acid. Therefore, both formic acid and the base were recovered easily by filtering off the catalyst and by evaporation of the acid and aqueous solvent at 130 °C, yielding the ionic liquid. In the follow-up work a diamine-functionalized ionic liquid was used for a higher catalytic efficiency by improving the uptake of formic acid.<sup>85</sup> The precatalyst “Si”–(CH<sub>2</sub>)<sub>3</sub>NH(CSCH<sub>3</sub>)–{RuCl<sub>3</sub>–PPh<sub>3</sub>} was prepared by mixing beforehand synthesized

“Si”-(CH<sub>2</sub>)<sub>3</sub>NH(CSCH<sub>3</sub>) and RuCl<sub>3</sub>·3H<sub>2</sub>O with subsequent addition of the required PPh<sub>3</sub> ligand, as without it no reaction occurred. Though no metal leaching was detected for five times use, the nature of the catalytic species is not revealed, as no characterization of fresh or spent catalyst was reported. The activity of this system is also moderate (cf. Table 2).

Evidently, some but significant efforts have been devoted to immobilize molecular catalysts for the synthesis of formic acid and formates through coordination to ligand(s) grafted on a support material. The more coordination interactions, the better the binding, with P-based ligands as the preferred ones for an optimal performance. Unfortunately, to date the catalytic tests have been performed only in batch mode and surprisingly little is investigated into the stability of these grafted catalyst systems, even though many authors reported that the stability is the major challenge. To fully benefit from the heterogeneous nature of such catalysts, rigorous evaluation of catalyst leaching under continuous operation will be required, and innovative strategies for stable anchoring of molecular catalysts on grafted surfaces of solid materials are still to be identified.

**4.2.2.2. Molecular Catalysts Immobilized on Porous Polymers.** Grafting ligands on a solid support is one of the strategies to immobilize a molecular catalyst with a desired coordination environment for the reaction. The major challenge in this approach is the catalyst stability, as discussed above, besides minimizing the steps for catalyst synthesis. In these respects, another emerging immobilization strategy using porous polymers is highly attractive. Particularly, porous organic framework (POF) is a relatively new but promising class of porous materials to immobilize molecular catalysts. The term POF comprises a number of porous solids based on only organic constituents, encompassing covalent organic frameworks (COFs) and porous organic polymers (POPs). POFs possess high surface areas from a few hundred to several thousand m<sup>2</sup> g<sup>-1</sup>, tunable pore sizes from micro- to mesopores, and adjustable skeletons that offer unprecedented possibilities for the design of single-site catalysts.<sup>86</sup> Although the most interesting solids are not crystalline, still excellent pore size distributions and control can be achieved, in contrast to traditional polymers.<sup>87</sup> In principle, another class of well-known porous polymers, metal-organic framework (MOF), can also be used as the support of active single-metal site if the skeleton offers an appropriate coordination environment to the metal center. Recently, Beloqui Redondo et al. reported the first example of phosphine-containing MOF to heterogenize a Ru complex.<sup>88</sup> Although the catalyst was not tested for CO<sub>2</sub> hydrogenation to formic acid, the reverse reaction, namely, formic acid decomposition, was evaluated. The catalyst showed excellent activity and stability even when the reaction was operated continuously in the gas phase. A more straightforward approach is the use of POFs with coordinating functional groups in the skeleton, and the number of examples is rapidly increasing.

Yang et al. prepared a Tröger's base-derived microporous organic polymer (TB-MOP), and the nitrogen atoms of the framework coordinated a Ru(III) complex, obtaining a TB-MOP–Ru catalyst (Figure 4a) with high activity in the hydrogenation of CO<sub>2</sub> to formate.<sup>89</sup> At relatively low temperature (40 °C) the TON was 2254 after 24 h (Table 2, entry 13). However, the use of a PPh<sub>3</sub> ligand was essential and, in its absence, only fewer than 25 turnovers could be observed under similar reaction conditions. Also, the TON decreased when TB-MOP–Ru was reused for the second time, which was due to leaching of Ru species, as detected by ICP-OES. The weaker

complexing ability of Tröger's base compared to PPh<sub>3</sub> was found as the main cause for leaching.<sup>89</sup>

There has been tremendous research on Ir pentamethylcyclopentadienyl (Cp\*) complexes, where Ir is coordinated by two nitrogen atoms of the support ligand, and they have been tested for a wide range of hydrogenation reactions including CO<sub>2</sub> hydrogenation.<sup>92–95</sup> The record values in CO<sub>2</sub> hydrogenation to formic acid were obtained by Hull et al. with TON of 153,000 and TOF of 53,800 h<sup>-1</sup> using a homogeneous dinuclear IrCp\* catalyst stabilized by the ligand environment of 4,4',6,6'-tetrahydroxy-2,2'-bipyrimidine (thbpy).<sup>65</sup> Many groups were inspired by that work and developed different heterogeneous versions of that system mimicking the coordination environment to active Ru or Ir metal centers.

Some of us pioneered the use of covalent triazine frameworks (CTFs) as support. CTFs are porous aromatic frameworks made upon trimerization of aromatic nitriles,<sup>96</sup> which possess high thermal and chemical stability and a high surface area. CTFs open up a wide range of possibilities for heterogenizing metal complexes, since they contain a high density of quasi-bipyridine complexes. Inspired by the original work of Bavykina et al.,<sup>97</sup> Park et al. immobilized the [IrCp\*(bpy)Cl]Cl complex (Figure 4b).<sup>90</sup> The obtained complex was thoroughly characterized to prove that the obtained catalyst is similar to its homogeneous counterpart. Scanning electron microscopy (SEM) in combination with energy-dispersive X-ray spectroscopy (EDS) mapping revealed the even distribution of Ir and Cl atoms. XPS analysis of both homogeneous and heterogeneous versions showed the identical value of binding energy for Ir 4f<sub>7/2</sub> (62.1 eV), indicating similar electronic environment of the active Ir center. The catalyst showed activity increasing favorably with pressure (Table 2, entries 18 vs 20) as well-known for homogeneous systems<sup>69,71</sup> with an optimal temperature of 120 °C (Table 2, entries 17–19). The maximum TON was 5000 at 120 °C under 8 MPa of total pressure. Encouragingly, the catalyst stability could be improved by this immobilization method; the catalyst was recycled five times with only a slight loss of activity.<sup>90</sup> The same group immobilized a similar Ir complex to a heptazine-based framework (HBF, Figure 4c). The catalyst material showed initial TOF of 1500 h<sup>-1</sup> and TON of 6400 at 120 °C under 8 MPa total pressure (Table 2, entry 21).<sup>91</sup> Furthermore, in an attempt to bring the use of CTF-based molecular catalysts a step further to industrial applicability, Bavykina et al. reported a one-step approach for the production of porous, mechanically rigid, and easy-to-handle CTF-based spheres (Figure 5).<sup>98</sup> A phase inversion technique making use of a polymer as binder was followed by first preparing a slurry of the CTF powder and the dissolved polymer in an organic solvent followed by a rapid removal of the solvent by contacting the slurry with a nonsolvent (water in this case). Removal of the organic solvent by the nonsolvent led to a rapid solidification of the polymer binder and to the creation of additional porosity in the composite. After obtaining the spheres, Ir(III)Cp\* was coordinated to the bipyridine moieties of CTF to obtain efficient catalyst. Removing Cl<sup>-</sup> ions by washing the catalyst with DMF increases its efficiency and recyclability.<sup>97</sup> Both powder and shaped catalysts were evaluated in the reaction, and the spherical particulate catalyst was shown to be easily recyclable in the hydrogenation of CO<sub>2</sub>.<sup>98</sup> These studies show that the environment of POFs is excellent for stably immobilizing molecular complexes likely due to the intrinsic stability of the coordinating ligands in the skeleton of the framework and the abundantly available coordinating sites (e.g., N atoms) homogeneously distributed over the porous material.

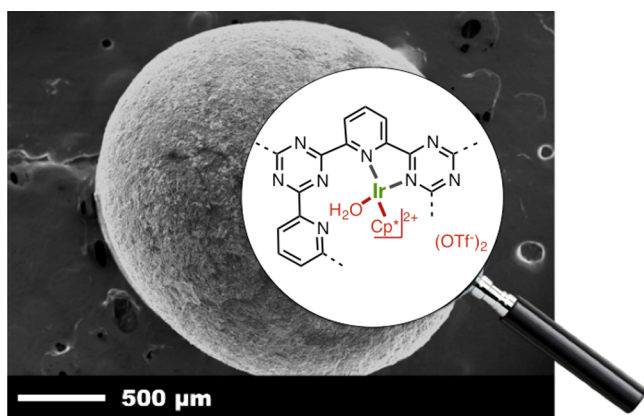


**Figure 5.** Immobilization of an Ir complex on CTF-based spheres. Reproduced with permission from ref 98. Copyright 2016 Wiley-VCH Verlag GmbH & Co. KGaA.

### 4.3. Reaction Mechanism

Formic acid synthesis by CO<sub>2</sub> hydrogenation is not thermodynamically favored as discussed in section 4.1. To facilitate this reaction, several strategies have been employed as mentioned earlier. In general, selection of a proper solvent for the reaction results in better catalytic performance owing to the solvation of product and reagents (entropic influence). However, in order to directly impact the thermodynamic equilibrium of the reaction, the use of strong bases able to form adducts with formic acid or formates has been proven as the most straightforward strategy. Typical base examples used in organic solvents are triethylamine and DBU (1,8-diazabicyclo[5,4,0]undec-7-ene). For the reaction in aqueous phase, hydroxides, bicarbonates, and carbonates are generally used, and the latter two are often employed as the source of CO<sub>2</sub> (*vide supra*). Therefore, the real substrate of the hydrogenation will not be only CO<sub>2</sub> but also HCO<sub>3</sub><sup>−</sup> or CO<sub>3</sub><sup>2−</sup>. The equilibrium between these compounds is influenced by many factors, e.g., pH, temperature, and CO<sub>2</sub> pressure. Therefore, when the term “CO<sub>2</sub> hydrogenation to formic acid” is used, it does not imply that CO<sub>2</sub> is the only and real substrate, but the above-mentioned equilibrium of many.<sup>39</sup>

Two main types of heterogeneous catalysts, namely, (un)-supported metal nanoparticles and immobilized organometallic complexes (Figure 2), have been reported to convert CO<sub>2</sub> to formic acid/formates, and consequently the reported reaction mechanisms are obviously different. Recently, Wang et al. summarized the main mechanistic aspects of homogeneous catalysts for the hydrogenation of CO<sub>2</sub> to formates.<sup>39</sup> The main differences in the reaction mechanisms among homogeneous catalysts reside in the way in which CO<sub>2</sub> coordinates to the metal center (through either C or O) as well as in the way in which hydrogen is activated. It is also worth mentioning that in most cases the performance of homogeneous catalysts is highly pH dependent as expected by thermodynamics. At low pH, active complexes preferentially catalyze hydrogen production from the decomposition of formic acid, whereas at high pH, formic acid is produced from CO<sub>2</sub> and H<sub>2</sub> using the same catalyst. Although various reaction mechanisms have been proposed and they are markedly different depending on the reactive environment like ligand and solvent (organic vs aqueous solvent),<sup>39</sup> most involve CO<sub>2</sub> activation with the M–H bond (M: metal) through nucleophilic attack of hydride to the carbon atom of CO<sub>2</sub> to form formates.<sup>69</sup> Then the formates are released as formic acid (or

derivatives, e.g., in the presence of amine or alcohol) through activation of H<sub>2</sub> at the metal center, yielding a product and regenerating the M–H bond. Related to the aforementioned promising heterogenized molecular catalysts supported on POFs with bipyridine-like skeletons, the reaction mechanism is expected to be similar to that reported for the homogeneous analogues (Figure 6).<sup>65</sup> For detailed reaction mechanisms

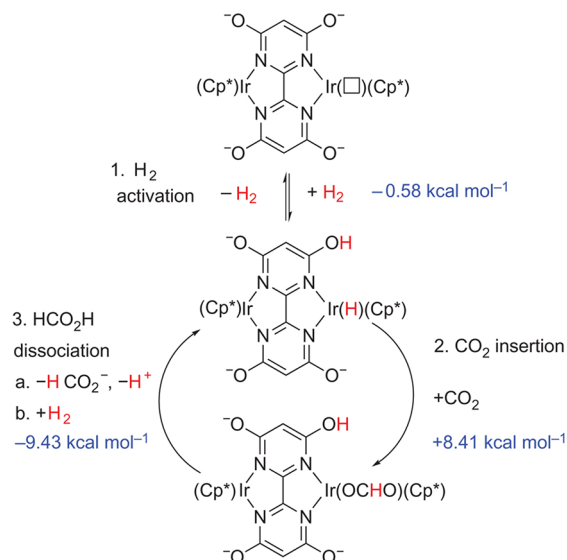


**Figure 6.** Proposed mechanism for reversible CO<sub>2</sub> hydrogenation to formic acid using binuclear IrCp\* catalyst with a thbpym ligand. Reproduced with permission from ref 65. Copyright 2012 Macmillan Publishers Ltd.

proposed to date for molecular complexes, we refer to the excellent review by Wang et al.<sup>39</sup> When it comes to the application of heterogenized molecular catalysts, reaction mechanisms similar to those found for their homogeneous counterparts can be expected. However, the role of support, especially its affinity to reactants, reaction products, and solvent, and potential mechanistic differences induced by the uniquely supported environment of active metals cannot be neglected. Further investigation on these aspects is awaited and expected to come in the near future.

Regarding these mechanistic aspects related to the application of metal nanoparticle based catalysts, it would not be overly controversial to state that this field is still in its infancy and only a few works have dealt with this aspect. Filonenko et al.<sup>58</sup> proposed a mechanism of hydrogenation of CO<sub>2</sub> to formates on Al<sub>2</sub>O<sub>3</sub> supported Au nanoparticles (Figure 7). It was proposed that formates and bicarbonates are the key intermediates in the catalytic cycle. They proposed that hydrogenation starts with the heterolytic dissociation of hydrogen at the Au/support interface, producing surface hydroxyl and metal hydride species. Since the reaction was performed in DMF, which adsorbed on the catalyst surface, the H<sub>2</sub> dissociation step may be preceded by DMF desorption, therefore liberating a vacant site for H<sub>2</sub> activation. This is followed by CO<sub>2</sub> reaction with surface OH groups, forming bicarbonates on the surface. Au–hydride reacts with the bicarbonates, and adsorbed formate species are formed on the Au–support interface; formates can subsequently migrate to more thermodynamically stable locations to generate alumina-bound formates.

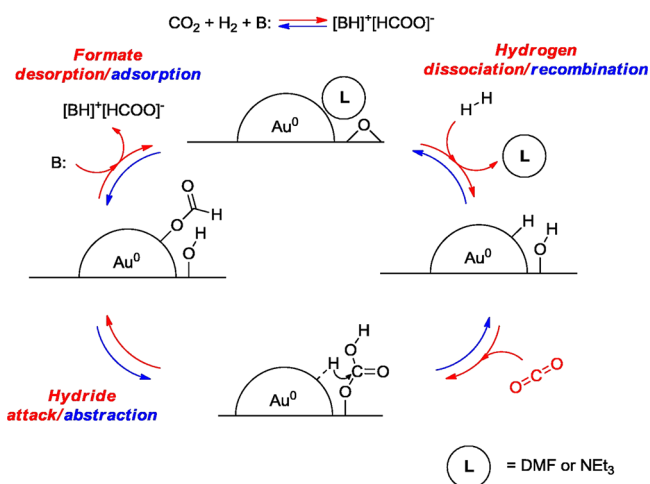


**Figure 7.** Mechanism of  $\text{CO}_2$  hydrogenation over supported Au nanoparticles. Reproduced with permission from ref 58. Copyright 2016 Elsevier.

Lee et al.<sup>99</sup> investigated the mechanism of  $\text{CO}_2$  hydrogenation to formic acid over carbon nanotube-graphene supported PdNi alloys. The proposed mechanism is illustrated in Figure 8. As the first step, an electron transfer from Ni to Pd atoms occurs. Therefore, Pd and Ni are in the electron-rich and -deficient state, respectively. It is followed by  $\text{H}_2$  dissociative adsorption on Pd surface and  $\text{CO}_2$  adsorption through its O atoms on the Ni surface. Reaction between H on Pd and adsorbed  $\text{CO}_2$  leads to the formation of adsorbed  $\text{HCOOH}$ . In this mechanism, the advantage and even necessity for bimetallic surfaces is clearly highlighted.

## 5. DIRECT HYDROGENATION OF $\text{CO}_2$ TO METHANOL AND DME

The “methanol economy” proposed by Nobel Laureate George Olah positions  $\text{CO}_2$  hydrogenation to methanol and derived products at its core. In the simplest form, the concept involves the capture of  $\text{CO}_2$  from any natural, human, or industrial source and its effective catalytic transformation into methanol, DME,

and a large variety of secondary methanol/DME-based products (Figure 9).

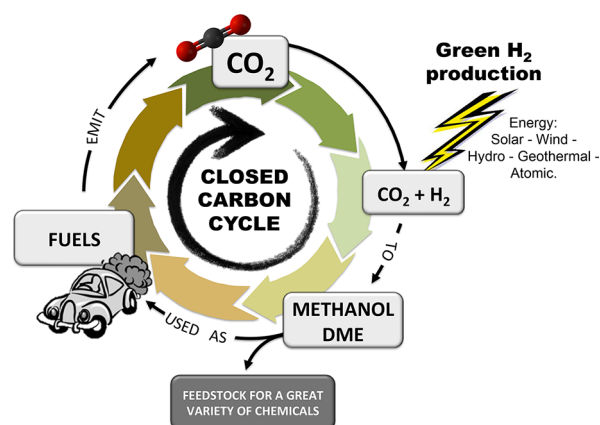


**Figure 9.** Chemical recycling of  $\text{CO}_2$  to methanol and DME.

The catalytic conversion of  $\text{CO}_2$  into methanol and DME bears a strong potential to transform large amounts of  $\text{CO}_2$  in a short span of time due to the commonly reported high reaction rates. This feature is translated into high process efficiency in practice. As described in section 3, for the process to be sustainable in the light of the carbon cycle,  $\text{H}_2$  should be produced in a greener way, e.g., photocatalytic water splitting and water electrolysis sourced by natural/renewable energy sources.

Historically, methanol was obtained as a byproduct in the charcoal production by wood, thus called *wood alcohol*.<sup>100</sup> Methanol produced in this way was used in the 19th century for lighting, cooking, and heating purposes, until it was replaced by cheaper fuels like kerosene. Until 1923 the *wood alcohol* was the only source of methanol. In early 1920s, Mittasch et al. at BASF (Badische Anilin and Soda Fabrik) successfully produced organic oxygenates, including methanol, from syngas during the developmental work on the ammonia synthesis. Later on, BASF went on commercializing this syngas-to-methanol synthesis process consisting of sulfur resistant zinc chromite ( $\text{ZnO}$ –

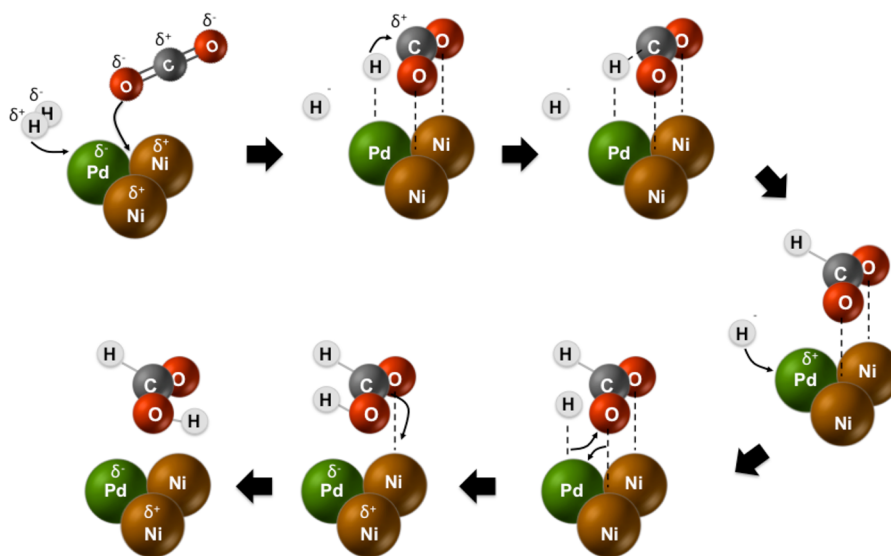


**Figure 8.** Mechanism of  $\text{CO}_2$  hydrogenation over PdNi bimetallic surface. Reproduced with permission from ref 60. Copyright 2015 The Royal Society of Chemistry.



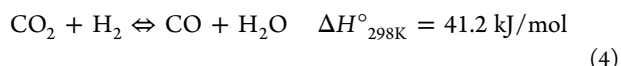
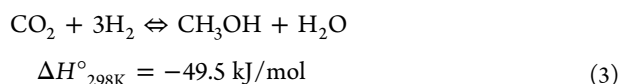
Cr<sub>2</sub>O<sub>3</sub>) catalysts and typical operating conditions of 320–450 °C and 250–350 bar.<sup>101</sup>

Today, methanol is one of the top five commodity chemicals shipped around the world each year. It is a primary raw material for the chemical industry, increasingly used in the methanol to olefins (MTO) process, an intermediate for the production of a variety of chemicals including formaldehyde, methyl *tert*-butyl ether, and acetic acid among others.<sup>100</sup> Most of these chemicals are the basic building blocks of many commodity products in our daily life including paints, plastics, resins, adhesives, and antifreezes. Furthermore, methanol can be directly employed in fuel cells, and it has also been proven to be an excellent fuel blend for internal combustion engines. Methanol itself has low cetane number, which makes it impractical as sole fuel in diesel engines, but the derivative of methanol, DME, with its high cetane number (higher than 55 as compared to with 40–55 of common diesel fuel<sup>102</sup>), offers several attractive properties such as very low emissions of pollutants (particulate matter, NO<sub>x</sub>, and CO) and biodegradability over the conventional fuels. Dehydration of methanol over solid acid catalysts yields DME. Integrating this dehydration reaction into CO<sub>2</sub> hydrogenation to methanol adds another dimension in CO<sub>2</sub> recycling strategy in terms of final product selection. The novel “one-step” approach of DME synthesis from CO<sub>2</sub>, i.e., via *in situ* transformation of methanol to DME, is meritorious thanks to the lower thermodynamic limitation in CO<sub>2</sub> hydrogenation than in methanol synthesis.<sup>103</sup> In addition, the methanol dehydration toward DME proceeds in a very similar temperature region as that of methanol synthesis, making the single step process viable.

Recently, trends of R&D in methanol synthesis are shifting toward a greener process, where CO<sub>2</sub> is reduced by H<sub>2</sub> generated from the technology sourced by natural/renewable energies. Mitsui Chemicals and Carbon Recycling International (CRI) Inc. are the two well-known companies, among others, and they have demonstrated such processes for production of methanol. The plant of the latter, CRI, located in Iceland has a production capacity of around 5 million liters of methanol per year (4 kta). The H<sub>2</sub> for this reaction is produced by water electrolysis using energy produced from natural sources, mainly geothermal, hydro, and wind.<sup>104</sup>

### 5.1. Thermodynamic Considerations

Methanol synthesis and reverse water-gas shift (RWGS) are the two major competing reactions in the process of CO<sub>2</sub> hydrogenation to methanol (eqs 3 and 4).<sup>105</sup>



It is also possible and likely that CO formed via RWGS undergoes further hydrogenation toward methanol as per eq 5.<sup>106</sup>



It is evident from eqs 3–5 that thermodynamically, according to Le Châtelier's principle, the use of high pressures and low temperatures should be advantageous due to the exothermic nature of the methanol formation reactions (eqs 3 and 5) and to the decrease in the number of molecules when the reactions proceed forward. The reaction characteristics are contrasting for

RWGS; the reaction is endothermic without a change in the total number of molecules.

Some of the first thermodynamic studies on the methanol synthesis from CO, CO<sub>2</sub>, and H<sub>2</sub> were performed by Graaf et al.<sup>107</sup> They studied the chemical equilibria of the associated reactions and proposed the expressions for the equilibrium constants by assuming the ideal gas behavior with nonideality corrections predicted by the Soave–Redlich–Kwong equation of state. In 2016, Graaf and Winkelman<sup>108</sup> refined the expressions by taking a large number of experimental data. They showed that in the literature the equilibrium constants for the methanol formation from CO and H<sub>2</sub> have a considerable variation as much as 40%. They explained that these variations are, on the basis of sensitivity analysis, due to the very small differences in the employed basic thermochemical data, especially the Gibbs energy of formation for CH<sub>3</sub>OH and CO. By fitting the Gibbs energy values they established highly reliable expressions for the equilibrium constants.

The thermodynamic and kinetic analysis of methanol synthesis from only CO<sub>2</sub> and H<sub>2</sub> has not been performed as frequently as conventional methanol synthesis using CO, CO<sub>2</sub>, and H<sub>2</sub> mixture. In the available literature, the kinetic expressions of Graaf et al.<sup>107,109</sup> as well as Bussche and Froment<sup>110</sup> are frequently applied to model reaction profiles in methanol synthesis with an industrial Cu–ZnO–Al<sub>2</sub>O<sub>3</sub> catalyst from syngas and also from CO<sub>2</sub> and H<sub>2</sub>.<sup>111–115</sup> These two widely applied kinetic models are based on different assumptions: the model of Graaf et al. assumes the formation of methanol from both CO and CO<sub>2</sub>, while the model of Bussche and Froment assumes that CO<sub>2</sub> is the main source of carbon for the synthesis of methanol and considered the inhibitory effect of water formed by the RWGS reaction.

Galluci and Basile<sup>111</sup> evaluated the performance of a membrane reactor in comparison to a traditional reactor for methanol synthesis by CO<sub>2</sub> hydrogenation over a commercial catalyst using the kinetic model of Graaf et al. and showed potential advantages of a zeolite membrane reactor. On the one hand Fornero et al.<sup>112</sup> applied the same kinetic model to theoretically study the effects of H<sub>2</sub>/CO<sub>2</sub> feed ratio, ranging from 1.5 to 4, and stream recycle ratio on the reaction performance under the conditions of thermodynamic and kinetic controls. On the other hand, Van-Dal and Bouallou<sup>113</sup> selected the kinetic model of Bussche and Froment arguing that this model was in better agreement with the recent experimental findings on the role of CO<sub>2</sub> on these catalysts. Meyer et al.<sup>114</sup> compared the two models and discussed the differences. Their results revealed that the two models behave differently in the first half of the reactor where the reaction is controlled by the kinetics. The difference become negligible and the results of both models become similar when the reaction is limited by thermodynamic equilibrium, i.e., close to the reactor outlet.

As mentioned earlier, high-pressure and low-temperature conditions are thermodynamically favorable. Van Bennekom et al.<sup>116</sup> reported a model based on a modified Soave–Redlich–Kwong equation of state which enabled the calculation of the simultaneous phase and chemical equilibria that occur during high-pressure methanol synthesis (200 bar, 190–280 °C). The model included the treatment of the dew point as a function of temperature and conversion. Additionally, the predictions were verified experimentally and the authors found that the condensation of methanol and water had beneficial consequences in methanol synthesis with carbon oxide conversions higher than that of the one-phase chemical equilibrium.<sup>117</sup>

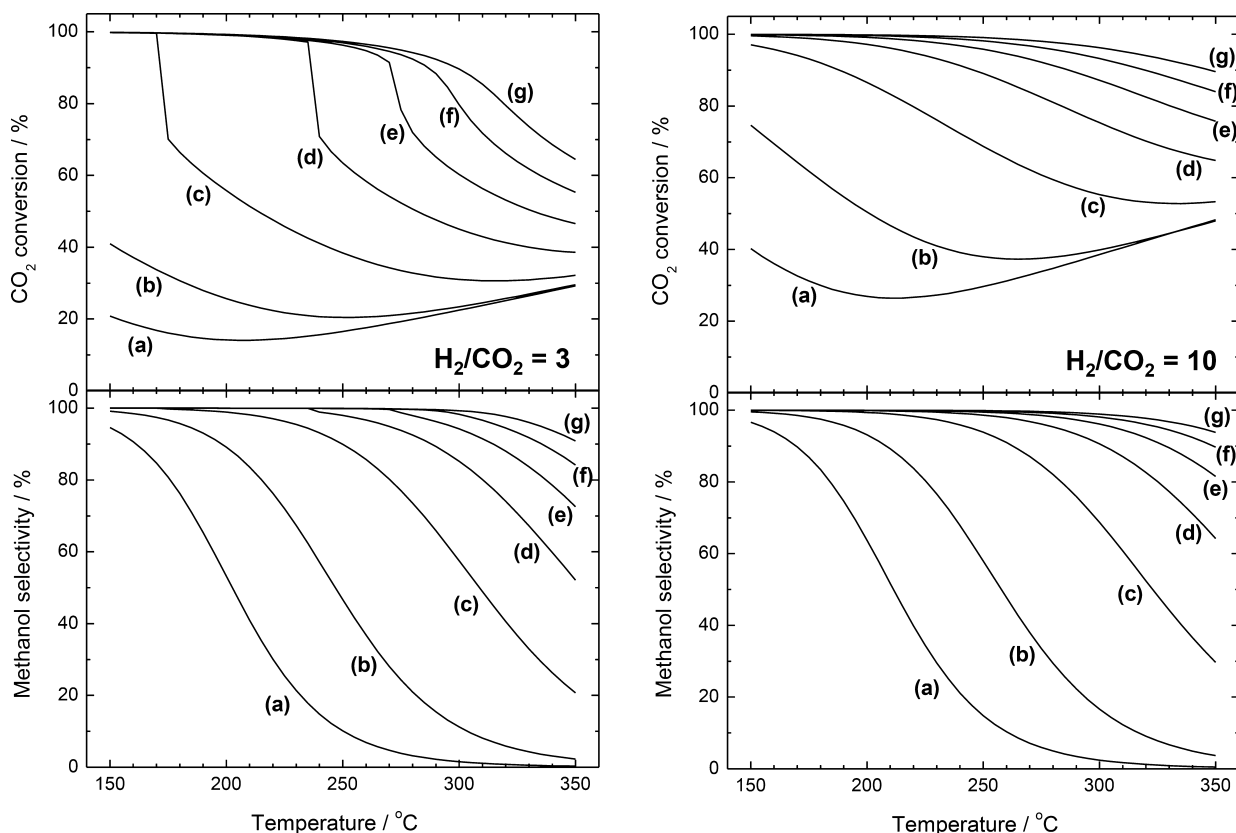


**Figure 10.** Equilibrium  $\text{CO}_2$  conversion and methanol selectivity at different temperatures with initial  $\text{H}_2/\text{CO}_2$  mixtures of 3 (left) and 10 (right), and at (a) 10 bar, (b) 30 bar, (c) 100 bar, (d) 200 bar, (e) 300 bar, (f) 400 bar, and (g) 500 bar. The calculation was performed with the same method as described in refs 115 and 118.

Figure 10 shows the equilibrium  $\text{CO}_2$  conversion and methanol selectivity over a wide range of pressures and temperatures (the other possible product is  $\text{CO}$ ; only the reactions of eqs 3–5 were assumed to take place).

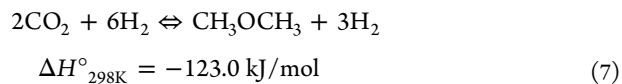
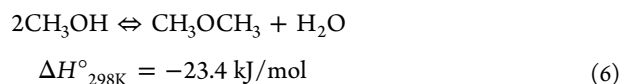
Interestingly, there is an abrupt change in  $\text{CO}_2$  conversion at 100–300 bar within the temperature range shown. This is due to the formation of a liquid phase and phase separation. This change takes place at about 240 °C at 200 bar, which is close to the condition reported by van Bennekom et al. Also, the abrupt change in  $\text{CO}_2$  conversion diminishes at higher pressure (>400 bar), transforming to a smooth decrease of  $\text{CO}_2$  conversion toward higher temperature. This is indicative of one dense phase at very high pressure conditions. Recent works by Gaikwad et al.<sup>115,118</sup> showed experimentally the advantage of high-pressure conditions in  $\text{CO}_2$  hydrogenation to methanol.

At the stoichiometric molar ratio ( $\text{H}_2/\text{CO}_2 = 3$ ) about 90%  $\text{CO}_2$  conversion and >95% methanol selectivity could be attained at 442 bar. It was also shown that, under such high-pressure conditions, a dense phase formation by product condensation takes place and internal mass transfer limits the overall reaction rate depending on the catalyst pellet size. Furthermore, as expected thermodynamically, high-pressure operation at higher  $\text{H}_2/\text{CO}_2$  ratio is greatly advantageous in  $\text{CO}_2$  conversion. At  $\text{H}_2/\text{CO}_2 = 10$ ,  $\text{CO}_2$  equilibrium conversion is boosted and also phase condensation does not seem to take place at these pressure conditions (Figure 10). Experimentally at 331 bar (partial pressure of the reactants), 260 °C, almost full (>95%)  $\text{CO}_2$  conversion and >98% methanol selectivity was demonstrated.<sup>118</sup>

As another example taking advantage of the reaction thermodynamics, a novel reactor configuration with two

temperature zones inside the reactor to shift the chemical equilibrium was reported by Bos et al.<sup>119</sup> The authors showed that the conversion limitations due to thermodynamic equilibrium could be bypassed via *in situ* condensation of a water/methanol mixture.

It is widely known that DME is formed via the dehydration reaction of methanol over solid acid catalysts, which is mildly exothermic (eq 6<sup>105</sup>; eq 7<sup>120</sup> is the overall reaction).



Because of the consecutive nature of DME formation through methanol formation when  $\text{CO}_2$  is used as the starting raw material, the thermodynamic aspects of DME synthesis are closely related to that of methanol synthesis. In addition to increasing the reaction pressure, the thermodynamic limitation of  $\text{CO}_2$  conversion could also be mitigated if methanol is continuously removed from the product side of eq 3 via its effective transformation to DME.

The study by Aguayo et al.<sup>121</sup> provided a kinetic model for one step DME synthesis over  $\text{Cu-ZnO-Al}_2\text{O}_3/\gamma\text{-Al}_2\text{O}_3$  bifunctional catalyst from  $\text{CO} + \text{H}_2$  or  $\text{CO}_2 + \text{H}_2$  mixture (notation “//” indicates the bifunctionality of the catalysts). They showed considerable increase in both methanol and DME yields when the DME synthesis was performed in one step. According to the kinetic study, methanol dehydration is very fast and the water-gas

shift reaction remains in equilibrium, rendering methanol synthesis to be the rate-determining step.<sup>121</sup> The same conclusion was drawn by Qin et al.,<sup>122</sup> who developed an intrinsic kinetic model for CO<sub>2</sub> hydrogenation to DME over a Cu–Fe<sub>2</sub>O<sub>3</sub>–ZrO<sub>2</sub>/H-ZSM-5 catalyst. Erefia et al.<sup>123</sup> further extended the kinetic model for a Cu–ZnO–Al<sub>2</sub>O<sub>3</sub>/γ-Al<sub>2</sub>O<sub>3</sub> bifunctional catalyst taking the catalyst deactivation into account. The model considered the attenuation of methanol synthesis and the formation of paraffin byproducts due to CO<sub>2</sub> and water in the reaction medium. The thermodynamic investigations by Shen et al.<sup>120</sup> revealed that the CO<sub>2</sub> equilibrium conversion to DME was considerably and consistently higher than that only to methanol without further transformation to DME. For any feed composition of CO<sub>2</sub>/H<sub>2</sub>, the equilibrium yield of DME increased with pressure and decreased with temperature as expected.<sup>120,124</sup> The above studies clearly indicate the thermodynamic advantages of CO<sub>2</sub> hydrogenation to DME in terms of CO<sub>2</sub> conversion efficiency by coupling CO<sub>2</sub> hydrogenation and methanol dehydration, although achieving complete transformation of methanol to DME, thus full DME selectivity, seems difficult or not possible.

## 5.2. Catalytic Systems

### 5.2.1. Catalysts for the Direct Hydrogenation of CO<sub>2</sub> to CH<sub>3</sub>OH.

The very first commercialized methanol synthesis process from CO<sub>2</sub>-containing syngas developed by BASF was using the ZnO–Cr<sub>2</sub>O<sub>3</sub>-based catalysts. In the 1960s, changing feedstock from coal to naphtha/natural gas led to fewer impurities in the synthesis gas and ultimately resulted the introduction of highly selective copper-zinc oxide-alumina catalyst (Cu–ZnO–Al<sub>2</sub>O<sub>3</sub>) developed by ICI (Imperial Chemical Industries). Due to the greatly enhanced activity, the ternary catalyst required significantly milder reaction conditions of temperature and pressure. Since then, the research trend has been shifted to investigate Cu–ZnO-based materials (the two major components of the above catalyst), which resulted in a large number of publications on the theme. Although many catalyst materials with various compositions have been found active and selective for methanol synthesis from CO<sub>2</sub>, the Cu–ZnO system prepared by coprecipitation still remains the most investigated due to its high activity and high product selectivity besides economic advantages. Numerous reports and reviews describing the various material aspects of the methanol synthesis catalysts have been published. For example, Jadhav et al.<sup>125</sup> summarized the main catalytic features of Cu- and Pd-based catalysts. Liu et al.<sup>126</sup> reviewed the advances until 2003 for the methanol synthesis via hydrogenation of CO and CO<sub>2</sub> making special emphasis on metallic Cu as active phase and ZnO as active promoter. Wang et al.<sup>127</sup> reported the main features of Cu-based catalysts and focused on the methanol production from CO<sub>2</sub> as an environmental strategy. A highly concise review of R&D activities in Japan reflecting the global trends until 1998 was reported by Saito, covering the aspects of catalysts, reaction mechanisms, and processes including pilot plant scale operation of CO<sub>2</sub> hydrogenation to methanol.<sup>128</sup>

A walkthrough of research articles published in the past 10 years on CO<sub>2</sub> hydrogenation to methanol (ca. 200 publications to have an idea, not a complete list) shows that three main branches of catalyst families can be recognized (Figure 11).

The statistical breakdown shows that 79% of the reports published in the past 10 years on CO<sub>2</sub> hydrogenation to methanol describe catalysts based on Cu, followed by 11.5% based on Pd, and 9.5% on bimetallic systems. Among the 79% of

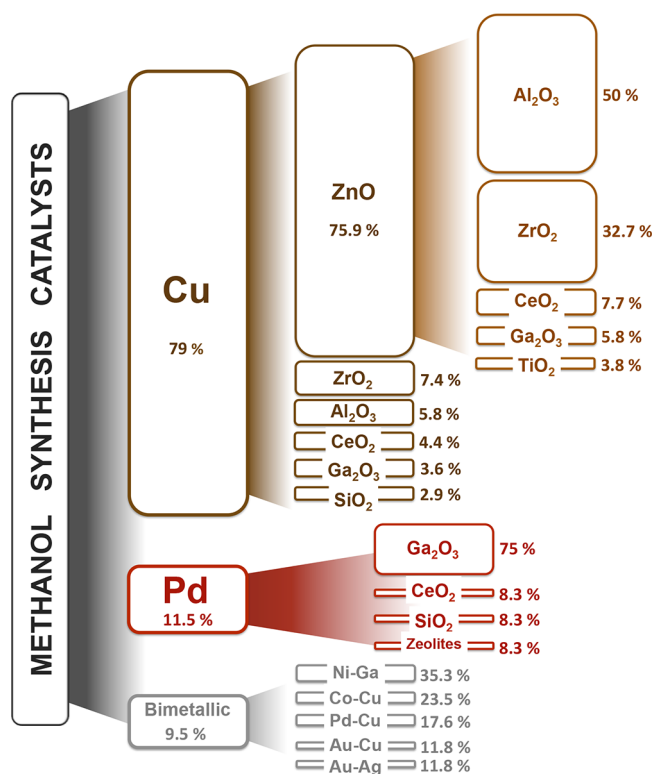


**Figure 11.** Types of catalyst material reported for CO<sub>2</sub> hydrogenation to methanol. The percentages have been calculated based on ca. 200 papers selected from a Scopus search from 2006 to 2016 on the principal catalyst materials.

the Cu-based catalysts, 75.9% deal with Cu–ZnO composites and, among these, the addition of Al<sub>2</sub>O<sub>3</sub> and ZrO<sub>2</sub> appears to be the most popular. For Pd-based catalysts, the most widely used support is Ga<sub>2</sub>O<sub>3</sub>, followed by CeO<sub>2</sub> and SiO<sub>2</sub>. For bimetallic catalysts, there is no chemical element combination that is prominently chosen. Several authors have investigated bimetallic Ni–Ga, Co–Cu, Pd–Cu, Au–Cu, and Au–Ag as effective couples in the CO<sub>2</sub> hydrogenation to methanol.

#### 5.2.1.1. Cu–ZnO-Based Catalysts.

Among the 92 naturally occurring elements in the Earth's crust, Cu is the 25th most abundant element, which makes the use of Cu in catalysis sustainable and economically attractive. This could be also a strong reason that, apart from its highly active nature, even almost after 60 years of the first introduction of the Cu–ZnO–Al<sub>2</sub>O<sub>3</sub> catalyst for methanol synthesis by ICI, today the Cu–ZnO combination remains the core of the industrial methanol synthesis catalysts.

Typically, commercial methanol synthesis catalysts (Cu–ZnO–Al<sub>2</sub>O<sub>3</sub>) are prepared by a coprecipitation and usually contain around 50–70 mol % of CuO, 20–50% ZnO, and 5–20% of Al<sub>2</sub>O<sub>3</sub>. Generally, these catalysts are calcined and reduced prior to the reaction in order to obtain specific Cu<sup>0</sup> surface areas (SA<sub>Cu</sub>) between 18–23 m<sup>2</sup>/g<sup>118</sup> (generally estimated by reactive N<sub>2</sub>O titration<sup>129</sup>). The high metal dispersion and high stability of this catalyst are due to the unique microstructure that is achieved after reduction, where ZnO nanoparticles act as spacers between the Cu<sup>0</sup> particles (Figure 12) and Al<sub>2</sub>O<sub>3</sub> enhances the thermal and chemical stability.<sup>130</sup> Frequently, the SA<sub>Cu</sub> has been directly related to the activity of Cu-based catalyst in CO<sub>2</sub> hydrogenation to methanol, but this relationship is not as direct in all the cases



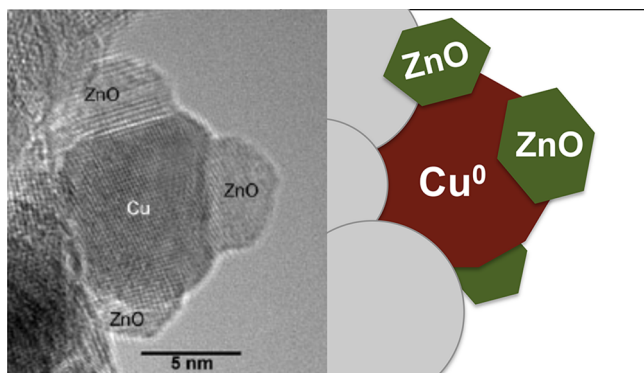


**Figure 12.** Microstructural features revealed by TEM of Cu–ZnO–Al<sub>2</sub>O<sub>3</sub> catalyst. Adapted with permission from ref 132. Copyright 2007 Wiley-VCH Verlag GmbH & Co. KGaA.

and is usually observed only for samples with similar preparation history.<sup>131</sup>

Besides the structural role of ZnO, it is widely reported that a peculiar solid-state interaction between ZnO and Cu is responsible for the outstanding activity presented by this type of catalysts. In 2016, Kuld et al.<sup>133</sup> reported how methanol synthesis from syngas over Cu<sup>0</sup> nanoparticles was boosted by Zn atoms migrating over the Cu surface. Also, Le Valant et al.<sup>134</sup> developed a mathematical model from Cu–ZnO core–shell nanoparticles that successfully related the number of contact points between Cu and ZnO with the observed catalytic activity. Generally, this Cu–ZnO synergy, where SA<sub>Cu</sub> is maximized and the Cu–ZnO interaction is enhanced, is often determined by and strictly related to the catalyst synthesis method.

Figure 13 shows the distribution of synthesis methods of Cu–ZnO-based catalysts found in the publications on CO<sub>2</sub>

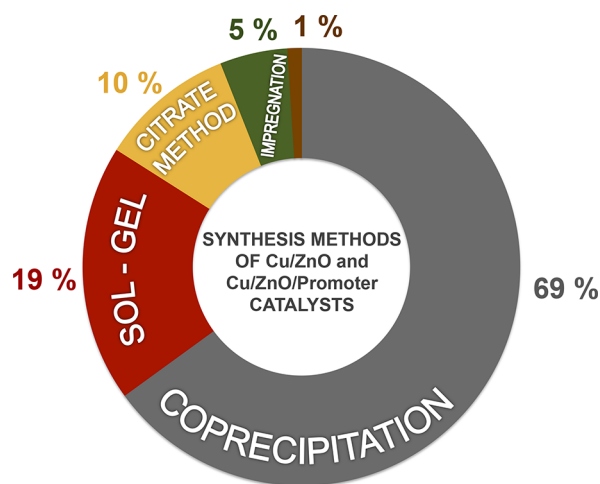


**Figure 13.** Synthesis methods of Cu–ZnO and Cu–ZnO–promoter catalysts. The percentage was calculated based on the publications over the past 10 years.

hydrogenation to methanol over the past 10 years. It clearly shows that coprecipitation is still the most widely used method of choice.

A coprecipitation process (Figure 14) can be described as the precipitation of metallic hydroxycarbonates or hydroxides by mixing a metal precursor solution (e.g., aqueous nitrates of Cu, Zn, and/or Al) with a solution containing a basic precipitating agent (e.g., carbonates, bicarbonates, or hydroxides). The order

of addition can differ; the two solutions can be added to the precipitation vessel, the base can be added to the metal salts, or vice versa. Since the structural and catalytic properties of the final catalyst are highly influenced by all the precipitation conditions, precise control of experimental parameters such as temperature and pH is required.

Precipitation is often followed by an aging period. Aging refers to the period of time in which the precipitate is left in its mother liquor typically under agitation. Several physicochemical processes take place during the aging. One of the most important ones is the crystallization of the freshly formed precipitates (usually amorphous) toward crystalline phases such as aurichalcite or zincian malachite. The solid-state chemistry of this step has been studied,<sup>135–138</sup> and zincian malachite has been reported as the ideal precursor to obtain highly active catalysts.<sup>138–141</sup> The conditions of aging and following processes, such as drying, calcining, and reduction treatment (the last one before the reaction), determine the microstructural properties of final catalyst.

Nevertheless, despite the fact that this synthesis method has been known for at least 60 years, no standard “recipe” has been identified, and several optimized conditions have been suggested since then. In 2008, Baltes et al.<sup>142</sup> prepared a ternary Cu–ZnO–Al<sub>2</sub>O<sub>3</sub> catalyst through a coprecipitation route. According to the study, the best catalytic performance was obtained when the precursors were precipitated at the pH of 6 to 8 at 70 °C followed by an aging time of 20–60 min and a final calcination at 300 °C. Fan et al.<sup>143</sup> reported the assistance of microwave (MW) irradiation in the coprecipitation and in the aging steps for the synthesis of Cu–ZnO–Al<sub>2</sub>O<sub>3</sub> catalysts. Their results on one hand showed that MW irradiation at the coprecipitation step could improve the activity of the catalyst, but not the stability. On the other hand, MW irradiation during aging showed great benefits in both activity and stability of the catalyst. Jung et al.<sup>144</sup> established that adjustment of the aging time could influence and optimize the final SA<sub>Cu</sub> of Cu–ZnO–Al<sub>2</sub>O<sub>3</sub> catalysts. Kühl et al.<sup>145</sup> employed a coprecipitation method to prepare a pure phase of Cu, Zn, Al hydrotalcite as the precursor of a very active catalyst. The authors described the calcined catalyst as well-dispersed “CuO” within ZnAl<sub>2</sub>O<sub>4</sub> matrix. Due to the strong interaction of Cu and the oxide matrix, the small Cu particles (7 nm) of this catalyst were partially embedded, leading to lower catalytic activity. However, the intrinsic activity (normalized against the Cu surface area) was superior compared with a conventionally prepared reference catalyst.

Furthermore, Behrens et al.<sup>137</sup> demonstrated how the catalytic activity of Cu–ZnO–Al<sub>2</sub>O<sub>3</sub> catalyst could be further improved by the optimization of ZnO and Al<sub>2</sub>O<sub>3</sub> components. They synthesized novel Cu–ZnO–Al<sub>2</sub>O<sub>3</sub> catalysts by varying the precipitating agent and a direct spray-drying of the fresh precipitate suspension without the aging phase. Not only the SA<sub>Cu</sub> but also the Cu–oxide interface played decisive roles in the activity of this type of catalyst. Besides these studies, several other authors have reported improvements in the coprecipitation procedure toward a more “eco-friendly” one. As described before, the precipitation of the Cu–Zn precursors is commonly done by mixing the metal nitrates with a precipitation agent, for which Na<sub>2</sub>CO<sub>3</sub> is commonly used. However, the presence of residues, such as nitrates or Na during the calcination of the precursors, promotes Cu agglomeration and, thereby, decreases the final metal dispersion, leading to a loss in the catalytic performance.<sup>146</sup> To overcome this problem, the prepared catalyst precursors are extensively washed with water in order



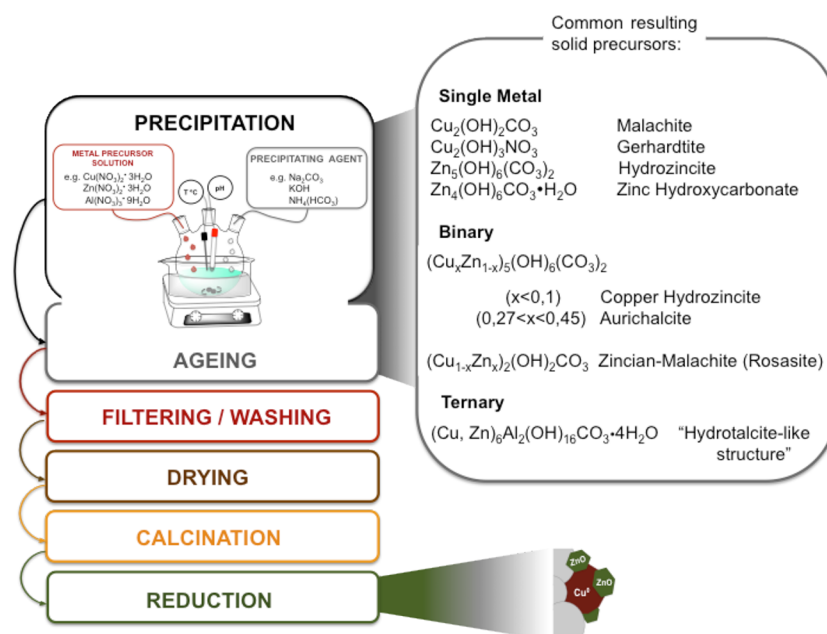


**Figure 14.** Simplified preparation procedure of Cu–ZnO or Cu–ZnO–Al<sub>2</sub>O<sub>3</sub> via coprecipitation with widely used chemicals and resulting solid precursor phases.

to remove nitrates and sodium species before the thermal treatments. In order to avoid the washing treatment, Behrens et al.<sup>147</sup> reported the synthesis of mixed basic formates  $(\text{Cu}_{1-x}\text{Zn}_x)_2(\text{OH})_3\text{HCO}_2$  by coprecipitation from Cu and Zn formate solutions leading to a nitrate-free mother liquor. In another study, Prieto et al.<sup>146</sup> reported the successful synthesis of a highly active catalyst by coprecipitation of Cu and Zn nitrates with  $(\text{NH}_4)\text{HCO}_3$  rather than  $\text{Na}_2\text{CO}_3$ . The modification of the precipitating agent resulted in Na-free hydroxycarbonate precursors, and hence washing treatment could be skipped.

In addition to coprecipitation, several other catalyst synthesis methods have been reported. Wang et al.<sup>148</sup> prepared a Cu–ZnO–Al<sub>2</sub>O<sub>3</sub> catalyst by the DMAC method (decomposition of metal ammonia complexes) under subatmospheric pressure at various temperatures. The precursor prepared at 70 °C was rich in the aurichalcite phase, and this enrichment improved Cu dispersion and catalytic activity. Kondrat et al.<sup>149</sup> reported the synthesis of georgeite, an amorphous form of malachite, as a stable amorphous precursor for a high activity catalyst. The precursor was synthesized by supercritical antisolvent (SAS) precipitation resulting in low amounts of Na and an interesting microstructure. Its calcination yielded a complex mixture of CuO and exceptionally small disordered ZnO with notable interactions between Cu and ZnO after reduction. The catalytic performance of selected materials described above is compared in Table 3.

**5.2.1.2. Cu-Based Catalysts Containing Other Metal/Metal Oxide Components.** Despite the good fame of Cu–ZnO–Al<sub>2</sub>O<sub>3</sub> catalysts, unsatisfactory CO<sub>2</sub> hydrogenation performance has been attributed to the presence of water combined with the strong hydrophilic character of alumina.<sup>150,151</sup> In order to address this issue, the addition of less hydrophilic promoters, like ZrO<sub>2</sub>, has been proposed. Wambach et al.<sup>152</sup> reviewed the CO<sub>2</sub> hydrogenation over various metal/zirconia catalysts. Several catalyst preparation methods were addressed, and a large influence of the interface between the metal and the zirconia was remarked. Raudaskoski et al.<sup>153</sup> reviewed some Cu-based zirconia catalysts for methanol synthesis. They described how the

addition of ZrO<sub>2</sub> to Cu catalyst enhanced Cu dispersion improving the activity and selectivity toward methanol. Frei et al.<sup>154</sup> studied the influence of the temperature during the precipitation and aging in the coprecipitation of a Cu–ZnO–ZrO<sub>2</sub> catalyst. High temperature (70 °C) in the precipitation step increased the crystallinity of the sample, however, the catalyst precipitated at room temperature showed better catalytic activity. Curiously, they also reported that the typical aurichalcite/malachite phases and structural peculiarities known for the Cu–ZnO system were observed in the presence of zirconia. Li et al.<sup>155</sup> synthesized a series of CuO–ZnO–ZrO<sub>2</sub> catalysts by a surfactant-assisted coprecipitation method. The solid prepared by this new method showed higher methanol selectivity than the conventional one prepared by coprecipitation. This higher selectivity was attributed to the enhanced Cu–Zn and Cu–Zr interaction. In 2014, Samson et al.<sup>156</sup> reported that the final activity of the catalyst was highly dependent on the crystallographic structure of ZrO<sub>2</sub>. The tetrahedral phase was found more beneficial since complexes formed on the tetragonal ZrO<sub>2</sub> phase and Cu<sup>+</sup> cations were identified as acidic centers active in methanol synthesis. This finding was in disagreement with that of Witton et al.,<sup>157</sup> who reported higher methanol yields when Cu was impregnated over an amorphous ZrO<sub>2</sub>.

Addition of ZrO<sub>2</sub> to Cu-based ternary catalysts has also been reported. Xiao et al.<sup>151</sup> described the synthesis of a quaternary Cu–ZnO–ZrO<sub>2</sub>–TiO<sub>2</sub> catalyst through the oxalate coprecipitation method. They found that the methanol yield increased with the addition of promoters, and the highest methanol productivity was achieved when both promoters (Zr and Ti) were added. They explained that the addition of Zr and Ti led to a decrease in crystallite size of CuO and ZnO, increasing SA<sub>Cu</sub> and thus the Cu–ZnO interaction. Angelo et al.<sup>158</sup> synthesized Cu–ZnO–Al<sub>2</sub>O<sub>3</sub> promoted with ZrO<sub>2</sub> and CeO<sub>2</sub> by sol–gel and coprecipitation methods. The best results were obtained with the ZrO<sub>2</sub> promoted catalyst prepared by coprecipitation. The addition of CeO<sub>2</sub> did not bring any benefit to the catalyst, and the copper dispersion was much lower.

Table 3. Catalytic Performance of Selected Catalysts in CO<sub>2</sub> Hydrogenation to Methanol in the Past 10 Years

|  | reaction conditions          |   |  | catalytic performance              |                                      |  |   | ref |
|--|------------------------------|---|--|------------------------------------|--------------------------------------|--|---|-----|
|  | temp (°C),<br>pressure (bar) | space velocity                                | H <sub>2</sub> /CO <sub>2</sub>                                | X <sub>CO<sub>2</sub></sub><br>(%) | S <sub>CH<sub>3</sub>OH</sub><br>(%) | Y <sub>CH<sub>3</sub>OH</sub><br>(g <sub>cat</sub> <sup>-1</sup> h <sup>-1</sup> ) | SA <sub>Cu</sub><br>(m <sup>2</sup> g <sup>-1</sup> ) |     |
| Cu–ZnO–Al <sub>2</sub> O <sub>3</sub> , coprecipitation  | 260, 331                     | (G) <sup>a</sup> 182,000 h <sup>-1</sup>      | 10   | 65.8                               | 77.3                                 | 7.73   | 17.5  | 118 |
| Cu–ZnO–Al <sub>2</sub> O <sub>3</sub> , coprecipitation  | 260, 331                     | (G) 20,000 h <sup>-1</sup>                    | 10   | 95.7                               | 98.2                                 | 1.58   | 17.5  | 118 |
| Cu–ZnO–Al <sub>2</sub> O <sub>3</sub> , coprecipitation  | 280, 442                     | (G) 100,000 h <sup>-1</sup>                   | 3  | 65.3                               | 91.9                                 | 15.2   | 17.5  | 115 |
| Cu(core)ZnO(shell), core–shell   | 250, 30                      | (W) 18,000 mL g <sup>-1</sup> h <sup>-1</sup> | 3  | 2.3                                | 100                                  | 0.147  |   | 134 |
| Cu–ZnO–Al <sub>2</sub> O <sub>3</sub> coprecipitation + MW   | 240, 40                      | (W) 1,620 mL g <sup>-1</sup> h <sup>-1</sup>  | CO/CO <sub>2</sub> /H <sub>2</sub> = 24/5/68 + He              |                                    | 99.4                                 | 0.312  |   | 143 |
| Cu–ZnO–Al <sub>2</sub> O <sub>3</sub> coprecipitation  | 245, 45                      | (W) 4,000 mL g <sup>-1</sup> h <sup>-1</sup>  | CO/CO <sub>2</sub> /H <sub>2</sub> = 24/6/70                   |                                    |                                      | 1.6  | 28  | 142 |
| Cu–ZnO, SAS precipitation  | 235, 25                      | (W) 7,200 mL g <sup>-1</sup> h <sup>-1</sup>  | CO/CO <sub>2</sub> /H <sub>2</sub> = 6/9.2/67 + N <sub>2</sub> |                                    |                                      | 0.32   | 53  | 149 |
| Cu–ZnO–ZrO <sub>2</sub> , coprecipitation + US   | 200, 10                      | (W) 4,400 mL g <sup>-1</sup> h <sup>-1</sup>  | 3  | 5.8                                | 55.2                                 | 0.049  | 63  | 150 |
| Cu–ZnO–ZrO <sub>2</sub> , coprecipitation  | 230, 30                      | (W) 3,000 mL g <sup>-1</sup> h <sup>-1</sup>  | 3  | 15.2                               | 35.1                                 |  |   | 153 |
| Cu–ZnO–ZrO <sub>2</sub> , coprecipitation  | 240, 40                      | (G) 4,000 h <sup>-1</sup>                     | 3  |                                    |                                      | 0.293  | 29  | 154 |
| Cu–ZnO–ZrO <sub>2</sub> , surfactant assisted coprecipitation  | 240, 30                      | (G) 3,600 h <sup>-1</sup>                     | 3  | 12.1                               | 54.1                                 | 6.5%   | 3.2   | 155 |
| Cu/ZrO <sub>2</sub> , impregnation   | 280, 30                      | (W) 7,200 mL g <sup>-1</sup> h <sup>-1</sup>  | 3  | 12                                 | 32                                   | 0.09   | 7.8   | 157 |
| Cu–ZnO–ZrO <sub>2</sub> , coprecipitation  | 280, 50                      | (G) 10,000 h <sup>-1</sup>                    | 3  | 23                                 | 33                                   | 0.33   | 12.7  | 158 |
| Cu–Ga <sub>2</sub> O <sub>3</sub> –ZrO <sub>2</sub> , solid state reaction + deposition–coprecipitation                | 250, 20                      | (G) 2,500 h <sup>-1</sup>                     | 3  | 13.7                               | 75.6                                 | 0.061  |   | 183 |
| Cu/Ga <sub>2</sub> O <sub>3</sub> /ZrO <sub>2</sub> , ZrO <sub>2</sub> support + Cu (ion exchange) + Ga (impregnation) | 250, 30                      | (G) 20,000 h <sup>-1</sup>                    | 3.4  | 1.3                                | 74                                   | 0.162  |   | 160 |
| Cu/Al <sub>2</sub> O <sub>3</sub> , impregnation   | 280, 950                     | (G) ~12,000 h <sup>-1</sup>                   | 4  | 30                                 | 80                                   | 0.32   | 2.2   | 184 |
| La <sub>0.8</sub> Zr <sub>0.2</sub> Cu <sub>0.7</sub> Zn <sub>0.3</sub> O <sub>x</sub> , sol–gel                       | 250, 50                      | (G) 3,600 h <sup>-1</sup>                     | 3  | 12.6                               | 52.5                                 | 0.10   | 6.5   | 185 |
| Cu–ZnO–ZrO <sub>2</sub> , microfluidic continuous coprecipitation  | 280, 50                      | (G) 10,000 h <sup>-1</sup>                    | 4  | 21                                 | 34                                   | 0.49   | 14.5  | 186 |
| Pd–Cu/SiO <sub>2</sub> , impregnation  | 300, 41                      | (W) 3,600 mL g <sup>-1</sup> h <sup>-1</sup>  | 3  | 6.6                                | 34                                   | 0.04   |   | 151 |
| Pd/ZnO, sol-immobilization   | 250, 20                      | (G) ~1,000 h <sup>-1</sup>                    | 3  | 10.7                               | 60                                   | 0.08   |   | 171 |
| In <sub>2</sub> O <sub>3</sub> /ZrO <sub>2</sub> , impregnation  | 300, 50                      | (G) 16,000 h <sup>-1</sup>                    | 4  | 5.2                                | 99.8                                 | 0.29   |   | 178 |
| Pd/ZnO–Al <sub>2</sub> O <sub>3</sub> , deposition–precipitation   | 180, 30                      | (W) 3,600 mL g <sup>-1</sup> h <sup>-1</sup>  | 3  | 2.9                                | 79.4                                 | 2.3%   |   | 172 |
| Au/Cu–ZnO–Al <sub>2</sub> O <sub>3</sub> , coprecipitation and deposition precipitation                                | 260, 40                      | (G) 70,000 h <sup>-1</sup>                    | 6  | 28                                 | 55                                   | 16.6%  |   | 176 |
| Au/ZnO, deposition–precipitation   | 240, 50                      | (G) 7,200 h <sup>-1</sup>                     | 3  | 1                                  | 70                                   | 0.023/g Au   |   | 175 |

<sup>a</sup>(G) = GHSV = volume flow rate/bed volume, (W) = WHSV = mass flow rate/catalyst mass.

Other metal oxides like CeO<sub>2</sub> and Ga<sub>2</sub>O<sub>3</sub> have also been reported to be beneficial in terms of activity and stability as support and promoter of Cu-based catalysts. Graciani et al.<sup>159</sup> presented theoretical and experimental evidence of a new site for the activation of CO<sub>2</sub> by the copper–ceria interface. The rate of methanol production on CeO<sub>x</sub>/Cu(111) was 200 times higher than that on Cu(111) and 14 times higher than that on Cu–ZnO. Recently, Fornero et al.<sup>160</sup> reported the synthesis of a ternary Cu/Ga<sub>2</sub>O<sub>3</sub>/ZrO<sub>2</sub> catalyst. They concluded that the ternary mixture performed better than that of the comparative binary Cu–ZrO<sub>2</sub> and Cu–Ga<sub>2</sub>O<sub>3</sub> catalysts. Importantly, better catalytic activity could be attained when the following conditions were met: ZrO<sub>2</sub> (dried and calcined) was used as the base support, Cu was incorporated by ion exchange, and then Ga was added by incipient wetness impregnation. The catalytic performance of selected materials described above is compared in Table 3.

**5.2.1.3. Pd-Based Catalysts.** First reports on the use of Pd-based catalysts for methanol synthesis can be traced back in the early studies of CO hydrogenation.<sup>161,162</sup> Simultaneously,

researchers have also reported a good activity of this type of catalyst in the hydrogenation of CO<sub>2</sub>. Fujitani et al.<sup>163</sup> were the first to report the use of a coprecipitated Pd–Ga<sub>2</sub>O<sub>3</sub>-based catalyst for the hydrogenation of CO<sub>2</sub> to methanol as an alternative to Cu–ZnO catalyst. More recently, Collins et al.<sup>164</sup> investigated the interaction of CO<sub>2</sub> and H<sub>2</sub>/CO<sub>2</sub> over an impregnated Pd/ $\beta$ -Ga<sub>2</sub>O<sub>3</sub> catalyst. They proposed that the addition of Pd to the oxide support increases the hydrogenation rate of all the carbon-containing species bound to the  $\beta$ -Ga<sub>2</sub>O<sub>3</sub> surface by spillover of atomic hydrogen from metallic Pd to Ga<sub>2</sub>O<sub>3</sub>. Further studies<sup>165,166</sup> on Ga<sub>2</sub>O<sub>3</sub>-promoted Pd/SiO<sub>2</sub> catalyst similarly revealed that atomic hydrogen can be generated by Pd<sup>0</sup> far away from Ga<sub>2</sub>O<sub>3</sub> and spills over on Ga<sub>2</sub>O<sub>3</sub> to reach the other reactive species (formates) to complete the reaction cycle. Chiavassa et al.<sup>167</sup> reported that the synthesis of methanol from CO<sub>2</sub> and H<sub>2</sub> by this type of catalysts is strongly influenced by the formed intermediates. At high conversions using ternary H<sub>2</sub>/CO<sub>2</sub>/CO mixtures, the surface CO competes with hydrogen on the Pd crystallites, thus severely limiting the availability of atomic hydrogen spilling-over to Ga<sub>2</sub>O<sub>3</sub> surface. Oyola-Rivera et al.<sup>168</sup>

reported the production of methanol and DME using Pd catalysts supported on different  $\text{Ga}_2\text{O}_3$  polymorphs. Higher catalytic activity in methanol synthesis was observed at a larger amount of  $\text{Pd}_2\text{Ga}$  intermetallic compounds; however, the selectivity toward DME was found to be rather dependent on the catalyst acidity but not on the  $\text{Pd}_2\text{Ga}$  content because of the consecutive nature of DME formation from methanol as will be discussed later.

Besides the combination of Pd and Ga, there are other reports on the catalysts containing Pd. Koizumi et al.<sup>169</sup> reported that supported Pd catalysts for  $\text{CO}_2$  hydrogenation could be improved by two different strategies: First, the use of uniform mesoporous supports (MCM-41, SBA-15) for better Pd dispersion, and second, the use of alkali/alkaline earth metal additives. Jiang et al.<sup>151</sup> reported a novel Pd–Cu bimetallic catalyst with a strong synergistic effect on promoting methanol formation when both metals were supported on  $\text{SiO}_2$ . J. Díez-Ramírez et al.<sup>170</sup> studied the influence of metal precursors on the performance of a supported Pd/ZnO catalyst. The authors reported that the use of tetraamminepalladium(II) nitrate led to Pd sintering during reduction, hindering the formation of PdZn alloy particles and thus resulting in low catalytic activity. These authors also studied the influence of the reduction temperature and observed that higher reduction temperatures led to the formation of more PdZn alloy particles that were directly related to a major conversion of  $\text{CO}_2$  and  $\text{H}_2$  to methanol. The importance of the PdZn alloy was also confirmed by Bahruji et al.<sup>171</sup> and Xu et al.<sup>172</sup>

**5.2.1.4. Bimetallic Catalysts and Others.** Other than Cu- and Pd-based systems, other metal-based and metal oxide based catalysts have been examined for the synthesis of methanol by  $\text{CO}_2$  hydrogenation. Co<sup>173</sup> and CoPt<sup>174</sup> bimetallic catalysts have been reported by Malaet et al. and Alayogou et al., respectively. The catalytic activity for  $\text{CO}_2$  hydrogenation was found low (around 5%  $\text{CO}_2$  conversion), and the major products obtained in the reaction were CO and  $\text{CH}_4$  as expected for these metals.

Recently, Hartadi et al.<sup>175</sup> reported a couple of studies on Au/ZnO catalysts. Kinetic measurements revealed that Au/ZnO catalysts showed similar formation rates of and superior selectivity to methanol compared to Cu–ZnO– $\text{Al}_2\text{O}_3$  over a wide range of reaction pressures. Additionally, isotopic labeling experiments showed that when using these catalysts, a shift in the preferred carbon source for methanol synthesis from  $\text{CO}_2$  to CO was observed with increasing reaction temperatures. The influence of gold in the conventional Cu–ZnO– $\text{Al}_2\text{O}_3$  catalyst has also been studied. Pasupulety et al.<sup>176</sup> reported a positive influence of 1% of Au on a coprecipitated Cu–ZnO– $\text{Al}_2\text{O}_3$  catalyst. The authors emphasized that the hydrogen spillover and enhanced adsorption capacities for CO and  $\text{H}_2$  at the Cu–Au interface increased the  $\text{CO}_2$  conversion and methanol yield. Sharafutdinov et al.<sup>177</sup> reported intermetallic compounds of Ni and Ga as catalysts for methanol synthesis reaction. The catalytic properties of the Ni–Ga materials were dependent on the type of intermetallic compound formed. The  $\text{Ni}_2\text{Ga}_3/\text{SiO}_2$  solid was reported as the most active and stable in  $\text{CO}_2$  hydrogenation.<sup>177</sup> In another recent study of 2016, Martin et al.<sup>178</sup> reported a highly active and methanol selective  $\text{In}_2\text{O}_3$  catalyst supported on  $\text{ZrO}_2$  with remarkable stability. The high methanol selectivity and stability of the catalyst was attributed to the reaction mechanism based on the creation and annihilation of oxygen vacancies as active sites. The amount of oxygen vacancies could be modulated by cofeeding CO and boosted through the electronic interactions

with the zirconia. The catalytic performance of the materials described above is compared in Table 3.

**5.2.2. Catalysts for the Direct Hydrogenation of  $\text{CO}_2$  to DME.** Direct transformation of  $\text{CO}_2$  to DME involves a bifunctional catalyst capable of performing two reactions, methanol synthesis and methanol dehydration, simultaneously. Often termed as “hybrid”, the active elements of these bifunctional catalysts inherently include a component active in the methanol synthesis, which is the preceding reaction in this process, while the methanol dehydration functionality of this hybrid catalyst relies on the solid acid catalyst component such as  $\gamma\text{-Al}_2\text{O}_3$  and H-ZSM-5. The notation “//” is used to indicate the formula of catalysts containing these two functions. The use of hybrid catalysts was initially investigated and practiced for direct conversion of syngas to DME. Similar to the methanol synthesis reaction, the hybrid catalysts developed for the syngas-to-DME/gasoline conversion are also known to be active for  $\text{CO}_2$  hydrogenation to DME.<sup>179–181</sup>

The two functions, namely, methanol synthesis and methanol dehydration, of a hybrid catalyst can be combined mainly in two ways, similarly as in the gas-to-liquid process.<sup>182</sup> The first one is a *physical mixture* where a methanol synthesis catalyst and a solid acid catalyst are simply mixed together, thus the functions of the two reactions are spatially well separated. The second one is an *integrated mixture* where the catalytically active components for the two reactions are intentionally placed in closest vicinity with the aim to facilitate the target synthesis of DME. For the first type of hybrid catalyst, how the two catalysts are placed in a reactor has a substantial influence on the catalytic performance.

**5.2.2.1. Physically Mixed Hybrid Catalysts.** As the name implies, physically mixed hybrid catalysts are prepared by mixing the two catalysts using dry powder mixing or grinding or in some cases by mixing in an aqueous solution and its subsequent thermal treatment. The characteristic of the physically mixed hybrid catalyst is that both functions, methanol synthesis and methanol dehydration, are preformed before the mixing procedure.

Being acidic in nature and with relatively high surface area,  $\gamma$ -alumina is a widely suggested candidate for methanol dehydration reaction; however, as reported by Xu et al.<sup>187</sup> the presence of water has a strong inhibiting effect on the activity of  $\gamma$ -alumina. The amount of water produced in  $\text{CO}_2$  hydrogenation is significantly substantial in comparison to that of CO hydrogenation as evident from eqs 3 and 5. It is believed that water competes with methanol for its adsorption on the catalyst surface and blocks the active sites responsible for the methanol dehydration step.<sup>188</sup> Hence, one of the required properties for solid acid catalyst in this reaction could be a higher tolerance toward the water presence. Nevertheless, the physical mixture of  $\gamma$ -alumina as solid acid catalyst with  $\text{Ga}_2\text{O}_3$  or  $\text{Cr}_2\text{O}_3$  promoted Cu–ZnO methanol synthesis catalyst was reported for the direct DME synthesis.<sup>189</sup> The addition of  $\text{Ga}_2\text{O}_3$  increased the number of active sites, whereas the role of  $\text{Cr}_2\text{O}_3$  was highly remarkable in increasing intrinsic activity toward DME and methanol synthesis.

H-ZSM-5 zeolite, having both Lewis and comparatively more and stronger Brønsted acid sites than  $\gamma$ -alumina,<sup>190,191</sup> showed high activity<sup>192</sup> and excellent water resistance, improving long-term stability during the reaction.<sup>187</sup> Aguayo et al.<sup>188</sup> investigated the deactivation behavior of Cu–ZnO– $\text{Al}_2\text{O}_3$ //NaH-ZSM-5 and Cu–ZnO– $\text{Al}_2\text{O}_3$ // $\gamma\text{-Al}_2\text{O}_3$  hybrid catalysts. The catalyst was prepared by physically mixing methanol synthesis catalyst with methanol dehydration catalyst in an aqueous solution, which was dried subsequently in two steps. Curiously, the



catalyst with NaH-ZSM-5 as a solid acid component was less prone to deactivation by coke when water was present in the feed and totally recovers its catalytic performance (21% yield and 48% selectivity of DME) even after 10 reaction–regeneration cycles. The coke combustion method was used for the regeneration process, where the combustion was carried out at 260 °C with a mixture of air and He.

Due to high catalytic activity and stability of zeolite-based catalysts over other solid acid catalysts, several types of zeolites with different types of methanol synthesis catalysts have been evaluated. The combinations of Cu–ZnO–ZrO<sub>2</sub> or Cu–ZnO–Ga<sub>2</sub>O<sub>3</sub> as methanol synthesis catalyst and Na-ZSM-5, H-ZSM-5, H-Ga-silicate, or SAPO-34 zeolites were studied extensively by several researchers.<sup>193–195</sup> In conjunction with Cu–ZnO–ZrO<sub>2</sub> methanol synthesis catalyst, H-ZSM-5 showed very high DME (60.1%) selectivity at 35% CO<sub>2</sub> conversion,<sup>194</sup> while H-Ga-silicate showed 45% DME selectivity at 19% CO<sub>2</sub> conversion,<sup>193</sup> confirming the superior performance of H-ZSM-5 in the physically mixed state. It is important to note that the given catalytic activity values are merely performance-indicative and cannot be compared directly due to different reaction conditions used in the literature reports.

Less common chemical elements and materials have also been reported for the promotion of methanol synthesis catalyst and/or ZSM-5 as methanol dehydration catalyst. Superior catalytic performance was observed with La-promoted-Cu–ZnO–Al<sub>2</sub>O<sub>3</sub>/H-ZSM-5 bifunctional catalyst system yielding 71% DME selectivity at 43.8% CO<sub>2</sub> conversion. The addition of La had an effect on the strength of the acid sites, and this effect was maximized at 2% of La loading.<sup>196</sup> Also, addition of Zr as a structural promoter to Cu–ZnO–Al<sub>2</sub>O<sub>3</sub>/H-ZSM-5 bifunctional system was examined, leading to a slight improvement in catalytic activity.<sup>197</sup> In another study, the doping of Zr to Cu–Fe<sub>2</sub>O<sub>3</sub>/H-ZSM-5 system was evaluated and the presence of Zr affected the outer-shell electron density of Cu<sup>2+</sup>, the specific surface area, and the reducing behavior of CuO species. These property changes were concluded to be responsible for the enhanced catalytic activity toward DME.<sup>198</sup> Similarly, Wang et al.<sup>199</sup> reported that the reducibility of copper in methanol synthesis catalyst has a strong impact on DME yield. They examined various Ti/Zr molar ratios in Cu–TiO<sub>2</sub>–ZrO<sub>2</sub>/H-ZSM-5 to modulate the reducibility of copper. At a Ti/Zr molar ratio of 1, the first reduction peak of Cu was shifted to lower temperatures, leading to superior catalytic activity toward DME synthesis.<sup>199</sup> However, the relation between the reducibility of Cu and reaction mechanism leading to DME formation has not been clarified. In other studies, the promoting effects of carbon nanotubes (CNT) and multiwalled carbon nanotubes (MWCNT) in the one-step synthesis of DME have been reported. Addition of small amounts of Pd-decorated CNT, prepared by impregnation, to Cu–ZrO/H-ZSM-5 improved the adsorption performance of the catalyst for H<sub>2</sub> and CO<sub>2</sub>, thus ultimately increasing the rate of the surface hydrogenation reactions.<sup>200</sup> Also, the catalytic activity could be enhanced using Cu–ZnO–Al<sub>2</sub>O<sub>3</sub>/H-ZSM-5 hybrid catalyst supported over acid-treated MWCNT.<sup>201</sup>

Dubois et al.<sup>105</sup> reported several combinations of physically mixed Cu–ZnO–Al<sub>2</sub>O<sub>3</sub> and different solid acid catalysts. In their study, zeolites, particularly Y-zeolite (SiO<sub>2</sub>/Al<sub>2</sub>O<sub>3</sub> = 6) and mordenite (SiO<sub>2</sub>/Al<sub>2</sub>O<sub>3</sub> = 10), were proved to be efficient to achieve high DME selectivity and high yield of methanol and DME. Among a class of Y-zeolites as a methanol dehydration catalyst in physically mixed state with Cu–ZnO–Cr<sub>2</sub>O<sub>3</sub>, CuNaY

zeolite was the most promising catalyst owing to the presence of higher number of moderate acid sites, whereas NaY with only weak acid sites was not effective in DME synthesis.<sup>189</sup>

Apart from zeolites as solid acid catalyst, sulfated zirconia was also found to be active for DME synthesis. The physical mixture of sulfated zirconia and Cu–ZnO–ZrO<sub>2</sub> was able to produce DME due to the increased Brønsted acidity generated by protonated sulfate species.<sup>202</sup> However, the CO<sub>2</sub> conversion and DME yield were less than 4%, rendering the hybrids with zeolites the most promising option at present as physically mixed hybrid catalyst.

**5.2.2.2. Integrated Hybrid Catalyst.** An integrated catalyst is commonly prepared in a single pot synthesis and exhibits the catalytic functions for the two reactions by the distinct active sites residing in spatial proximity to promote the DME synthesis. It could be prepared by adding the methanol synthesis function over/in the presence of the solid acid catalyst, e.g., by precipitation method or by forming a new functionality to perform both functions. Typically, one of the functions is preformed and generally a solid acid catalyst is incorporated for the dehydration reaction.

One of the first examples of such integrated catalysts is the study reported by Naito et al. in 1972.<sup>203</sup> They reported the use of transition-metal chlorides (PdCl<sub>3</sub>, RhCl<sub>3</sub>, IrCl<sub>3</sub>, OsCl<sub>3</sub>, CoCl<sub>2</sub>, and FeCl<sub>3</sub>) in combination with graphite and sodium as a catalyst for direct DME synthesis. Although the details are not shown and the catalytic functionality of each component is not clear, PdCl<sub>3</sub>-based catalyst (graphite–PdCl<sub>3</sub>–Na) was found most effective for DME synthesis.

The combination of the most popular Cu-based methanol synthesis catalyst and ZSM-5-based solid acid catalyst has been studied using the approach of integrated catalyst design.<sup>204</sup> Low-temperature (200 °C) synthesis of DME over Pd-modified Cu–ZnO–Al<sub>2</sub>O<sub>3</sub>–ZrO<sub>2</sub>/H-ZSM-5 catalysts prepared by coprecipitating sedimentation method indicated that the addition of Pd strongly enhanced the DME production due to the promoted spillover of hydrogen from Pd<sup>0</sup> to the neighboring active phase.<sup>205</sup> A slight increase in DME yield (19.1%) was achieved by Cu–ZnO–ZrO<sub>2</sub>/H-ZSM-5 when promoted with V, in comparison to 15.9% DME yield for the unpromoted catalyst. V promotion aided to balance a proper acid amount and distribution, thereby improving the catalytic performance.<sup>206</sup> Addition of a small amount of Mo to Cu/H-ZSM-5 (Mo/Cu = 1/2 wt) markedly enhanced the catalytic activity toward DME synthesis by creating new adsorption sites and thus the density of the surface species to increase CO<sub>2</sub> hydrogenation rate.<sup>207</sup> Li et al.<sup>208</sup> developed a novel synthesis method to prepare a hybrid catalyst composed of CuO–ZnO as a core and H-ZSM-5 as a shell layer. The high catalytic activity of core–shell hybrid catalyst was mainly attributed to the orderly self-assembly of core–shell structure, which could optimize the reactant diffusion path and enhance the reaction rate. Similar to core–shell structure, H-ZSM-5 as shell and Cu–ZnO–Al<sub>2</sub>O<sub>3</sub> as a core type capsule catalyst was synthesized and tested in the reaction, exhibiting a good DME selectivity over the conventional hybrid catalyst.<sup>209</sup>

As integrated hybrid catalyst using  $\gamma$ -Al<sub>2</sub>O<sub>3</sub> as solid acid catalyst, Wang and Zeng investigated the effect of Al<sub>2</sub>O<sub>3</sub> content in Cu–ZnO–Al<sub>2</sub>O<sub>3</sub>–SiO<sub>2</sub> catalyst prepared by a pseudo sol–gel technique.<sup>210</sup> Al<sub>2</sub>O<sub>3</sub> incorporated in the SiO<sub>2</sub> structure presumably formed acid–base sites responsibly for the DME formation. The better synergistic effect between methanol



forming active sites and methanol dehydration active sites was found at 4 wt %  $\text{Al}_2\text{O}_3$  loading.

**5.2.2.3. Catalyst Bed Configuration.** The advantage of physically mixed hybrid catalysts is the ability to configure the two catalysts in different manners (e.g., pelleting and packing) in fixed bed continuous flow reactor. Many researchers have studied different approaches and their impact on catalytic performance.<sup>118,195,211,212</sup> Summarizing, there are three configurations (Figure 15): (1) methanol synthesis catalyst and solid acid

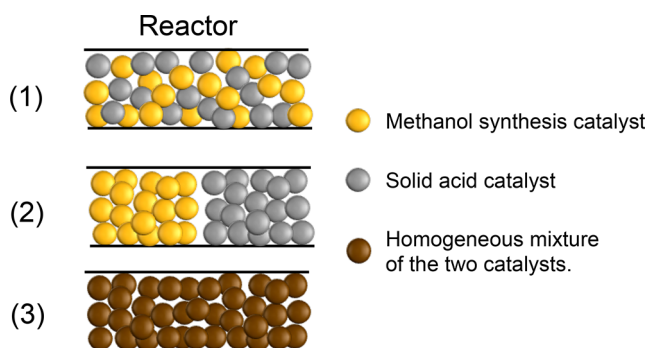


**Figure 15.** Reported bed configurations of physically mixed catalysts in a fixed bed reactor.

catalyst are pelletized separately and placed in a well-mixed manner; (2) the pellets of the two catalysts are placed sequentially, with the methanol synthesis catalyst being the first; (3) a homogeneous solid mixture of two catalysts, prepared by grinding mixing and pelletization and placed in reactor.

Each configuration type has its own characteristics and unique effects on the catalytic performance. Bonura et al.<sup>195,211</sup> investigated the catalytic behavior of a hybrid  $\text{Cu-ZnO-ZrO}_2/\text{H-ZSM5}$  system with different configurations of catalyst bed. They found that configuration 1 prepared by physical mixing of prepelletized catalysts exhibited superior catalytic performance, whereas configuration 2, where two catalyst beds were placed sequentially, did not show any catalytic advantage. The same observation was confirmed in the direct transformation of  $\text{CO}_2$  and  $\text{H}_2$  to DME under high-pressure reaction conditions (331 bar).<sup>118</sup> Therein, a similar level of catalytic performance was reported using the sequential bed of configuration 2 due to the methanol conversion level at thermodynamic equilibrium.<sup>118</sup> The advantages of configuration 2 are the ability to vary the temperature of the two catalyst beds independent of each other and ease in catalyst recovery, refilling, and regeneration in case the catalyst deactivates (e.g., solid acid catalyst). Interestingly, configuration 3 leads to poorer catalytic performance, which has been explained by redistribution/destruction of surface active sites due to the grinding procedure,<sup>195</sup> although further investigation is necessary.

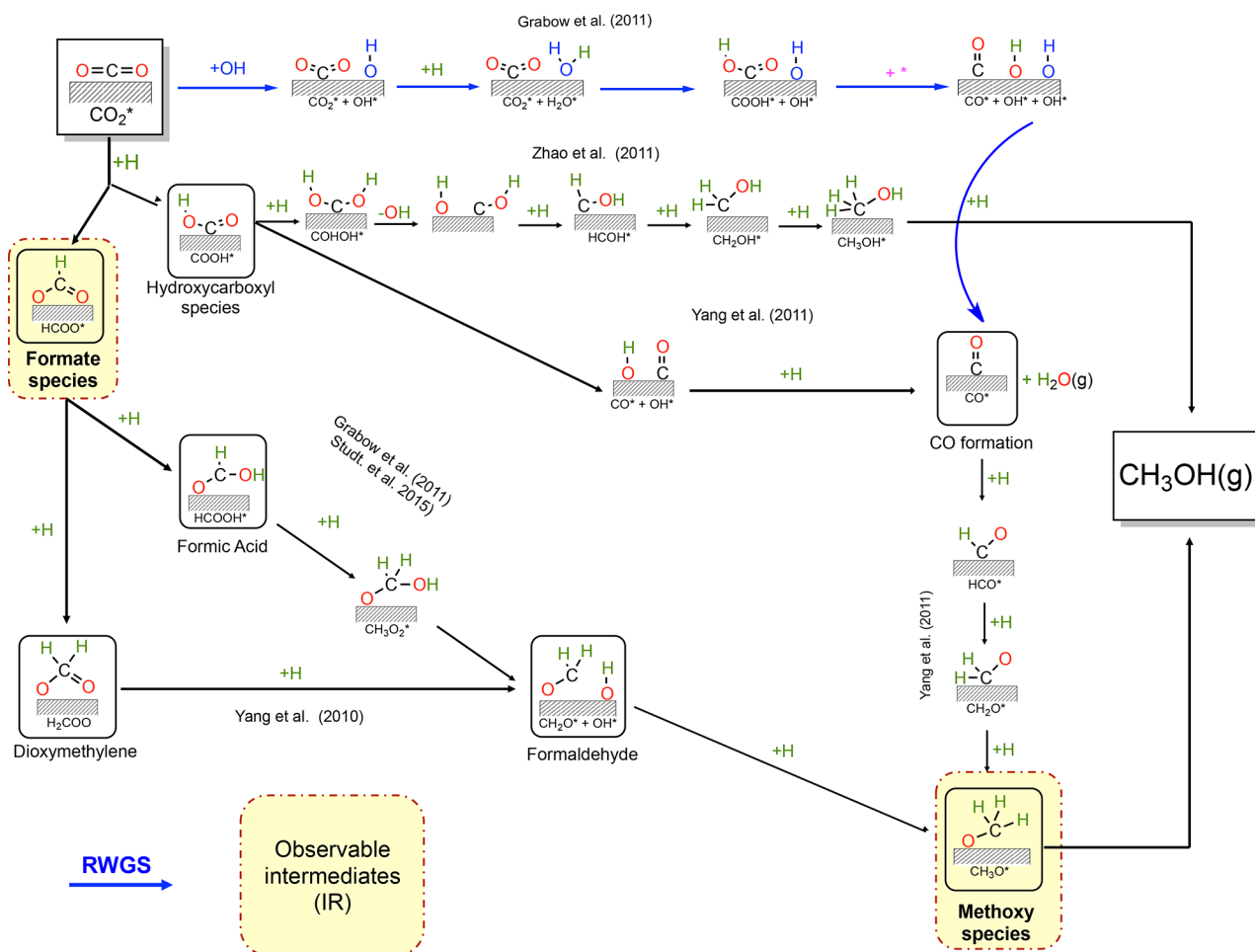


**Figure 16.** Proposed reaction mechanisms for the  $\text{CO}_2$  hydrogenation toward methanol.

### 5.3. Reaction Mechanism

**5.3.1. Reaction Mechanism of CO<sub>2</sub> Hydrogenation to Methanol.** The mechanism of CO<sub>2</sub> hydrogenation has been studied by numerous researchers urged by the importance of the methanol synthesis processes. However, the mechanism on the molecular level is not well understood and is widely debated to date, including the carbon source in methanol, i.e., methanol formation via either CO or CO<sub>2</sub>.

There are two important aspects of the reaction mechanisms: (1) the nature of the active site and (2) the reaction path. Considering the first aspect of the active site, it is widely believed that bare Cu<sup>0</sup> metal is the origin of the reactivity in the hydrogenation of CO<sub>2</sub> to methanol.<sup>213–215</sup> This statement has been supported by numerous reports taking single crystal and polycrystalline Cu films in experiments as well as by DFT calculations. Additionally, a direct relationship between the SA<sub>Cu</sub> and the activity of the catalysts has been reported, pointing out that Cu<sup>0</sup> is indeed the active phase.<sup>216–218</sup>

Nevertheless, some literature reports recognized the promoting influence of many metal oxides to the reactivity of Cu, showing structural, chemical, and electronic effects on Cu, thereby, enhancing exposure of Cu surface and unique reactivity.<sup>103,219</sup> Among these, the most discussed interaction is between Cu<sup>0</sup> and the most popular promoter, ZnO. In order to explain the Cu–Zn synergy, Arena et al.<sup>103</sup> proposed that ZnO could act as a reservoir for atomic hydrogen speeding up the hydrogenation of the intermediates. They also proposed that either ZnO could confer a peculiar morphology to the Cu particles or ZnO was able to create additional active sites on the Cu surface. The proposals are in agreement with the finding of Studt et al.,<sup>220</sup> who showed how the presence or absence of the Zn drastically altered not only the activity but also the reaction mechanism. Based on the DFT calculations, they concluded that in CO<sub>2</sub> hydrogenation the intermediates are bound to the surface through an oxygen atom and the addition of Zn acted as a promoter. In the case of the CO hydrogenation, in contrast, the intermediates are bound to the surface through C atoms and a full layer of Zn blocked these sites and hindered CO hydrogenation.

There are mainly two models proposed to describe the Cu–Zn “active site”. The first one assumes the active site to be a fully Zn-decorated surface step of Cu,<sup>220–223</sup> and the second one is an electron-deficient Cu<sup>δ+</sup> species dissolved across the ZnO promoter as the active site.<sup>126,224,225</sup> This first “Zn-decorated” model site was based on the experiments and theoretical studies, where the surface enrichment of Zn on the Cu particles was observed by XPS and HRTEM.<sup>221</sup> Kuld et al.<sup>222</sup> found metallic Zn on the surface of reduced Cu–ZnO catalyst by Auger emission spectroscopy, and Lunkenbein et al.<sup>226</sup> showed clear evidence of the formation of metastable ZnO layer during reductive activation. On the other hand, the electron-deficient Cu<sup>δ+</sup> species has been widely used to explain the differences in catalytic activity of the Cu–ZnO–ZrO<sub>2</sub> systems.<sup>103,150,219,224,227–229</sup> This hypothesis has been supported by chemisorption and FTIR studies and proved that the interaction of Cu particles with ZnO and ZrO<sub>2</sub> phases leads to the stabilization of Cu<sup>δ+</sup> sites at the metal oxide interface.<sup>227,228</sup>

Besides the open discussion about the nature of the active site, the second point described above on the reaction pathway is also still a matter of active debate. The initial adsorption of CO<sub>2</sub> has been reported to occur in several ways. Some researchers claim that CO<sub>2</sub> can dissociatively adsorb over bare Cu,<sup>0,230,231</sup> while others report that preadsorbed H species are crucial to ensure CO<sub>2</sub> adsorption on Cu.<sup>0,232,233</sup> In addition, the type of species

that are formed after the successful adsorption of CO<sub>2</sub> is also widely debated. Some researchers support the formation of formate species (HCOO\*) as the first hydrogenated species in the mechanism, whereas others propose the formation of hydrocarboxyl (COOH\*).

The very first studies supported the formate route via transformation to dioxymethylene (CH<sub>2</sub>O<sub>2</sub>\*), formaldehyde (CH<sub>2</sub>O\*), and then to methoxy (CH<sub>3</sub>O\*) (Figure 16). However, the only observable intermediates were formate and methoxy species.<sup>213</sup> Grabow and Mavrikakis<sup>229</sup> proposed a mean-field microkinetic model that fitted the experimental results obtained under realistic conditions on commercial Cu–ZnO–Al<sub>2</sub>O<sub>3</sub>. In their proposed mechanism (Figure 16), besides the formate (HCOO\*) and methoxy (CH<sub>3</sub>O\*) species, they also considered intermediates such as formic acid HCOOH\* and CH<sub>3</sub>O<sub>2</sub>\*. The DFT calculations showed that CO<sub>2</sub> hydrogenation goes through the formate route, where formate (HCOO\*) preferentially leads to the formation of formic acid (HCOOH\*) rather than dioxymethylene (CH<sub>2</sub>O<sub>2</sub>\*). This formic acid would be further hydrogenated to CH<sub>3</sub>O<sub>2</sub>\*, which is subsequently transformed to CH<sub>2</sub>O\* by splitting off its OH group. In the final step, the hydrogenation of CH<sub>2</sub>O\* would yield methoxy (CH<sub>3</sub>O\*). As a favorable support of the formate route, Tabatabaei et al.<sup>234</sup> reported the presence of formate species in the CO<sub>2</sub> hydrogenation by pulses and desorption analysis. They noted that the bidentate formate was an intermediate for the RWGS reaction while a monodentate formate was the intermediate for CH<sub>3</sub>OH synthesis on ZnO from CO<sub>2</sub>/H<sub>2</sub> feeds. Yang et al.<sup>232</sup> showed that methanol synthesis on Cu surfaces proceeds through a formate intermediate to formaldehyde, but in this case via a dioxomethylene intermediate (Figure 16). The overall reaction rate was found limited by both formate and dioxomethylene hydrogenation. In a recently study, Kattel et al. reported the synergy of Cu–ZnO and the transformation of formate to methanol via \*HCOOH, \*H<sub>2</sub>COOH, and \*CH<sub>3</sub>O intermediates.<sup>235</sup>

Furthermore, the synergistic effects of Cu–ZrO<sub>2</sub> were evidently reported recently by Larmier et al. using a tailored catalyst with highly dispersed Cu on ZrO<sub>2</sub>. They have shown by NMR, DRIFTS, and DFT calculations that formate is an intermediate and its transformation to methanol is highly favored at the interface of Cu and ZrO<sub>2</sub> owing to lowered activation barrier by the interface. Interestingly, the unique interface of Cu and ZrO<sub>2</sub> facilitated transformation of formate to an acetal-like species (H<sub>2</sub>C(O)<sub>2</sub>\*), which is further hydrogenated to methoxy and finally to methanol.<sup>236</sup>

Contrary to the formate route, Zhao et al.<sup>237</sup> reported that formation of methanol from direct hydrogenation of formate (HCOO\*) on Cu(111) is not feasible due to the high activation barriers in some of the elementary steps. Instead, CO<sub>2</sub> hydrogenation to hydrocarboxyl (*trans*-COOH) is kinetically more favorable than formate in the presence of water via a unique hydrogen transfer mechanism (Figure 16). In agreement with Zhao et al., Yang et al.<sup>238</sup> concluded that the direct hydrogenation of bidentate formate (HCOO\*) on metallic Cu does not produce methanol. Interestingly, they found that a significant amount of methanol is formed if the Cu catalyst is pretreated by N<sub>2</sub>O or O<sub>2</sub>, which implies that surface oxygen or possibly water-derived species may play a critical role in the reaction mechanism.

Besides the CO<sub>2</sub> hydrogenation, RWGS reaction and the CO hydrogenation also play important roles in the overall reaction network. In the early days, when methanol was only produced via syngas hydrogenation, it was widely assumed that CO hydro-

genation was the main reaction pathway for methanol synthesis. However, substantial research work<sup>220,239,240</sup> based on isotope labeling experiments suggested that carbon dioxide is the sole carbon source for methanol synthesis. These findings have been corroborated by numerous other studies, including DFT calculations.<sup>232</sup> Nevertheless, since Cu is also an excellent RWGS catalyst facilitating the conversion of CO to CO<sub>2</sub> and *vice versa*, the controversy about the carbon source in methanol synthesis lives onward. Grabow and Mavrikakis<sup>229</sup> proposed that both CO and CO<sub>2</sub> hydrogenation pathways could be active under typical methanol synthesis conditions (Figure 16). They also found that under typical industrial reaction conditions 2/3 of the methanol is produced from CO<sub>2</sub> hydrogenation. Based on DFT calculations, Yang et al.<sup>232</sup> reported that the CO produced by the fast RWGS does not undergo subsequent hydrogenation to methanol, but simply accumulates as a product. This was explained by the hydrogenation of CO into unstable formyl (HCO\*), which prefers to dissociate into CO and H on Cu surface.

**5.3.2. Reaction Mechanism of CO<sub>2</sub> Hydrogenation to DME.** One-step direct transformation of CO<sub>2</sub> to DME essentially involves the dehydration of methanol to DME, which is a mature industrial process and mostly conducted on the H-form of zeolite. Specifically, H-ZSM-5 is the most popular and versatile zeolite catalyst for this reaction as evident from the earlier section on the catalyst materials. Several studies reported two possible reaction pathways, dissociative and associative, for the dehydration of methanol to DME over acid catalysts (Figure 17).<sup>241–246</sup> However, there is no definitive conclusion regarding the most prevailed reaction mechanism. In the case of protonated zeolites both pathways are catalyzed by Brønsted acid sites. In the dissociative mechanism on the one hand, methanol becomes adsorbed at the Brønsted acid site and transformed into a surface methoxy group by losing a water molecule. Subsequently, the nucleophilic attack by a second methanol molecule on surface methoxy leads to formation of DME. On the other hand, in the associative mechanism, two methanol molecules coadsorb at the Brønsted acid site and are transformed to DME and water.

The recent DFT study by Ghorbanpour et al.<sup>247</sup> shows on the basis of Gibbs free energies that the dissociative mechanism is dominant for a particular set of reaction conditions irrespective of the active site. At higher temperatures where entropic contributions are high, however, the mechanism shifts from the associative to the dissociative one due to the crossover temperature for each active site.

#### 5.4. Process and Economic Aspects

When a chemical process is evaluated, economic aspects, energetic aspects, and environmental and ecological impacts need to be carefully and holistically examined. The aspects on economy and energy are highly related, while in the light of CO<sub>2</sub> utilization the energy aspects can also impact human and environment considering the CO<sub>2</sub> emission associated with energy production. Greenliness of a chemical process in terms of net reduction in CO<sub>2</sub> emission, i.e., lower carbon footprint, thus requires careful inspection of CO<sub>2</sub> emission and utilization in all steps including raw material processing, product transport, and even how electric energies are generated. The commonly reported processes for CO<sub>2</sub> hydrogenation to methanol are based on packed-bed reactors, and they are generally identical to those used for conventional methanol production from syngas. This is also a natural choice since the large-scale conventional methanol processes utilize CO<sub>2</sub> to produce methanol. CO<sub>2</sub> is

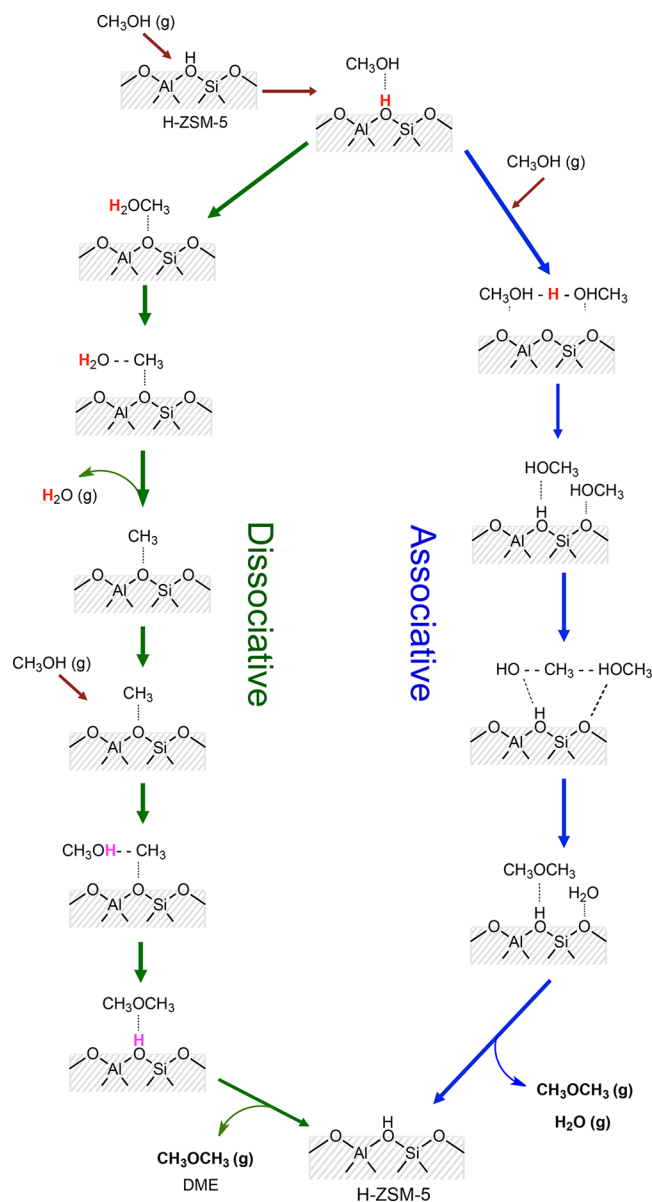


**Figure 17.** Proposed reaction mechanism of methanol dehydration to DME. Adapted with permission from ref 247. Copyright 2016 American Chemical Society.

intentionally added to a syngas stream to balance the H<sub>2</sub>/(CO + CO<sub>2</sub>) ratio appropriate for methanol synthesis utilizing the CO<sub>2</sub> captured in another process as well as to improve the catalytic performance. In this section, methanol synthesis processes mainly based on syngas are described due to the high similarities. Then the aspects of greenliness of CO<sub>2</sub>-to-methanol processes are discussed based on carbon footprints evaluated by life cycle assessment (LCA).

The commercial syngas-to-methanol technologies feature three main processes: syngas preparation, methanol synthesis, and methanol purification. The syngas preparation is performed with highly energy-demanding processes such as steam reforming, partial oxidation, or pyrolysis of fossil fuels.<sup>248</sup> Economically, this process accounts for more than a half of the total investment and consumes the major energy of the overall methanol process. For this reason, there is a great motivation to use CO<sub>2</sub> as a cost-competitive carbon source in methanol production. However, the other reactant in CO<sub>2</sub> hydrogenation,



namely, hydrogen, needs to be produced separately in this case. The greenliness and carbon footprint of  $H_2$  production process should be improved with the emerging technologies (*vide supra*), but at present they are not economically competitive and/or scalable, thus rendering the price of “green hydrogen” high in the scenario of renewable/natural energy as activation source of water for hydrogen production.

The heart of the second process, methanol synthesis, is the reactor. Various types of reactors and catalyst arrangements have been reported. The shared aspects in the different designs are to remove the heat of reaction efficiently and economically and at the same time to equilibrate the reaction at lower temperature ensuring high conversion per pass.<sup>248</sup> Conversely, the per-pass conversion is kept moderate in all designs, and recirculation of unreacted gases and CO produced by RWGS is required to achieve reasonable methanol yields.

Mainly three types of reactors are used in industry. The first one, the tubular boiling water reactor used, e.g., by Lurgi, includes indirect cooling of catalyst-packed tubes with boiling water (Figure 18a). By controlling the pressure of the circulating

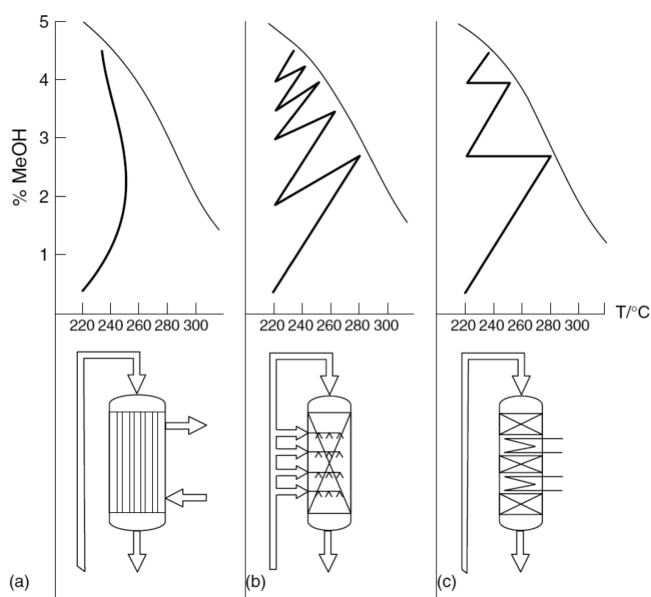


**Figure 18.** Conversion profiles (upper panel, bold lines) and equilibrium curve (upper panel, thin lines) for three types of conventional methanol synthesis reactors (lower panels): (a) tubular boiling water reactor; (b) series quench reactor; (c) series adiabatic reactor with interstage cooling. Reproduced with permission from ref 135. Copyright 1997 Wiley-VCH Verlag GmbH & Co. KGaA.

boiling water, the reaction temperature is regulated and optimized. The isothermal nature of the reactor gives a high conversion and a long catalyst life (5 years) due to the low average operating temperature which minimizes the sintering rate of active catalyst components, although the complex mechanical design of this type of reactor results in relatively high investment costs.

The second reactor type, called series quench reactor, was developed by ICI Syntex (now Johnson Matthey) containing several adiabatic catalyst beds installed in series (Figure 18b). Internal cooling is achieved by passing cold feed gas into the chambers between the catalyst beds. Although these types of reactors are relatively inexpensive, the reaction trajectory is far from ideal due to the dilution of the gas and the fact that not all

the gas passes through the total catalyst volume, causing lower catalyst utilization and a larger amount of byproduct formation compared to other reactor types.<sup>135</sup> The third type is a series adiabatic reactor (Figure 18c). The spherical model of the reactor type used in the Kellogg and Haldor-Topsøe processes has advantages over cylindrical ones in better pressure resistance by the spherical shape with thinner wall (cost reduction), low pressure drops, and high methanol production rates.<sup>249</sup>

Besides these common reactor types, the operation of slurry phase systems, e.g., liquid phase methanol process (LPMEOH) by Air Products and Chemicals, has also been demonstrated, although never commercially operated. In the process a powdered catalyst is suspended in inert oil, providing an efficient means to remove the heat of reaction and control the reaction temperature. The syngas is simply bubbled into the liquid. This process promotes a higher syngas-to-methanol conversion so that a single pass through the reactor is generally sufficient.<sup>250</sup>

For the conversion of pure  $CO_2$  stream to methanol, the CAMERE process (carbon dioxide hydrogenation to form methanol via a reverse water-gas shift reaction) has been developed. In this two-step process, first the feed gas is passed to a RWGS reactor and  $H_2O$  is removed after the first reactor. Second, the composition of the feed gas at the second reactor is closer to the common syngas used in the conventional methanol synthesis, and the negative effects of the water presence on the catalyst stability are minimized.<sup>251</sup> For this process, and as is widely suggested, an infrastructure identical or similar to that of the conventional syngas-to-methanol processes can be used for  $CO_2$  hydrogenation to methanol. That said, there is a fundamental difference in the scopes of the two methanol processes. Namely,  $CO_2$  hydrogenation is generally aimed at reducing  $CO_2$  emission and the dependency on fossil fuels, and at converting the carbon in  $CO_2$  to chemical fuels and useful materials. However, are such apparently greener processes economically viable? What is the actual, exact carbon footprint of the overall  $CO_2$ -to-methanol process, taking into account the method of  $H_2$  production and the energy necessary to capture  $CO_2$ , to run the plant, and to generate  $H_2$ ? Reliable, quantitative and complete assessment of a chemical process is required to address this point. Currently, LCA serves as the most established protocol to evaluate the carbon footprint and impacts on environment. LCA takes into account all up- and downstream processes and establishes a direct link to environmental impacts.<sup>252</sup>

Aresta et al.<sup>253</sup> performed LCAs on methanol processes to compare the environmental impacts by the use of syngas or by the use of  $CO_2$  and  $H_2$  from renewables. The objective was to evaluate the best path for sustainable methanol synthesis process by assuming  $CO_2$  from a steam reforming process of natural gas or captured from a thermal power plant. Their results showed that extraction and the steam reforming of natural gas were remarkably more energy-demanding than the process of  $CO_2$  capture from flue gases.  $CO_2$  capture and  $H_2$  production from renewables or nuclear/photovoltaic power were obviously favorable in terms of carbon footprint, and therefore the hydrogenation of the captured  $CO_2$  to methanol made sense. From an environmental point of view, the comparison of the processes showed that the most friendly one was based on  $CO_2$  recovered from flue gases and  $H_2$  from electrolysis with photovoltaic energy. Nevertheless, the authors emphasized the low efficiency of the water splitting by photovoltaic energy as a limitation.



Recently, von der Assen et al.<sup>254</sup> performed thorough LCAs to evaluate the environmental impacts of possible future methanol production processes, assuming five different potential scenarios:

1. Production of H<sub>2</sub> via electrolysis powered by photovoltaics and direct utilization of atmospheric CO<sub>2</sub>.
2. Production of H<sub>2</sub> via electrolysis powered by photovoltaics, but with provision of CO<sub>2</sub> from point sources.
3. Production of H<sub>2</sub> via electrolysis with wind power and with provision of CO<sub>2</sub> from point sources.
4. Production of H<sub>2</sub> via steam reforming of natural gas and provision of CO<sub>2</sub> from point sources.
5. H<sub>2</sub> and CO<sub>2</sub> via steam reforming of natural gas.

The results of LCA are expressed in terms of global warming impact score (GW).

The GW includes the contributions from all greenhouse gas (GHG) emission along a life cycle, and the score is calculated by the sum of all the global warming potential (GWP<sub>i</sub>) of each GHG multiplied by its amount ( $m_i$ ). GWP<sub>i</sub> is the measure of the relative global warming strength scaled by the radiation absorption by a single GHG emission. In practice, GW can be considered as the measure of “carbon footprint”. Table 4 summarizes the GWs of the above five scenarios.

**Table 4. Comparison of GWs for the Five Different Scenarios**

| scenario | GW (H <sub>2</sub> production), kg CO <sub>2</sub> /kg H <sub>2</sub> | GW (CO <sub>2</sub> feed), kg CO <sub>2</sub> /kg CO <sub>2</sub> | GW (methanol), kg CO <sub>2</sub> /kg methanol |
|----------|---|---|--|
| 1        | 6.0 <sup>255</sup>  | −1  | 0.45   |
| 2        | 6.0 <sup>255</sup>  | −0.41 <sup>256</sup>  | 1.26   |
| 3        | 1.0 <sup>257</sup>  | −0.41 <sup>256</sup>  | 0.32   |
| 4        | 11.9 <sup>258</sup>   | −0.41 <sup>256</sup>  | 2.37   |
| 5        |   |   | 0.75 <sup>259</sup>                            |

In the assessment, H<sub>2</sub> production by electrolysis powered by photovoltaics (scenarios 1 and 2) is found significantly more CO<sub>2</sub> emitting than the case of electrolysis powered by wind energy (scenario 3); in other words, the use of wind energy to power a water electrolyzer is significantly more attractive in comparison with the current route of hydrogen production based on steam reforming (scenario 4). From the LCA perspective there is no great difference between CO<sub>2</sub> capture from the atmosphere and from point sources. The GW value of −0.41 for the net “reduction” of CO<sub>2</sub> by the CO<sub>2</sub> capture process can be further reduced (more negative; more net CO<sub>2</sub> reduction) when CO<sub>2</sub> is captured from more concentrated CO<sub>2</sub> emission sources due to easier capture and less energy requirements. It is still not a carbon-neutral or carbon-negative process, but by choosing appropriate energy sources a CO<sub>2</sub>-to-methanol process can become greener (scenario 3) with less than half the GW of the conventional methanol process. Importantly, the LCA shows that the use of conventional H<sub>2</sub> from steam reforming in CO<sub>2</sub>-to-methanol process is extremely unfavorable for the environmental impact (scenario 4), emitting CO<sub>2</sub> nearly three times more than the conventional methanol process (scenario 5).

Related to the reaction conditions and the process energy costs, Tidona et al.<sup>260</sup> investigated the energy requirements of high-pressure CO<sub>2</sub>-to-methanol process, assuming direct capture from air as CO<sub>2</sub> source and water electrolysis as H<sub>2</sub> source, and evaluated the effects of high-pressure operations on the process performance and energy requirement as a function of the reactor pressure. The study showed that the energy requirement lowers at higher pressures roughly up to 400 bar due to better

performance given by the thermodynamic advantages, but then it goes slightly up at higher pressures for compression (Figure 19).

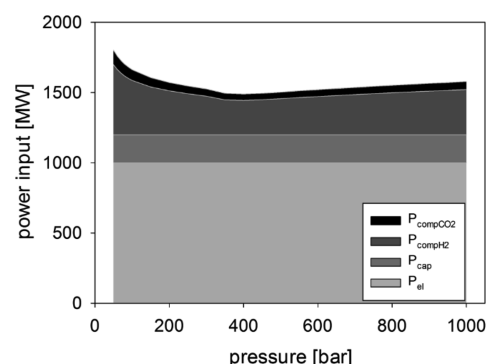


**Figure 19.** Power requirements for water electrolysis ( $P_{el}$ ), CO<sub>2</sub> capture ( $P_{cap}$ ), and compression of hydrogen ( $P_{compH2}$ ) and CO<sub>2</sub> ( $P_{compCO2}$ ) at various reaction pressures in methanol synthesis by CO<sub>2</sub> hydrogenation. Reprinted with permission ref 184. Copyright 2016 Elsevier.

Nevertheless, it is important to note that roughly 60–70% of the total energy was required to generate H<sub>2</sub>, confirming once again that the H<sub>2</sub> and its production method, energy, and cost in greener CO<sub>2</sub>-to-methanol process greatly matter.

There are increasing actions to develop and install CO<sub>2</sub>-to-methanol processes worldwide urged by environmental concerns. Mitsui Chemicals and Carbon Recycling International (CRI) are well-recognized companies that demonstrated the methanol synthesis from sustainable CO<sub>2</sub> and H<sub>2</sub> as raw materials. It is claimed that Mitsui Chemicals has invented catalysts operated in the process of CO<sub>2</sub>-to-methanol at the capacity of 100 tons of methanol per year with CO<sub>2</sub> released in ethylene production and H<sub>2</sub> generated by photochemical water splitting using solar energy.<sup>261</sup> CRI in Iceland is considered to be the leader in commercializing CO<sub>2</sub>-to-methanol processes, where the CO<sub>2</sub> is captured from flue gas released by a geothermal power plant and the H<sub>2</sub> in the process is produced by water electrolysis powered by green (geothermal, hydro, and wind) energy. The capital investment for a methanol plant using CO<sub>2</sub> and H<sub>2</sub> is estimated to be about the same as that for a conventional syngas-based plant. Still, the limiting factor for wide introduction of such processes is the economics of the process, currently unfavorable due to the low price of natural gas and consequently the low methanol price. To be commercially viable, the methanol produced by greener CO<sub>2</sub>-to-methanol processes needs to be in the same or similar price range as that produced by the conventional process. Obviously, lower costs of renewable energies and additional social drivers to lower the dependency on fossil fuels and a higher carbon tax, besides technological developments like novel catalysts and catalytic process design, are required to facilitate widespread introduction of carbon-neutral/negative CO<sub>2</sub>-to-methanol and CO<sub>2</sub>-to-DME processes.

## 6. SUMMARY AND FUTURE PERSPECTIVES

To tackle the challenges imposed by global warming, an urgent action in terms of decreasing (and eventually stopping) CO<sub>2</sub> emissions is necessary. Over the past decade, a drastic change in public opinion, driven by new governmental policy (although this may swiftly vary considerably geographically and in time), has boosted intense research not only into the development of more efficient CO<sub>2</sub> capture technologies but also into methods for the valorization of this carbon containing feedstock. In this

review, we have highlighted the most important advances in the development of heterogeneous catalysts for the hydrogenation of CO<sub>2</sub>, with special emphasis on selective processes. Not surprisingly, for these processes to become economically attractive, several advancements on the feedstock side will be needed. First, efficient capture technologies need to be available, and these should provide, in massive amounts, sufficiently pure CO<sub>2</sub>. We strongly believe that, in the short term, only capture technologies applied at point sources are a feasible possibility. If recent efforts in membrane technology crystallize into large scale deployment, a price of 20 \$/ton of CO<sub>2</sub> will be sufficiently attractive as to boost the development of an alternative petrochemical industry where CO<sub>2</sub> may become the main feedstock. At this point, it is necessary to stress that research into CO<sub>2</sub> capture from the atmosphere should by no means be abandoned. However, one must consider that this is a different ball game, where most likely adsorption and absorption driven processes making use of green energy sources will be the main workhorse, as recently reviewed by Sanz-Pérez and colleagues.<sup>262</sup> Nevertheless, the potential implementation of such technology may very well take several decades.

Second, advances in CO<sub>2</sub> capture need to go hand in hand with advances in the production of green hydrogen. It would indeed make very little sense to use H<sub>2</sub> derived from hydrocarbons for the hydrogenation of CO<sub>2</sub>. This leg seems, at present, to advance at a good pace: as briefly discussed in section 3, recent advances in PV- and wind-based electricity generation along with improvements in electrolyzer technologies promise cheap and abundant hydrogen soon, especially utilizing unconsumed excess electricity.<sup>263</sup> Once this technology is massively applied, the parallel production of highly pure O<sub>2</sub> along with the desired hydrogen may offer additional advantages. Considering that distillation is one of the most energy consuming (and therefore CO<sub>2</sub> emitting) technologies applied by the chemical industry and the importance of O<sub>2</sub> distillation, the globalization of electrolyzers will be doubly beneficial in the fight against global warming. When it comes to catalysis to produce chemical commodities from CO<sub>2</sub>, in this review we have focused on the most important developments in the hydrogenation to formate and to methanol/DME. From a technology readiness level perspective (TRL), it is fair to admit that methanol synthesis is a far more advanced technology, with already examples at the industrial level (TRL 6–7 at least). Considering the high selectivities obtained with heterogeneous catalysts, practical implementation of homogeneous catalysts will be doubtful for methanol synthesis. Regarding the hydrogenation of CO<sub>2</sub> to formates, the TRL of this technology is far lower (TRL 1–2). Although several catalytic systems have been proven to work and to produce formates at decent reaction rates, to the best of our knowledge, the economic feasibility of this technology has not been demonstrated. Currently formic acid (in the form of formates) is produced in industry from methanol and carbon monoxide in the presence of strong bases under relatively mild reaction conditions (40 bar, 80 °C). Considering the potential amount of CO<sub>2</sub> available in the future and the relatively small demand for formic acid (ca. 800 kton/year), even if deployed commercially, this technology would only be a niche application, unless formic acid is used as a hydrogen carrier.

At this point, it should be stressed that formic acid is currently seen as a potential way of chemically storing hydrogen. The main advantages of formic acid over other alternatives for H<sub>2</sub> storage include easy handling, refueling, and transportation. Moreover, recent advances in the development of catalysts for its

decomposition to CO<sub>2</sub> and H<sub>2</sub> are promising and able to meet DOE targets.<sup>97</sup> Therefore, research into more efficient systems for the formation of formates may eventually lead to the massive use of this chemical as alternative to the traditional liquid fuels.<sup>264</sup> Although the immobilization of homogeneous catalysts has been shown successful for the hydrogenation of CO<sub>2</sub> to formic acid, a better characterization of the working and deactivated catalysts would certainly help understanding and designing new catalyst generations. Indeed, as discussed above, while in many cases the structure of the as synthesized solids (or precatalysts) seems to be more or less clear, surprisingly little is known about the very likely changes that may occur upon activation under reaction conditions and the consequences for catalyst stability and reuse, the main objective for immobilization.

In addition, the development of catalysts for the hydrogenation of CO<sub>2</sub> to formates has the potential to open the door to low-temperature, mild condition routes for the synthesis of methanol through collaborative/domino catalysis. Indeed, as discussed above, the synthesis of methanol takes place via formates (Figure 16). If catalysts able to form formates at milder conditions are eventually combined with an additional catalyst (or catalytic function) able to selectively transform carboxylic acids into alcohols, such technology has the potential to promote a paradigm shift in CO<sub>2</sub> hydrogenation. Homogeneous catalysts for the direct hydrogenation of carboxylic acids (including formic acid) have already been described in the literature, although these usually require a stoichiometric hydrogen donor, something not feasible in the process hypothesized above.<sup>265,266</sup> To the best of our knowledge, Liu et al. and Yao et al. reported first the reduction of formic acid to methanol with H<sub>2</sub> over Cu–Zn<sup>267</sup> and Cu–Al<sup>268</sup> catalysts. A maximum methanol yield of 32% under batch conditions was achieved at 300 °C after 5 h. However, the reaction pathway was proven to be more likely through hydrogenation of CO<sub>2</sub> produced via the decomposition of formic acid under reaction conditions. On a more promising note, recently the group of De Bruijn has reported the application of a homogeneous Co catalyst able to hydrogenate a wide scope of carboxylic acids, including formic acid, to alcohols under relatively mild reaction conditions (76% isolated yield to methanol at 100 °C and 80 bar, although using environmentally unfriendly THF as solvent).<sup>269</sup> Indeed, the approach of combined synthesis of formate, often transformed into alkyl formate via esterification in the presence of ethanol or methanol, and methanol by formate hydrogenation using molecular catalysts has been recently demonstrated.<sup>41,270</sup> Some Ru and Co catalysts<sup>271,272</sup> could also transform CO<sub>2</sub> and H<sub>2</sub> to methanol in the absence of alcohol in the medium, achieving direct methanol synthesis with a comparable TOF as the most common Cu–ZnO heterogeneous catalyst.<sup>270</sup> In the coming years, we expect further development and application of these catalysts or the molecular systems described in section 4, and even of immobilized molecular catalysts with the dual functionality for formate and consecutive methanol synthesis via CO<sub>2</sub> hydrogenation.

Technologically, CO<sub>2</sub> hydrogenation to methanol and DME over heterogeneous catalyst is matured and can become economic and more widespread at the current TRL when other limitations such as high energy cost for CO<sub>2</sub> capture, H<sub>2</sub> production, and high carbon footprint (sections 2, 3, 5) are mitigated. Conversely, such limiting and unsustainable aspects should be equally considered upon development and possible commercialization of the technology. While most research on methanol synthesis is focused on the development of active and

selective catalysts, the thermodynamics of the methanol synthesis should not be forgotten (Figure 10). Its practical importance is evident from almost full CO<sub>2</sub> conversion to methanol at high weight time yield (WTY) with and without benefiting from product phase condensation.<sup>115,117,118</sup> In theory, almost full CO<sub>2</sub> conversion and full methanol selectivity are possible below 170 °C at 100 bar or below 230 °C at 200 bar at the stoichiometric ratio of CO<sub>2</sub> and H<sub>2</sub> feed (see Figure 10). To achieve this, however, more active catalysts are required. Often catalysts with exceptionally high methanol selectivity at low CO<sub>2</sub> conversion level (kinetic regime) are reported, but these features may be meaningless in practice when high or full CO<sub>2</sub> conversion, thus operation under thermodynamic control, is a must. Along the same line, rates of the reaction must be critically evaluated to assess practical viability of the process in terms of WTY, as this quantity describes the methanol yield taking reaction time and reactor size into account so that different types of catalysts can be critically compared.

From an industrial point of view, the Cu-based catalyst, particularly containing Cu–ZnO, is expected to remain the benchmark to beat for CO<sub>2</sub>-to-methanol transformation because of the superior activity, stability, and economic advantages. Although the Cu–ZnO catalyst has been used for decades, still a number of mysteries exist associated with its synthesis, active site, and the reaction mechanism. The Cu surface is commonly related to the catalytic activity, but the interaction of Cu with ZnO is reported to be as critical. The major challenge in our view is that the true understanding of the active sites and reaction mechanism (surface intermediates) under relevant reaction conditions has not yet been achieved. Coprecipitation is the standard method to synthesize methanol synthesis catalysts (Figure 14), which is often considered as an art, but there are advances, e.g., by Behrens,<sup>131</sup> to do science with this synthetic process identifying precursors leading to highly active phases upon calcination treatment. Still, there are several parameters in coprecipitation (Figure 14) that can greatly affect catalytic performance, and the optimum condition is probably not yet reached. In this context, true understanding on the exact form of the active site and the reaction mechanism should facilitate maximizing the desired active phase in a catalyst. In reality, the difficulty is that such a phase may be formed only under reaction conditions of specific pressure and temperature. Therefore, *operando* spectroscopic investigations under a catalyst's working conditions with high sensitivity to the minute fraction of active phase formed at Cu and ZnO interfaces are crucial toward rational catalyst design. Once an excellent catalyst is in hand, catalyst stability also needs to be maximized. Employing highly active catalyst, one can reduce the reaction temperature, which could potentially prevent the destruction of active Cu surface or Cu–ZnO interfaces, thereby improving the longevity of catalyst.

A more environmentally benign process operated at low temperature and pressure and at the same time giving high methanol yield would require a radically different, unconventional approach, for example, by adding another interface to shift or bias the equilibrium. Among them, a more established one is the use of membrane reactor,<sup>273,274</sup> and the concept has been demonstrated. Another approach is electrocatalysis to influence the reaction thermodynamics at the electrode surface by altering the redox properties of catalyst. Although no outstanding result using these approaches has been reported to date, further development along this direction is anticipated, and highly innovative methodologies are awaited to enable low-temperature and low-pressure methanol processes.

On the other hand, DME synthesis by dehydration of methanol is a more mature process. On an industrial scale this reaction is often coupled with the syngas-to-methanol process to yield DME or olefins as final product. Although several strategies and catalysts have been developed for direct transformation of CO<sub>2</sub> to DME (section 5), this process essentially remains a two-step reaction. The bottleneck of this reaction could be the deactivation of methanol dehydration catalyst due to water poisoning. Comparing with the syngas–methanol–DME process, starting from CO<sub>2</sub> would yield significantly more water and hence the catalysts must be highly water-tolerant while maintaining the high activity. Among others, H-ZSM-5 holds the first position as highly active, widely available, water tolerant catalyst for methanol dehydration. A factor not yet well understood is the required intimacy of the two catalysts (Figure 15) because the DME yield drops when the active sites for methanol synthesis and dehydration are located too close to each other. Besides, formation of coke is the major cause of catalyst deactivation especially in a long-term operation. In such cases, high-temperature reactivation treatment to burn off the coke would be needed to regain the methanol dehydration activity. However, the reactivation treatment may ruin the active site for methanol synthesis under most circumstances, and development of water- and coke-resistant methanol dehydration catalysts needs to be addressed.

In this review we have examined the current state of the art in CO<sub>2</sub> capture, H<sub>2</sub> production, and CO<sub>2</sub> hydrogenation to formate/formic acid and methanol/DME and evaluated where we stand technologically. We should not forget that these technologies should be seen as a path forward into a carbon neutral society with a lower, or eventually negative, carbon footprint. As briefly touched upon in the Introduction, we should keep in mind that our society largely depends on chemicals, such as polymers, which, in the long run, will require an alternative feedstock. The development of competitive technologies for the capture and transformation of CO<sub>2</sub> will play an instrumental role in providing such alternative carbon source. In this review, promising advances as well as clear issues have been identified. Detailed economic analysis of the processes was out of the scope of this review, but it is imperative to keep this aspect in mind to remove the economic bottlenecks and facilitate the commercialization of these technologies. Currently, the theme of this special issue has become a subject where science, society, and policy have to join forces for much faster progress although it is slowly but steadily moving ahead. We hope this review will catalyze further technological developments into CO<sub>2</sub> hydrogenation processes and, even more importantly, promote scientific discussions toward accelerated installation of greener catalytic processes.

## AUTHOR INFORMATION

### Corresponding Authors

\*E-mail: f.kapteijn@tudelft.nl.

\*E-mail: aurakawa@iciq.es.

\*E-mail: j.gascon@tudelft.nl.

### ORCID

Atsushi Urakawa: 0000-0001-7778-4008

Jorge Gascon: 0000-0001-7558-7123

Freek Kapteijn: 0000-0003-0575-7953

### Notes

The authors declare no competing financial interest.



## Biographies

Andrea Álvarez (1985) obtained her MSc in Materials Science at the University of Sevilla in 2010. For her PhD she joined the group of Prof. Odriozola at the same university and developed her thesis in catalytic reforming of biomass with Ni-based catalysts (2015). She is currently a postdoctoral researcher at Prof. Urakawa's group, where her research is focused on the usage of CO<sub>2</sub> as a chemical feedstock.

Atul Bansode (1984) obtained his MSc in Physical Chemistry from University of Pune (India) in 2006 and then moved to National Chemical Laboratory (India) to work on catalytic reforming of hydrocarbons for H<sub>2</sub> production. In early 2008, he joined Dow Chemical's R&D center (India), where he continued his research on several industrially important catalytic reactions. In 2010 he moved to ICIQ (Spain) and finished his PhD in 2014 on high-pressure catalytic hydrogenation of CO<sub>2</sub> to chemicals and fuels. Since 2014 he is working as group scientific coordinator in the Urakawa research group at ICIQ and actively involved in developing efficient catalytic CO<sub>2</sub> conversion processes and *operando* spectroscopic tools.

Atsushi Urakawa (1976) was educated in an international environment and obtained his BSc in Applied Chemistry at Kyushu University with one year stay in the USA, MSc in Chemical Engineering at Delft University of Technology, and PhD in Natural Science at ETH Zürich. In 2006, he undertook a position as Senior Scientist/Lecturer at ETH Zürich. Since January 2010, he has joined ICIQ as Group Leader with particular research emphasis on the development of heterogeneous catalysts and processes based on rational understanding aided by *in situ* and *operando* spectroscopic methods aiming at accelerated tech transfer of innovative catalytic technologies to industry.

Anastasiya V. Bavykina (1988) obtained two Master degrees, the first at Novosibirsk State University in 2010 and the second jointly from the University of Barcelona and the Gdansk University of Technology in 2012, within Erasmus Mundus program. She obtained her PhD at Delft University of Technology on "Porous Organic Frameworks in Catalysis" in 2017. From July 1, 2017, she is a postdoctoral researcher at KAUST.

Tim A. Wezendonk (1986) obtained his MSc in Chemical Engineering at the Delft University of Technology in 2013. For his thesis work on MOF-based catalyst synthesis for Fischer–Tropsch to Olefins, he was awarded with The Netherlands Process Technology best research thesis 2013 prize. He continued working in this topic at the TU Delft as a PhD under the supervision of Prof. Gascon and Prof. Kapteijn, elaborating on the mechanisms at play in this synthesis method and focusing on structuring of these catalysts.

Michiel Makkee (1954) received his Master degree in Chemical Engineering and did PhD studies on catalysis and organic chemistry at the Delft University of Technology. After more than 6 years at Exxon Chemicals he was nominated as associate professor in the field of Catalysis Engineering and process development at the Delft University of Technology (1990). He was nominated as special parttime professor at the Politecnico di Torino (2011). He has supervised more than 150 Master students and 25 PhD students. He is (co-) inventor of 25 patents/patent applications and (co-) author of over 240 peer reviewed papers with an H-factor of 52. He received three personal grants from Aramco (\$325,000). He lectured in several courses on chemical and reactor engineering and is coauthor of the book *Chemical Process Technology* (2nd edition).

Jorge Gascon (1977) received his MSc in Chemistry in 2002 and his PhD in Chemical Engineering in 2006, both at the University of Zaragoza (Spain). Starting as postdoc at TUDelft he is since 2014 "Anthonie van Leeuwenhoek Professor" of Catalysis Engineering. Research interests include fundamental aspects and applications of new

nanostructured materials and composites. He has coauthored over 100 publications and several patents and has edited the book *Metal Organic Frameworks as Heterogeneous Catalysts*. He has been the recipient of the prestigious VENI (2010), VIDI (2013), and ERC Starting (2013) personal grants and of the 2013 ExxonMobil Chemical European Science and Engineering Award.

Freek Kapteijn (1952), MSc in Chemistry and Mathematics, received his PhD on "Metathesis of alkenes" in 1980 at the University of Amsterdam. After postdoc positions (Coal Science) in Amsterdam and Nancy (ENSIC), he became Associate professor in Amsterdam. He moved to Delft University of Technology in 1992, became "Anthonie van Leeuwenhoek professor" in 1999, and is since 2008 chair of Catalysis Engineering, with visiting professorships at ETH Zürich, Tianjin and Zhejiang Normal University. Research interest focuses on the interplay of catalysis and engineering, comprising structured and multifunctional catalysts, adsorption, separation, and (catalytic) membranes. He has coauthored over 500 publications in peer-reviewed journals and as book chapters.

## ACKNOWLEDGMENTS

A.A., A.B., and A.U. thank Generalitat de Catalunya for financial support through the CERCA Programme and recognition (2014 SGR 893) and thank MINECO (CTQ2012-34153) for financial support and support through Severo Ochoa Excellence Accreditation 2014-2018 (SEV-2013-0319).

## REFERENCES

- (1) Princiotta, F. *Global Climate Change—The Technology Challenge*; Springer: 2011; p 420.
- (2) 2011 *Technology Map of the European Strategic Energy Technology Plan (SET-Plan)*, 3rd ed.; European Commission, Joint Research Centre, Institute for Energy and Transport; © European Union: Luxembourg, 2011.
- (3) *The Global Status of CCS: 2011*; The Global CCS Institute: Canberra, Australia, 2011.
- (4) *CCS EII Implementation Plan 2010–2012*; Zero Emissions Platform: 2010.
- (5) Rubin, E. S.; Mantripragada, H.; Marks, A.; Versteeg, P.; Kitchin, J. The Outlook for Improved Carbon Capture Technology. *Prog. Energy Combust. Sci.* **2012**, *38*, 630–671.
- (6) Merkel, T. C.; Lin, H.; Wei, X.; Baker, R. Power Plant Post-Combustion Carbon Dioxide Capture: An Opportunity for Membranes. *J. Membr. Sci.* **2010**, *359*, 126–139.
- (7) Franz, J.; Maas, P.; Scherer, V. Economic Evaluation of Pre-Combustion CO<sub>2</sub>-capture in IGCC Power Plants by Porous Ceramic Membranes. *Appl. Energy* **2014**, *130*, 532–542.
- (8) Ku, A. Y.; Kulkarni, P.; Shisler, R.; Wei, W. Membrane Performance Requirements for Carbon Dioxide Capture using Hydrogen-selective Membranes in Integrated Gasification Combined Cycle (IGCC) Power Plants. *J. Membr. Sci.* **2011**, *367*, 233–239.
- (9) Lin, H.; He, Z.; Sun, Z.; Knip, J.; Ng, A.; Baker, R. W.; Merkel, T. C. CO<sub>2</sub>-Selective Membranes for Hydrogen Production and CO<sub>2</sub> Capture – Part II: Techno-Economic Analysis. *J. Membr. Sci.* **2015**, *493*, 794–806.
- (10) EPRI, *Program on Technology Innovation: Post-combustion CO<sub>2</sub> Capture Technology Development*; Electric Power Research Institute: Palo Alto, 2008; p 136.
- (11) Acar, C.; Dincer, I. Comparative Assessment of Hydrogen Production Methods from Renewable and Non-Renewable Sources. *Int. J. Hydrogen Energy* **2014**, *39*, 1–12.
- (12) Holladay, J. D.; Hu, J.; King, D. L.; Wang, Y. An Overview of Hydrogen Production Technologies. *Catal. Today* **2009**, *139*, 244–260.
- (13) Parthasarathy, P.; Narayanan, K. S. Hydrogen Production from Steam Gasification of Biomass: Influence of Process Parameters on Hydrogen Yield – A Review. *Renewable Energy* **2014**, *66*, 570–579.



- (14) Gaudernack, B.; Lynum, S. Hydrogen from Natural Gas without Release of CO<sub>2</sub> to the Atmosphere. *Int. J. Hydrogen Energy* **1998**, *23*, 1087–1093.
- (15) Nasir Uddin, M.; Daud, W. M. A. W.; Abbas, H. F. Potential Hydrogen and Non-Condensable Gases Production from Biomass Pyrolysis: Insights into the Process Variables. *Renewable Sustainable Energy Rev.* **2013**, *27*, 204–224.
- (16) Ursua, A.; Gandia, L. M.; Sanchis, P. Hydrogen Production From Water Electrolysis: Current Status and Future Trends. *Proc. IEEE* **2012**, *100* (2), 410–426.
- (17) Dincer, I. Green Methods for Hydrogen Production. *Int. J. Hydrogen Energy* **2012**, *37*, 1954–1971.
- (18) Dincer, I.; Acar, C. Review and Evaluation of Hydrogen Production Methods for Better Sustainability. *Int. J. Hydrogen Energy* **2015**, *40*, 11094–11111.
- (19) Wang, M.; Wang, Z.; Gong, X.; Guo, Z. The Intensification Technologies to Water Electrolysis for Hydrogen Production – A Review. *Renewable Sustainable Energy Rev.* **2014**, *29*, 573–588.
- (20) Carmo, M.; Fritz, D. L.; Mergel, J.; Stolten, D. A Comprehensive Review on PEM Water Electrolysis. *Int. J. Hydrogen Energy* **2013**, *38*, 4901–4934.
- (21) Zeng, K.; Zhang, D. Recent Progress in Alkaline Water Electrolysis for Hydrogen Production and Applications. *Prog. Energy Combust. Sci.* **2010**, *36*, 307–326.
- (22) Kalinci, Y.; Hepbasli, A.; Dincer, I. Biomass-based Hydrogen Production: A Review and Analysis. *Int. J. Hydrogen Energy* **2009**, *34*, 8799–8817.
- (23) Zhu, C.; Guo, L.; Jin, H.; Huang, J.; Li, S.; Lian, X. Effects of Reaction Time and Catalyst on Gasification of Glucose in Supercritical Water: Detailed Reaction Pathway and Mechanisms. *Int. J. Hydrogen Energy* **2016**, *41*, 6630–6639.
- (24) Ni, M.; Leung, D. Y. C.; Leung, M. K. H.; Sumathy, K. An Overview of Hydrogen Production from Biomass. *Fuel Process. Technol.* **2006**, *87*, 461–472.
- (25) Teets, T. S.; Nocera, D. G. Photocatalytic Hydrogen Production. *Chem. Commun.* **2011**, *47*, 9268–9274.
- (26) Maeda, K.; Domen, K. Photocatalytic Water Splitting: Recent Progress and Future Challenges. *J. Phys. Chem. Lett.* **2010**, *1*, 2655–2661.
- (27) Khan, S. U. M.; Al-Shahry, M.; Ingler, W. B. Efficient Photochemical Water Splitting by a Chemically Modified n-TiO<sub>2</sub>. *Science* **2002**, *297* (5590), 2243.
- (28) Kudo, A.; Miseki, Y. Heterogeneous Photocatalyst Materials for Water Splitting. *Chem. Soc. Rev.* **2009**, *38*, 253–278.
- (29) Xiao, J.-D.; Shang, Q.; Xiong, Y.; Zhang, Q.; Luo, Y.; Yu, S.-H.; Jiang, H.-L. Boosting Photocatalytic Hydrogen Production of a Metal–Organic Framework Decorated with Platinum Nanoparticles: The Platinum Location Matters. *Angew. Chem., Int. Ed.* **2016**, *55*, 9389–9393.
- (30) Li, Q.; Guo, B.; Yu, J.; Ran, J.; Zhang, B.; Yan, H.; Gong, J. R. Highly Efficient Visible-Light-Driven Photocatalytic Hydrogen Production of CdS-Cluster-Decorated Graphene Nanosheets. *J. Am. Chem. Soc.* **2011**, *133*, 10878–10884.
- (31) Jing, D.; Guo, L.; Zhao, L.; Zhang, X.; Liu, H.; Li, M.; Shen, S.; Liu, G.; Hu, X.; Zhang, X.; Zhang, K.; Ma, L.; Guo, P. Efficient Solar Hydrogen Production by Photocatalytic Water Splitting: From Fundamental Study to Pilot Demonstration. *Int. J. Hydrogen Energy* **2010**, *35*, 7087–7097.
- (32) Wang, Q.; Hisatomi, T.; Jia, Q.; Tokudome, H.; Zhong, M.; Wang, C.; Pan, Z.; Takata, T.; Nakabayashi, M.; Shibata, N.; Li, Y.; Sharp, I. D.; Kudo, A.; Yamada, T.; Domen, K. Scalable Water Splitting on Particulate Photocatalyst Sheets with a Solar-to-Hydrogen Energy Conversion Efficiency Exceeding 1%. *Nat. Mater.* **2016**, *15*, 611–615.
- (33) Grasemann, M.; Laurenczy, G. Formic Acid as a Hydrogen Source – Recent Developments and Future Trends. *Energy Environ. Sci.* **2012**, *5* (8), 8171–8181.
- (34) Reutemann, W.; Kieczka, H. Formic Acid. In *Ullmann's Encyclopedia of Industrial Chemistry*; Wiley-VCH Verlag GmbH & Co. KGaA: 2000.
- (35) Wang, W.-H.; Himeda, Y. Hydrogenation. In *Recent Advances in Transition Metal-Catalysed Homogeneous Hydrogenation of Carbon Dioxide in Aqueous Media* [Online]; Karamé, I., Ed.; InTechOpen: 2012.
- (36) Xu, W.; Ma, L.; Huang, B.; Cui, X.; Niu, X.; Zhang, H. In *Thermodynamic Analysis of Formic Acid Synthesis from CO<sub>2</sub> Hydrogenation*, 2011 International Conference on Materials for Renewable Energy & Environment, 20–22 May 2011; 2011; pp 1473–1477.
- (37) Jessop, P. G.; Ikariya, T.; Noyori, R. Homogeneous Catalysis in Supercritical Fluids. *Chem. Rev.* **1999**, *99*, 475–493.
- (38) Inoue, Y.; Izumida, H.; Sasaki, Y.; Hashimoto, H. Catalytic Fixation of Carbon Dioxide to Formic Acid by Transition-Metal Complexes under Mild Conditions. *Chem. Lett.* **1976**, *5* (8), 863–864.
- (39) Wang, W.-H.; Himeda, Y.; Muckerman, J. T.; Manbeck, G. F.; Fujita, E. CO<sub>2</sub> Hydrogenation to Formate and Methanol as an Alternative to Photo- and Electrochemical CO<sub>2</sub> Reduction. *Chem. Rev.* **2015**, *115*, 12936–12973.
- (40) Jessop, P. G.; Ikariya, T.; Noyori, R. Homogeneous Hydrogenation of Carbon-Dioxide. *Chem. Rev.* **1995**, *95*, 259–272.
- (41) Klankermayer, J.; Wesselbaum, S.; Beydoun, K.; Leitner, W. Selective Catalytic Synthesis Using the Combination of Carbon Dioxide and Hydrogen: Catalytic Chess at the Interface of Energy and Chemistry. *Angew. Chem., Int. Ed.* **2016**, *55*, 7296–7343.
- (42) Leitner, W. Carbon-Dioxide as A Raw-Material - The Synthesis of Formic-Acid and its Derivatives from CO<sub>2</sub>. *Angew. Chem., Int. Ed. Engl.* **1995**, *34*, 2207–2221.
- (43) Jessop, P. G.; Joo, F.; Tai, C. C. Recent Advances in the Homogeneous Hydrogenation of Carbon Dioxide. *Coord. Chem. Rev.* **2004**, *248*, 2425–2442.
- (44) Filonenko, G. A.; van Putten, R.; Schulpen, E. N.; Hensen, E. J. M.; Pidko, E. A. Highly Efficient Reversible Hydrogenation of Carbon Dioxide to Formates Using a Ruthenium PNP-Pincer Catalyst. *ChemCatChem* **2014**, *6*, 1526–1530.
- (45) Gunasekar, G. H.; Park, K.; Jung, K.-D.; Yoon, S. Recent Developments in the Catalytic Hydrogenation of CO<sub>2</sub> to Formic Acid/Formate using Heterogeneous Catalysts. *Inorg. Chem. Front.* **2016**, *3*, 882–895.
- (46) Bredig, G.; Carter, S. R. Katalytische Synthese der Ameisensäure unter Druck. *Ber. Dtsch. Chem. Ges.* **1914**, *47*, 541–545.
- (47) Farlow, M. W.; Adkins, H. The Hydrogenation of Carbon Dioxide and a Correction of the Reported Synthesis of Urethans. *J. Am. Chem. Soc.* **1935**, *57*, 2222–2223.
- (48) Srivastava, V. In Situ Generation of Ru Nanoparticles to Catalyze CO<sub>2</sub> Hydrogenation to Formic Acid. *Catal. Lett.* **2014**, *144*, 1745–1750.
- (49) Umegaki, T.; Enomoto, Y.; Kojima, Y. Metallic Ruthenium Nanoparticles for Hydrogenation of Supercritical Carbon Dioxide. *Catal. Sci. Technol.* **2016**, *6*, 409–412.
- (50) Stalder, C. J.; Chao, S.; Summers, D. P.; Wrighton, M. S. Supported Palladium Catalysts for the Reduction of Sodium Bicarbonate to Sodium Formate in Aqueous Solution at Room Temperature and One Atmosphere of Hydrogen. *J. Am. Chem. Soc.* **1983**, *105*, 6318–6320.
- (51) Su, J.; Yang, L.; Lu, M.; Lin, H. Highly Efficient Hydrogen Storage System Based on Ammonium Bicarbonate/Formate Redox Equilibrium over Palladium Nanocatalysts. *ChemSusChem* **2015**, *8*, 813–816.
- (52) Bi, Q.-Y.; Lin, J.-D.; Liu, Y.-M.; Du, X.-L.; Wang, J.-Q.; He, H.-Y.; Cao, Y. An Aqueous Rechargeable Formate-Based Hydrogen Battery Driven by Heterogeneous Pd Catalysis. *Angew. Chem., Int. Ed.* **2014**, *53*, 13583–13587.
- (53) Lee, J. H.; Ryu, J.; Kim, J. Y.; Nam, S.-W.; Han, J. H.; Lim, T.-H.; Gautam, S.; Chae, K. H.; Yoon, C. W. Carbon Dioxide Mediated, Reversible Chemical Hydrogen Storage using a Pd Nanocatalyst Supported on Mesoporous Graphitic Carbon Nitride. *J. Mater. Chem. A* **2014**, *2*, 9490–9495.
- (54) Joo, F.; Joo, F.; Nadasdi, L.; Elek, J.; Laurenczy, G.; Nadasdi, L. Homogeneous Hydrogenation of Aqueous Hydrogen Carbonate to Formate under Exceedingly Mild Conditions—a Novel Possibility of Carbon Dioxide Activation. *Chem. Commun.* **1999**, *11*, 971–972.

- (55) Su, J.; Lu, M.; Lin, H. High Yield Production of Formate by Hydrogenating CO<sub>2</sub> Derived Ammonium Carbamate/Carbonate at Room Temperature. *Green Chem.* **2015**, *17*, 2769–2773.
- (56) Preti, D.; Resta, C.; Squarcialupi, S.; Fachinetti, G. Carbon Dioxide Hydrogenation to Formic Acid by Using a Heterogeneous Gold Catalyst. *Angew. Chem., Int. Ed.* **2011**, *50*, 12551–12554.
- (57) Preti, D.; Squarcialupi, S.; Fachinetti, G. Conversion of Syngas into Formic Acid. *ChemCatChem* **2012**, *4*, 469–471.
- (58) Filonenko, G. A.; Vrijburg, W. L.; Hensen, E. J. M.; Pidko, E. A. On the Activity of Supported Au Catalysts in the Liquid Phase Hydrogenation of CO<sub>2</sub> to Formates. *J. Catal.* **2016**, *343*, 97–105.
- (59) Hao, C.; Wang, S.; Li, M.; Kang, L.; Ma, X. Hydrogenation of CO<sub>2</sub> to Formic Acid on Supported Ruthenium Catalysts. *Catal. Today* **2011**, *160*, 184–190.
- (60) Nguyen, L. T. M.; Park, H.; Banu, M.; Kim, J. Y.; Youn, D. H.; Magesh, G.; Kim, W. Y.; Lee, J. S. Catalytic CO<sub>2</sub> Hydrogenation to Formic Acid over Carbon Nanotube-Graphene Supported PdNi Alloy Catalysts. *RSC Adv.* **2015**, *5*, 105560–105566.
- (61) Takahashi, H.; Liu, L. H.; Yashiro, Y.; Ioku, K.; Bignall, G.; Yamasaki, N.; Kori, T. CO<sub>2</sub> Reduction using Hydrothermal Method for the Selective Formation of Organic Compounds. *J. Mater. Sci.* **2006**, *41*, 1585–1589.
- (62) Federsel, C.; Jackstell, R.; Beller, M. State-of-the-Art Catalysts for Hydrogenation of Carbon Dioxide. *Angew. Chem., Int. Ed.* **2010**, *49*, 6254–6257.
- (63) Filonenko, G. A.; Hensen, E. J. M.; Pidko, E. A. Mechanism of CO<sub>2</sub> Hydrogenation to Formates by Homogeneous Ru-PNP Pincer Catalyst: from a Theoretical Description to Performance Optimization. *Catal. Sci. Technol.* **2014**, *4*, 3474–3485.
- (64) Huff, C. A.; Sanford, M. S. Catalytic CO<sub>2</sub> Hydrogenation to Formate by a Ruthenium Pincer Complex. *ACS Catal.* **2013**, *3*, 2412–2416.
- (65) Hull, J. F.; Himeda, Y.; Wang, W.-H.; Hashiguchi, B.; Periana, R.; Szalda, D. J.; Muckerman, J. T.; Fujita, E. Reversible Hydrogen Storage using CO<sub>2</sub> and a Proton-Switchable Iridium Catalyst in Aqueous Media under Mild Temperatures and Pressures. *Nat. Chem.* **2012**, *4*, 383–388.
- (66) Moret, S.; Dyson, P. J.; Laurency, G. Direct Synthesis of Formic Acid from Carbon Dioxide by Hydrogenation in Acidic Media. *Nat. Commun.* **2014**, *5*, 4017.
- (67) Tanaka, R.; Yamashita, M.; Nozaki, K. Catalytic Hydrogenation of Carbon Dioxide Using Ir(III)–Pincer Complexes. *J. Am. Chem. Soc.* **2009**, *131*, 14168–14169.
- (68) Urakawa, A.; Iannuzzi, M.; Hutter, J.; Baiker, A. Towards a Rational Design of Ruthenium CO<sub>2</sub> Hydrogenation Catalysts by Ab Initio Metadynamics. *Chem. - Eur. J.* **2007**, *13*, 6828–6840.
- (69) Urakawa, A.; Jutz, F.; Laurency, G.; Baiker, A. Carbon Dioxide Hydrogenation Catalyzed by a Ruthenium Dihydride: A DFT and High-Pressure Spectroscopic Investigation. *Chem. - Eur. J.* **2007**, *13*, 3886–3899.
- (70) Hübner, S.; de Vries, J. G.; Farina, V. Why Does Industry Not Use Immobilized Transition Metal Complexes as Catalysts? *Adv. Synth. Catal.* **2016**, *358*, 3–25.
- (71) Jessop, P. G.; Hsiao, Y.; Ikariya, T.; Noyori, R. Homogeneous Catalysis in Supercritical Fluids: Hydrogenation of Supercritical Carbon Dioxide to Formic Acid, Alkyl Formates, and Formamides. *J. Am. Chem. Soc.* **1996**, *118*, 344–355.
- (72) Jessop, P. G.; Ikariya, T.; Noyori, R. Homogeneous Catalysis in Supercritical Fluids. *Science* **1995**, *269* (5227), 1065–1069.
- (73) Jessop, P. G.; Ikariya, T.; Noyori, R. Homogeneous Catalytic-Hydrogenation Of Supercritical Carbon-Dioxide. *Nature* **1994**, *368* (6468), 231–233.
- (74) Kröcher, O.; Köppel, R. A.; Baiker, A. Highly Active Ruthenium Complexes with Bidentate Phosphine Ligands for the Solvent-free Catalytic Synthesis of N,N-dimethylformamide and Methyl Formate. *Chem. Commun.* **1997**, *5*, 453–454.
- (75) Rohr, M.; Günther, M.; Jutz, F.; Grunwaldt, J.-D.; Emerich, H.; Beek, W. v.; Baiker, A. Evaluation of Strategies for the Immobilization of Bidentate Ruthenium–phosphine Complexes used for the Reductive Amination of Carbon Dioxide. *Appl. Catal., A* **2005**, *296*, 238–250.
- (76) Schmid, L.; Kröcher, O.; Köppel, R. A.; Baiker, A. Silica Xerogels Containing Bidentate Phosphine Ruthenium Complexes: Textural Properties and Catalytic Behaviour in the Synthesis of N,N-dimethylformamide from Carbon Dioxide. *Microporous Mesoporous Mater.* **2000**, *35–36*, 181–193.
- (77) Schmid, L.; Rohr, M.; Baiker, A. A Mesoporous Ruthenium Silica Hybrid Aerogel with Outstanding Catalytic Properties in the Synthesis of N,N-diethylformamide from CO<sub>2</sub>, H<sub>2</sub> and Diethylamine. *Chem. Commun.* **1999**, *22*, 2303–2304.
- (78) Zhang, Y.; Fei, J.; Yu, Y.; Zheng, X. Silica Immobilized Ruthenium Catalyst used for Carbon Dioxide Hydrogenation to Formic Acid (I): the Effect of Functionalizing Group and Additive on the Catalyst Performance. *Catal. Commun.* **2004**, *5*, 643–646.
- (79) Yu, Y.-M.; Fei, J.-H.; Zhang, Y.-P.; Zheng, X.-M. MCM-41 Bound Ruthenium Complex as Heterogeneous Catalyst for Hydrogenation I: Effect of Support, Ligand and Solvent on the Catalyst Performance. *Chin. J. Chem.* **2006**, *24*, 840–844.
- (80) Yu, Y.-M.; Zhang, Y.-P.; Fei, J.-H.; Zheng, X.-M. Silica Immobilized Ruthenium Catalyst for Formic Acid Synthesis from Supercritical Carbon Dioxide Hydrogenation II: Effect of Reaction Conditions on the Catalyst Performance. *Chin. J. Chem.* **2005**, *23*, 977–982.
- (81) Baffert, M.; Maishal, T. K.; Mathey, L.; Copéret, C.; Thieuleux, C. Tailored Ruthenium–N-Heterocyclic Carbene Hybrid Catalytic Materials for the Hydrogenation of Carbon Dioxide in the Presence of Amine. *ChemSusChem* **2011**, *4*, 1762–1765.
- (82) Xu, Z.; McNamara, N. D.; Neumann, G. T.; Schneider, W. F.; Hicks, J. C. Catalytic Hydrogenation of CO<sub>2</sub> to Formic Acid with Silica-Tethered Iridium Catalysts. *ChemCatChem* **2013**, *5*, 1769–1771.
- (83) McNamara, N. D.; Hicks, J. C. CO<sub>2</sub> Capture and Conversion with a Multifunctional Polyethyleneimine-Tethered Iminophosphine Iridium Catalyst/Adsorbent. *ChemSusChem* **2014**, *7*, 1114–1124.
- (84) Zhang, Z.; Xie, Y.; Li, W.; Hu, S.; Song, J.; Jiang, T.; Han, B. Hydrogenation of Carbon Dioxide is Promoted by a Task-Specific Ionic Liquid. *Angew. Chem., Int. Ed.* **2008**, *47*, 1127–1129.
- (85) Zhang, Z.; Hu, S.; Song, J.; Li, W.; Yang, G.; Han, B. Hydrogenation of CO<sub>2</sub> to Formic Acid Promoted by a Diamine-Functionalized Ionic Liquid. *ChemSusChem* **2009**, *2*, 234–238.
- (86) Feng, X.; Ding, X.; Jiang, D. Covalent Organic Frameworks. *Chem. Soc. Rev.* **2012**, *41*, 6010–6022.
- (87) Rogge, S. M. J.; Bavykina, A.; Hajek, J.; Garcia, H.; Olivos-Suarez, A. I.; Sepulveda-Escribano, A.; Vimont, A.; Clet, G.; Bazin, P.; Kapteijn, F.; Daturi, M.; Ramos-Fernandez, E. V.; Llabres i Xamena, F. X.; Van Speybroeck, V.; Gascon, J. Metal-organic and Covalent Organic Frameworks as Single-site Catalysts. *Chem. Soc. Rev.* **2017**, *46*, 3134–3184.
- (88) Redondo, A. B.; Morel, F. L.; Ranocchiar, M.; van Bokhoven, J. A. Functionalized Ruthenium-Phosphine Metal-Organic Framework for Continuous Vapor-Phase Dehydrogenation of Formic Acid. *ACS Catal.* **2015**, *5*, 7099–7103.
- (89) Yang, Z.-Z.; Zhang, H.; Yu, B.; Zhao, Y.; Ji, G.; Liu, Z. A Troger's Base-derived Microporous Organic Polymer: Design and Applications in CO<sub>2</sub>/H<sub>2</sub> Capture and Hydrogenation of CO<sub>2</sub> to Formic Acid. *Chem. Commun.* **2015**, *51*, 1271–1274.
- (90) Park, K.; Gunasekar, G. H.; Prakash, N.; Jung, K.-D.; Yoon, S. A Highly Efficient Heterogenized Iridium Complex for the Catalytic Hydrogenation of Carbon Dioxide to Formate. *ChemSusChem* **2015**, *8*, 3410–3413.
- (91) Gunniya Hariyanandam, G.; Hyun, D.; Natarajan, P.; Jung, K.-D.; Yoon, S. An Effective Heterogeneous Ir(III) Catalyst, Immobilized on a Heptazine-based Organic Framework, for the Hydrogenation of CO<sub>2</sub> to Formate. *Catal. Today* **2016**, *265*, 52–55.
- (92) Li, Z.-W.; Wang, T.-L.; He, Y.-M.; Wang, Z.-J.; Fan, Q.-H.; Pan, J.; Xu, L.-J. Air-Stable and Phosphine-Free Iridium Catalysts for Highly Enantioselective Hydrogenation of Quinoline Derivatives. *Org. Lett.* **2008**, *10*, 5265–5268.
- (93) Ogo, S.; Kabe, R.; Hayashi, H.; Harada, R.; Fukuzumi, S. Mechanistic Investigation of CO<sub>2</sub> Hydrogenation by Ru(II) and Ir(III) Aqua Complexes under Acidic Conditions: Two Catalytic Systems



Differing in the Nature of the Rate Determining Step. *Dalton Transactions* **2006**, 39, 4657–4663.

(94) Ogo, S.; Makiyama, N.; Watanabe, Y. pH-Dependent Transfer Hydrogenation of Water-Soluble Carbonyl Compounds with  $[\text{Cp}^*\text{IrIII}(\text{H}_2\text{O})_3]^{2+}$  ( $\text{Cp}^* = \eta^5\text{-C}_5\text{Me}_5$ ) as a Catalyst Precursor and  $\text{HCOONa}$  as a Hydrogen Donor in Water. *Organometallics* **1999**, 18, 5470–5474.

(95) Yamaguchi, R.; Ikeda, C.; Takahashi, Y.; Fujita, K.-i. Homogeneous Catalytic System for Reversible Dehydrogenation–Hydrogenation Reactions of Nitrogen Heterocycles with Reversible Interconversion of Catalytic Species. *J. Am. Chem. Soc.* **2009**, 131, 8410–8412.

(96) Kuhn, P.; Antonietti, M.; Thomas, A. Porous, Covalent Triazine-Based Frameworks Prepared by Ionothermal Synthesis. *Angew. Chem., Int. Ed.* **2008**, 47, 3450–3453.

(97) Bavykina, A. V.; Goesten, M. G.; Kapteijn, F.; Makkee, M.; Gascon, J. Efficient Production of Hydrogen from Formic Acid using a Covalent Triazine Framework Supported Molecular Catalyst. *ChemSusChem* **2015**, 8, 809–812.

(98) Bavykina, A. V.; Rozhko, E.; Goesten, M. G.; Wezendonk, T.; Seoane, B.; Kapteijn, F.; Makkee, M.; Gascon, J. Shaping Covalent Triazine Frameworks for the Hydrogenation of Carbon Dioxide to Formic Acid. *ChemCatChem* **2016**, 8, 2217–2221.

(99) Peng, G.; Sibener, S. J.; Schatz, G. C.; Ceyer, S. T.; Mavrikakis, M.  $\text{CO}_2$  Hydrogenation to Formic Acid on Ni(111). *J. Phys. Chem. C* **2012**, 116, 3001–3006.

(100) Olah, G. A.; Goepfert, A.; Prakash, G. K. Chemical Recycling of Carbon Dioxide to Methanol and DME: From Greenhouse Gas to Renewable, Environmentally Carbon Neutral Fuels and Synthetic Hydrocarbons. *J. Org. Chem.* **2009**, 74, 487–498.

(101) BASF 1923. German Patents 415686, 441433, 462837, 1923.

(102) Arcoumanis, C.; Bae, C.; Crookes, R.; Kinoshita, E. The Potential of di-methyl Ether (DME) as an Alternative Fuel for Compression-ignition Engines: A review. *Fuel* **2008**, 87, 1014–1030.

(103) Arena, F.; Mezzatesta, G.; Spadaro, L.; Trunfio, G. Latest Advances in the Catalytic Hydrogenation of Carbon Dioxide to Methanol/Dimethylether. In *Transformation and utilization of Carbon Dioxide*; Bhanage, B. M., Arai, M., Eds.; Springer: Berlin, 2014; Chapter 5, pp 103–130.

(104) Ganesh, I. Conversion of Carbon Dioxide into Methanol – a Potential Liquid Fuel: Fundamental Challenges and Opportunities (a Review). *Renewable Sustainable Energy Rev.* **2014**, 31, 221–257.

(105) Dubois, J.-L.; Sayama, K.; Arakawa, H. Conversion of  $\text{CO}_2$  to Dimethylether and Methanol over Hybrid Catalysts. *Chem. Lett.* **1992**, 21, 1115–1118.

(106) Chen, W.-H.; Lin, B.-J.; Lee, H.-M.; Huang, M.-H. One-step Synthesis of Dimethyl Ether from the Gas Mixture Containing  $\text{CO}_2$  with High Space Velocity. *Appl. Energy* **2012**, 98, 92–101.

(107) Graaf, G. H.; Sijtsma, P. J. J. M.; Stamhuis, E. J.; Joosten, G. E. H. Chemical Equilibria in Methanol Synthesis. *Chem. Eng. Sci.* **1986**, 41, 2883–2890.

(108) Graaf, G. H.; Winkelman, J. G. M. Chemical Equilibria in Methanol Synthesis Including the Water–Gas Shift Reaction: A Critical Reassessment. *Ind. Eng. Chem. Res.* **2016**, 55, 5854–5864.

(109) Graaf, G. H.; Stamhuis, E. J.; Beenackers, A. A. C. M. Kinetics of Low-pressure Methanol Synthesis. *Chem. Eng. Sci.* **1988**, 43, 3185–3195.

(110) Bussche, K. M. V.; Froment, G. F. A Steady-State Kinetic Model for Methanol Synthesis and the Water Gas Shift Reaction on a Commercial  $\text{Cu}/\text{ZnO}/\text{Al}_2\text{O}_3$  Catalyst. *J. Catal.* **1996**, 161, 1–10.

(111) Gallucci, F.; Basile, A. A Theoretical Analysis of Methanol Synthesis from  $\text{CO}_2$  and  $\text{H}_2$  in a Ceramic Membrane Reactor. *Int. J. Hydrogen Energy* **2007**, 32, 5050–5058.

(112) Fornero, E. L.; Chiavassa, D. L.; Bonivardi, A. L.; Baltanás, M. A.  $\text{CO}_2$  Capture via Catalytic Hydrogenation to Methanol: Thermodynamic Limit vs. ‘Kinetic Limit’. *Catal. Today* **2011**, 172, 158–165.

(113) Van-Dal, É.S.; Bouallou, C. Design and Simulation of a Methanol Production Plant from  $\text{CO}_2$  Hydrogenation. *J. Cleaner Prod.* **2013**, 57, 38–45.

(114) Meyer, J. J.; Tan, P.; Apfelbacher, A.; Daschner, R.; Hornung, A. Modeling of a Methanol Synthesis Reactor for Storage of Renewable Energy and Conversion of  $\text{CO}_2$  – Comparison of Two Kinetic Models. *Chem. Eng. Technol.* **2016**, 39, 233–245.

(115) Gaikwad, R.; Bansode, A.; Urakawa, A. High-pressure Advantages in Stoichiometric Hydrogenation of Carbon Dioxide to Methanol. *J. Catal.* **2016**, 343, 127–132.

(116) Bennekou, J. G. v.; Winkelman, J. G. M.; Venderbosch, R. H.; Nieland, S. D. G. B.; Heeres, H. J. Modeling and Experimental Studies on Phase and Chemical Equilibria in High-Pressure Methanol Synthesis. *Ind. Eng. Chem. Res.* **2012**, 51, 12233–12243.

(117) van Bennekou, J. G.; Venderbosch, R. H.; Winkelman, J. G. M.; Wilbers, E.; Assink, D.; Lemmens, K. P. J.; Heeres, H. J. Methanol Synthesis beyond Chemical Equilibrium. *Chem. Eng. Sci.* **2013**, 87, 204–208.

(118) Bansode, A.; Urakawa, A. Towards Full One-pass Conversion of Carbon Dioxide to Methanol and Methanol-derived Products. *J. Catal.* **2014**, 309, 66–70.

(119) Bos, M. J.; Brilman, D. W. F. A Novel Condensation Reactor for Efficient  $\text{CO}_2$  to Methanol Conversion for Storage of Renewable Electric Energy. *Chem. Eng. J.* **2015**, 278, 527–532.

(120) Shen, W.-J.; Jun, K.-W.; Choi, H.-S.; Lee, K.-W. Thermodynamic Investigation of Methanol and Dimethyl Ether Synthesis from  $\text{CO}_2$  Hydrogenation. *Korean J. Chem. Eng.* **2000**, 17, 210–216.

(121) Aguayo, A. T.; Ereña, J.; Mier, D.; Arandes, J. M.; Olazar, M.; Bilbao, J. Kinetic Modeling of Dimethyl Ether Synthesis in a Single Step on a  $\text{CuO}-\text{ZnO}-\text{Al}_2\text{O}_3/\gamma\text{-Al}_2\text{O}_3$  Catalyst. *Ind. Eng. Chem. Res.* **2007**, 46, 5522–5530.

(122) Qin, Z.-z.; Su, T.-m.; Ji, H.-b.; Jiang, Y.-x.; Liu, R.-w.; Chen, J.-h. Experimental and Theoretical Study of the Intrinsic Kinetics for Dimethyl Ether Synthesis from  $\text{CO}_2$  over  $\text{Cu}-\text{Fe}-\text{Zr}/\text{HZSM}-5$ . *AIChE J.* **2015**, 61, 1613–1627.

(123) Ereña, J.; Sierra, I.; Aguayo, A. T.; Ateka, A.; Olazar, M.; Bilbao, J. Kinetic Modelling of Dimethyl Ether Synthesis from  $(\text{H}_2 + \text{CO}_2)$  by Considering Catalyst Deactivation. *Chem. Eng. J.* **2011**, 174, 660–667.

(124) Jia, G.; Tan, Y.; Han, Y. Comparative Study on the Thermodynamics of Dimethyl Ether Synthesis from  $\text{CO}$  Hydrogenation and  $\text{CO}_2$  Hydrogenation. *Ind. Eng. Chem. Res.* **2006**, 45, 1152–1159.

(125) Jadhav, S. G.; Vaidya, P. D.; Bhanage, B. M.; Joshi, J. B. Catalytic Carbon Dioxide Hydrogenation to Methanol: A Review of Recent Studies. *Chem. Eng. Res. Des.* **2014**, 92, 2557–2567.

(126) Liu, X.-M.; Lu, G. Q.; Yan, Z.-F.; Beltrami, J. Recent Advances in Catalyst for Methanol Synthesis via Hydrogenation of  $\text{CO}$  and  $\text{CO}_2$ . *Ind. Eng. Chem. Res.* **2003**, 42, 6518–6530.

(127) Wang, W.; Wang, S.; Ma, X.; Gong, J. Recent Advances in Catalytic Hydrogenation of Carbon Dioxide. *Chem. Soc. Rev.* **2011**, 40, 3703–3727.

(128) Saito, M. R&D Activities in Japan on Methanol Synthesis from  $\text{CO}_2$  and  $\text{H}_2$ . *Catal. Surv. Jpn.* **1998**, 2, 175–184.

(129) Chinchin, G. C.; Hay, C. M.; Vandervell, H. D.; Waugh, K. C. The Measurement of Copper Surface Areas by Reactive Frontal Chromatography. *J. Catal.* **1987**, 103, 79–86.

(130) Twigg, M. V.; Spencer, M. S. Deactivation of Supported Copper Metal Catalysts for Hydrogenation Reactions. *Appl. Catal., A* **2001**, 212, 161–174.

(131) Behrens, M.; Schlögl, R. How to Prepare a Good  $\text{Cu}/\text{ZnO}$  Catalyst or the Role of Solid State Chemistry for the Synthesis of Nanostructured Catalysts. *Z. Anorg. Allg. Chem.* **2013**, 639, 2683–2695.

(132) Kasatkin, I.; Kurr, P.; Kniep, B.; Trunschke, A.; Schlögl, R. Role of Lattice Strain and Defects in Copper Particles on the Activity of  $\text{Cu}/\text{ZnO}/\text{Al}_2\text{O}_3$  Catalysts for Methanol Synthesis. *Angew. Chem., Int. Ed.* **2007**, 46, 7324–7327.

(133) Kuld, S.; Thorhauge, M.; Falsig, H.; Elkjaer, C. F.; Helveg, S.; Chorkendorff, I.; Sehested, J. Quantifying the Promotion of  $\text{Cu}$  Catalysts by  $\text{ZnO}$  for Methanol Synthesis. *Science* **2016**, 352 (6288), 969–974.

(134) Le Valant, A.; Comminges, C.; Tisseraud, C.; Canaff, C.; Pinard, L.; Pouilloux, Y. The  $\text{Cu}-\text{ZnO}$  Synergy in Methanol Synthesis from  $\text{CO}_2$ , Part 1: Origin of Active Site Explained by Experimental Studies



and a Sphere Contact Quantification Model on Cu+ZnO Mechanical Mixtures. *J. Catal.* **2015**, *324*, 41–49.

(135) Ertl, G.; Knözinger, H.; Schüth, F.; Weitkamp, J. *Handbook of Heterogeneous Catalysis*; Wiley-VCH: 1997; Vol. 1.

(136) de Jong, K. P. *Synthesis of Solid Catalysts*; Wiley-VCH: Weinheim, 2009.

(137) Behrens, M.; Lolli, G.; Muratova, N.; Kasatkin, I.; Havecker, M.; d'Alnoncourt, R. N.; Storcheva, O.; Kohler, K.; Muhler, M.; Schlögl, R. The Effect of Al-doping on ZnO Nanoparticles Applied as Catalyst Support. *Phys. Chem. Chem. Phys.* **2013**, *15*, 1374–1381.

(138) Behrens, M.; Brennecke, D.; Girgsdies, F.; Kießner, S.; Trunschke, A.; Nasrudin, N.; Zakaria, S.; Idris, N. F.; Hamid, S. B. A.; Kniep, B.; Fischer, R.; Busser, W.; Muhler, M.; Schlögl, R. Understanding the Complexity of a Catalyst Synthesis: Co-precipitation of Mixed Cu,Zn,Al Hydroxycarbonate Precursors for Cu/ZnO/Al<sub>2</sub>O<sub>3</sub> Catalysts Investigated by Titration Experiments. *Appl. Catal., A* **2011**, *392*, 93–102.

(139) Behrens, M. Meso- and Nano-structuring of Industrial Cu/ZnO/(Al<sub>2</sub>O<sub>3</sub>) catalysts. *J. Catal.* **2009**, *267*, 24–29.

(140) Behrens, M.; Girgsdies, F.; Trunschke, A.; Schlögl, R. Minerals as Model Compounds for Cu/ZnO Catalyst Precursors: Structural and Thermal Properties and IR Spectra of Mineral and Synthetic (Zincian) Malachite, Rosasite and Aurichalcite and a Catalyst Precursor Mixture. *Eur. J. Inorg. Chem.* **2009**, *2009*, 1347–1357.

(141) Behrens, M.; Girgsdies, F. Structural Effects of Cu/Zn Substitution in the Malachite-Rosasite System. *Z. Anorg. Allg. Chem.* **2010**, *636*, 919–927.

(142) Baltes, C.; Vukojevic, S.; Schuth, F. Correlations between Synthesis, Precursor, and Catalyst Structure and Activity of a Large Set of CuO/ZnO/Al<sub>2</sub>O<sub>3</sub> Catalysts for Methanol Synthesis. *J. Catal.* **2008**, *258*, 334–344.

(143) Fan, H.; Zheng, H.; Li, Z. Preparation of Cu/ZnO/Al<sub>2</sub>O<sub>3</sub> Catalyst under Microwave Irradiation for Slurry Methanol Synthesis. *Front. Chem. Eng. China* **2010**, *4*, 445–451.

(144) Jung, H.; Yang, D.-R.; Joo, O.-S.; Jung, K.-D. The Importance of the Aging Time to Prepare Cu/ZnO/Al<sub>2</sub>O<sub>3</sub> Catalyst with High Surface Area in Methanol Synthesis. *Bull. Korean Chem. Soc.* **2010**, *31*, 1241–1246.

(145) Kühn, S.; Tarasov, A.; Zander, S.; Kasatkin, I.; Behrens, M. Cu-Based Catalyst Resulting from a Cu,Zn,Al Hydrotalcite-Like Compound: A Microstructural, Thermoanalytical, and In Situ XAS Study. *Chem. - Eur. J.* **2014**, *20*, 3782–3792.

(146) Prieto, G.; de Jong, K. P.; de Jongh, P. E. Towards 'Greener' Catalyst Manufacture: Reduction of Wastewater from the Preparation of Cu/ZnO/Al<sub>2</sub>O<sub>3</sub> Methanol Synthesis Catalysts. *Catal. Today* **2013**, *215*, 142–151.

(147) Behrens, M.; Kießner, S.; Girgsdies, F.; Kasatkin, I.; Hermerschmidt, F.; Mette, K.; Ruland, H.; Muhler, M.; Schlögl, R. Knowledge-based Development of a Nitrate-free Synthesis Route for Cu/ZnO Methanol Synthesis Catalysts via formate Precursors. *Chem. Commun.* **2011**, *47*, 1701–1703.

(148) Wang, D.; Zhao, J.; Song, H.; Chou, L. Characterization and Performance of Cu/ZnO/Al<sub>2</sub>O<sub>3</sub> Catalysts Prepared via Decomposition of M(Cu, Zn)-ammonia Complexes under Sub-atmospheric Pressure for Methanol Synthesis from H<sub>2</sub> and CO<sub>2</sub>. *J. Nat. Gas Chem.* **2011**, *20*, 629–634.

(149) Kondrat, S.; Smith, P. J.; Wells, P. P.; Chater, P. A.; Carter, J. H.; Morgan, D. J.; Fiordaliso, E. M.; Wagner, J. B.; Davies, T. E.; Lu, L.; Bartley, J. K.; Taylor, S. H.; Spencer, M. S.; Kiely, C. J.; Kelly, G. J.; Park, C. W.; Rosseinsky, M. J.; Hutchings, G. J. Stable Amorphous Georgerite as a Precursor to a High-activity Catalyst. *Nature* **2016**, *531*, 83–87.

(150) Arena, F.; Barbera, K.; Italiano, G.; Bonura, G.; Spadaro, L.; Frusteri, F. Synthesis, Characterization and Activity Pattern of Cu–ZnO/ZrO<sub>2</sub> Catalysts in the Hydrogenation of Carbon Dioxide to Methanol. *J. Catal.* **2007**, *249*, 185–194.

(151) Jiang, X.; Koizumi, N.; Guo, X.; Song, C. Bimetallic Pd–Cu Catalysts for Selective CO<sub>2</sub> Hydrogenation to Methanol. *Appl. Catal., B* **2015**, *170–171*, 173–185.

(152) Wambach, J.; Baiker, A.; Wokaun, A. CO<sub>2</sub> Hydrogenation over Metal/zirconia Catalysts. *Phys. Chem. Chem. Phys.* **1999**, *1*, 5071–5080.

(153) Raudaskoski, R.; Niemelä, M. V.; Keiski, R. L. The Effect of Ageing Time on co-precipitated Cu/ZnO/ZrO<sub>2</sub> Catalysts used in Methanol Synthesis from CO<sub>2</sub> and H<sub>2</sub>. *Top. Catal.* **2007**, *45*, 57–60.

(154) Frei, E.; Schaadt, A.; Ludwig, T.; Hillebrecht, H.; Krossing, I. The Influence of the Precipitation/Ageing Temperature on a Cu/ZnO/ZrO<sub>2</sub> Catalyst for Methanol Synthesis from H<sub>2</sub> and CO<sub>2</sub>. *ChemCatChem* **2014**, *6*, 1721–1730.

(155) Li, L.; Mao, D.; Yu, J.; Guo, X. Highly Selective Hydrogenation of CO<sub>2</sub> to Methanol over CuO–ZnO–ZrO<sub>2</sub> Catalysts Prepared by a Surfactant-assisted co-precipitation Method. *J. Power Sources* **2015**, *279*, 394–404.

(156) Samson, K.; Sliwa, M.; Socha, R. P.; Gora-Marek, K.; Mucha, D.; Rutkowska-Zbik, D.; Paul, J.-F.; Ruggiero-Mikolajczyk, M.; Grabowski, R.; Sloczynski, J. Influence of ZrO<sub>2</sub> Structure and Copper Electronic State on Activity of Cu/ZrO<sub>2</sub> Catalysts in Methanol Synthesis from CO<sub>2</sub>. *ACS Catal.* **2014**, *4*, 3730–3741.

(157) Wittoon, T.; Chalorngtham, J.; Dumrongbunditkul, P.; Chareonpanich, M.; Limtrakul, J. CO<sub>2</sub> Hydrogenation to Methanol over Cu/ZrO<sub>2</sub> Catalysts: Effects of Zirconia Phases. *Chem. Eng. J.* **2016**, *293*, 327–336.

(158) Angelo, L.; Kobl, K.; Tejada, L. M. M.; Zimmermann, Y.; Parkhomenko, K.; Roger, A.-C. Study of CuZnMO<sub>x</sub> Oxides (M = Al, Zr, Ce, CeZr) for the Catalytic Hydrogenation of CO<sub>2</sub> into Methanol. *C. R. Chim.* **2015**, *18*, 250–260.

(159) Graciani, J.; Mudiyanse, K.; Xu, F.; Baber, A. E.; Evans, J.; Senanayake, S. D.; Stacchiola, D. J.; Liu, P.; Hrbek, J.; Fernandez Sanz, J.; Rodriguez, J. A. Highly Active Copper-ceria and Copper-ceria-titania Catalysts for Methanol Synthesis from CO<sub>2</sub>. *Science* **2014**, *345*, 546–550.

(160) Fornero, E. L.; Sanguineti, P. B.; Chiavassa, D. L.; Bonivardi, A. L.; Baltanás, M. A. Performance of Ternary Cu–Ga<sub>2</sub>O<sub>3</sub>–ZrO<sub>2</sub> Catalysts in the Synthesis of Methanol using CO<sub>2</sub>-rich gas Mixtures. *Catal. Today* **2013**, *213*, 163–170.

(161) Kikuzono, Y.; Kagami, S.; Naito, S.; Onishi, T.; Tamaru, K. Selective Hydrogenation of Carbon Monoxide on Palladium Catalysts. *Faraday Discuss. Chem. Soc.* **1981**, *72*, 135–143.

(162) Gotti, A.; Prins, R. Basic Metal Oxides as Cocatalysts for Cu/SiO<sub>2</sub> Catalysts in the Conversion of Synthesis Gas to Methanol. *J. Catal.* **1998**, *178*, 511–519.

(163) Fujitani, T.; Saito, M.; Kanai, Y.; Watanabe, T.; Nakamura, J.; Uchijima, T. Development of an Active Ga<sub>2</sub>O<sub>3</sub> Supported Palladium Catalyst for the Synthesis of Methanol from Carbon Dioxide and Hydrogen. *Appl. Catal., A* **1995**, *125*, L199–L202.

(164) Collins, S. E.; Baltanás, M. A.; Bonivardi, A. L. An Infrared Study of the Intermediates of Methanol Synthesis from Carbon Dioxide over Pd/β-Ga<sub>2</sub>O<sub>3</sub>. *J. Catal.* **2004**, *226*, 410–421.

(165) Collins, S. E.; Delgado, J. J.; Mira, C.; Calvino, J. J.; Bernal, S.; Chiavassa, D. L.; Baltanás, M. A.; Bonivardi, A. L. The role of Pd–Ga Bimetallic Particles in the Bifunctional Mechanism of Selective Methanol Synthesis via CO<sub>2</sub> Hydrogenation on a Pd/Ga<sub>2</sub>O<sub>3</sub> Catalyst. *J. Catal.* **2012**, *292*, 90–98.

(166) Collins, S. E.; Chiavassa, D. L.; Bonivardi, A. L.; Baltanás, M. A. Hydrogen Spillover in Ga<sub>2</sub>O<sub>3</sub>–Pd/SiO<sub>2</sub> Catalysts for Methanol Synthesis from CO<sub>2</sub>/H<sub>2</sub>. *Catal. Lett.* **2005**, *103*, 83–88.

(167) Chiavassa, D. L.; Collins, S. E.; Bonivardi, A. L.; Baltanás, M. A. Methanol Synthesis from CO<sub>2</sub>/H<sub>2</sub> using Ga<sub>2</sub>O<sub>3</sub>–Pd/silica Catalysts: Kinetic Modeling. *Chem. Eng. J.* **2009**, *150*, 204–212.

(168) Oyola-Rivera, O.; Baltanás, M. A.; Cardona-Martínez, N. CO<sub>2</sub> Hydrogenation to Methanol and Dimethyl Ether by Pd–Pd<sub>2</sub>Ga Catalysts Supported over Ga<sub>2</sub>O<sub>3</sub> Polymorphs. *Journal of CO<sub>2</sub> Utilization* **2015**, *9*, 8–15.

(169) Koizumi, N.; Jiang, X.; Kugai, J.; Song, C. Effects of Mesoporous Silica Supports and Alkaline Promoters on Activity of Pd Catalysts in CO<sub>2</sub> Hydrogenation for Methanol Synthesis. *Catal. Today* **2012**, *194*, 16–24.

(170) Díez-Ramírez, J.; Valverde, J. L.; Sánchez, P.; Dorado, F. CO<sub>2</sub> Hydrogenation to Methanol at Atmospheric Pressure: Influence of the

Preparation Method of Pd/ZnO Catalysts. *Catal. Lett.* **2016**, *146*, 373–382.

(171) Bahruji, H.; Bowker, M.; Hutchings, G.; Dimitratos, N.; Wells, P.; Gibson, E.; Jones, W.; Brookes, C.; Morgan, D.; Lalev, G. Pd/ZnO Catalysts for Direct CO<sub>2</sub> Hydrogenation to Methanol. *J. Catal.* **2016**, *343*, 133.

(172) Xu, J.; Su, X.; Liu, X.; Pan, X.; Pei, G.; Huang, Y.; Wang, X.; Zhang, T.; Geng, H. Methanol Synthesis from CO<sub>2</sub> and H<sub>2</sub> over Pd/ZnO/Al<sub>2</sub>O<sub>3</sub>: Catalyst Structure Dependence of Methanol Selectivity. *Appl. Catal., A* **2016**, *514*, 51–59.

(173) Melaet, G.; Lindeman, A. E.; Somorjai, G. A. Cobalt Particle Size Effects in the Fischer–Tropsch Synthesis and in the Hydrogenation of CO<sub>2</sub> Studied with Nanoparticle Model Catalysts on Silica. *Top. Catal.* **2014**, *57*, 500–507.

(174) Alayoglu, S.; Beaumont, S. K.; Zheng, F.; Pushkarev, V. V.; Zheng, H.; Iablokov, V.; Liu, Z.; Guo, J.; Kruse, N.; Somorjai, G. A. CO<sub>2</sub> Hydrogenation Studies on Co and CoPt Bimetallic Nanoparticles under Reaction Conditions using TEM, XPS and NEXAFS. *Top. Catal.* **2011**, *54*, 778–785.

(175) Hartadi, Y.; Widmann, D.; Behm, R. J. Methanol Synthesis via CO<sub>2</sub> Hydrogenation over a Au/ZnO Catalyst: an Isotope Labelling Study on the Role of CO in the Reaction Process. *Phys. Chem. Chem. Phys.* **2016**, *18*, 10781–10791.

(176) Pasupulety, N.; Driss, H.; Alhamed, Y. A.; Alzahrani, A. A.; Daous, M. A.; Petrov, L. Studies on Au/Cu–Zn–Al Catalyst for Methanol Synthesis from CO<sub>2</sub>. *Appl. Catal., A* **2015**, *504*, 308.

(177) Studt, F.; Sharafutdinov, I.; Abild-Pedersen, F.; Elkjaer, C. F.; Hummelshøj, J. S.; Dahl, S.; Chorkendorff, I.; Nørskov, J. K. Discovery of a Ni–Ga Catalyst for Carbon Dioxide Reduction to Methanol. *Nat. Chem.* **2014**, *6*, 320–324.

(178) Martin, O.; Martín, A. J.; Mondelli, C.; Mitchell, S.; Segawa, T. F.; Hauert, R.; Drouilly, C.; Curulla-Ferré, D.; Pérez-Ramírez, J. Indium Oxide as a Superior Catalyst for Methanol Synthesis by CO<sub>2</sub> Hydrogenation. *Angew. Chem., Int. Ed.* **2016**, *55*, 6261–6265.

(179) Fujimoto, K.; Shikada, T. Selective Synthesis of C<sub>2</sub>–C<sub>5</sub> Hydrocarbons from Carbon Dioxide Utilizing a Hybrid Catalyst Composed of a Methanol Synthesis Catalyst and Zeolite. *Appl. Catal.* **1987**, *31*, 13–23.

(180) Chang, C. D.; Silvestri, A. J. Conversion of Synthesis Gas to Gasoline. US3894102 A, 1975.

(181) Sofianos, A. C.; Scurrall, M. S. Conversion of Synthesis Gas to Dimethyl Ether over Bifunctional Catalytic Systems. *Ind. Eng. Chem. Res.* **1991**, *30*, 2372–2378.

(182) Sartipi, S.; Makkee, M.; Kapteijn, F.; Gascon, J. Catalysis Engineering of Bifunctional Solids for the one-Step Synthesis of Liquid fuels from Syngas: a Review. *Catal. Sci. Technol.* **2014**, *4*, 893–907.

(183) Liu, X.-M.; Yan, Z.-F.; Lu, G.-Q. Role of Nanosized Zirconia on the Properties of Cu/Ga<sub>2</sub>O<sub>3</sub>/ZrO<sub>2</sub> Catalysts for Methanol Synthesis. *Chin. J. Chem.* **2006**, *24*, 172–176.

(184) Tidona, B.; Koppold, C.; Bansode, A.; Urakawa, A.; Rudolf von Rohr, P. CO<sub>2</sub> Hydrogenation to Methanol at Pressures up to 950 bar. *J. Supercrit. Fluids* **2013**, *78*, 70–77.

(185) Zhan, H.; Li, F.; Gao, P.; Zhao, N.; Xiao, F.; Wei, W.; Zhong, L.; Sun, Y. Methanol Synthesis from CO<sub>2</sub> Hydrogenation over La–M–Cu–Zn–O (M = Y, Ce, Mg, Zr) Catalysts Derived from Perovskite-type Precursors. *J. Power Sources* **2014**, *251*, 113–121.

(186) Angelo, L.; Girleanu, M.; Ersen, O.; Serra, C.; Parkhomenko, K.; Roger, A.-C. Catalyst Synthesis by Continuous coprecipitation under Micro-fluidic Conditions: Application to the Preparation of Catalysts for Methanol Synthesis from CO<sub>2</sub>/H<sub>2</sub>. *Catal. Today* **2016**, *270*, 59–67.

(187) Xu, M.; Lunsford, J. H.; Goodman, D. W.; Bhattacharyya, A. Synthesis of Dimethyl Ether (DME) from Methanol over Solid-acid Catalysts. *Appl. Catal., A* **1997**, *149* (2), 289–301.

(188) Aguayo, A. T.; Ereña, J.; Sierra, I.; Olazar, M.; Bilbao, J. Deactivation and Regeneration of Hybrid Catalysts in the Single-step Synthesis of Dimethyl Ether from Syngas and CO<sub>2</sub>. *Catal. Today* **2005**, *106*, 265–270.

(189) Jun, K.-W.; Rama Rao, K. S.; Jung, M.-H.; Lee, K.-W. The CO<sub>2</sub> Hydrogenation toward the Mixture of Methanol and Dimethyl Ether:

Investigation of Hybrid Catalysts. *Bull. Korean Chem. Soc.* **1998**, *19*, 466–470.

(190) Sun, Y.; Campbell, S. M.; Lunsford, J. H.; Lewis, G. E.; Palke, D.; Tau, L. M. The Catalytic Conversion of Methyl Chloride to Ethylene and Propylene over Phosphorus-Modified Mg–ZSM-5 Zeolites. *J. Catal.* **1993**, *143*, 32–44.

(191) Topsøe, N.-Y.; Pedersen, K.; Derouane, E. G. Infrared and Temperature-programmed Desorption Study of the Acidic Properties of ZSM-5-type Zeolites. *J. Catal.* **1981**, *70*, 41–52.

(192) Stöcker, M. Methanol-to-hydrocarbons: Catalytic Materials and their Behavior. *Microporous Mesoporous Mater.* **1999**, *29*, 3–48.

(193) Son-Ki, I.; Se-Won, B.; Young-Kwon, P.; Jong-Ki, J. CO<sub>2</sub> Hydrogenation over Copper-Based Hybrid Catalysts for the Synthesis of Oxygenates. In *Utilization of Greenhouse Gases*; American Chemical Society: Washington, DC, 2003; Vol. 852, pp 183–194.

(194) Ge, Q.; Huang, Y.; Qiu, F.; Zhang, C. New Bifunctional Catalyst For Direct Synthesis Of Dimethyl Ether. *J. Nat. Gas Chem.* **1999**, *8*, 280–285.

(195) Bonura, G.; Cordaro, M.; Spadaro, L.; Cannilla, C.; Arena, F.; Frusteri, F. Hybrid Cu–ZnO–ZrO<sub>2</sub>/H-ZSM5 System for the Direct Synthesis of DME by CO<sub>2</sub> Hydrogenation. *Appl. Catal., B* **2013**, *140*–*141*, 16–24.

(196) Gao, W.; Wang, H.; Wang, Y.; Guo, W.; Jia, M. Dimethyl Ether Synthesis from CO<sub>2</sub> Hydrogenation on La-modified CuO–ZnO–Al<sub>2</sub>O<sub>3</sub>/HZSM-5 bifunctional Catalysts. *J. Rare Earths* **2013**, *31*, 470–476.

(197) Zhao, Y.; Chen, J.; Zhang, J. Effects of ZrO<sub>2</sub> on the Performance of CuO–ZnO–Al<sub>2</sub>O<sub>3</sub>/HZSM-5 Catalyst for Dimethyl Ether Synthesis from CO<sub>2</sub> Hydrogenation. *J. Nat. Gas Chem.* **2007**, *16*, 389–392.

(198) Liu, R.-w.; Qin, Z.-z.; Ji, H.-b.; Su, T.-m. Synthesis of Dimethyl Ether from CO<sub>2</sub> and H<sub>2</sub> Using a Cu–Fe–Zr/HZSM-5 Catalyst System. *Ind. Eng. Chem. Res.* **2013**, *52*, 16648–16655.

(199) Wang, S.; Mao, D.; Guo, X.; Wu, G.; Lu, G. Dimethyl Ether Synthesis via CO<sub>2</sub> Hydrogenation over CuO–TiO<sub>2</sub>–ZrO<sub>2</sub>/HZSM-5 Bifunctional Catalysts. *Catal. Commun.* **2009**, *10*, 1367–1370.

(200) Zhang, M.-H.; Liu, Z.-M.; Lin, G.-D.; Zhang, H.-B. Pd/CNT-promoted CuZrO<sub>2</sub>/HZSM-5 hybrid Catalysts for direct Synthesis of DME from CO<sub>2</sub>/H<sub>2</sub>. *Appl. Catal., A* **2013**, *451*, 28–35.

(201) Zha, F.; Tian, H.; Yan, J.; Chang, Y. Multi-walled Carbon Nanotubes as Catalyst Promoter for Dimethyl Ether Synthesis from CO<sub>2</sub> Hydrogenation. *Appl. Surf. Sci.* **2013**, *285* (Part B), 945–951.

(202) Witton, T.; Permsirivanich, T.; Kanjanasontorn, N.; Akkaraphataworn, C.; Seubsai, A.; Faungnawakij, K.; Warakulwit, C.; Chareonpanich, M.; Limtrakul, J. Direct Synthesis of Dimethyl Ether from CO<sub>2</sub> Hydrogenation over Cu–ZnO–ZrO<sub>2</sub>/SO<sub>4</sub>–ZrO<sub>2</sub> hybrid Catalysts: Effects of Sulfur-to-zirconia Ratios. *Catal. Sci. Technol.* **2015**, *5*, 2347–2357.

(203) Naito, S.; Ogawa, O.; Ichikawa, M.; Tamaru, K. Formation of Dimethyl Ether from Hydrogen and Carbon Dioxide over a Graphite–PdCl<sub>2</sub>–Na Catalyst. *J. Chem. Soc., Chem. Commun.* **1972**, *23*, 1266–1266.

(204) Frusteri, F.; Bonura, G.; Cannilla, C.; Drago Ferrante, G.; Aloise, A.; Catizzzone, E.; Migliori, M.; Giordano, G. Stepwise Tuning of Metal-oxide and Acid Sites of CuZnZr-MFI hybrid Catalysts for the Direct DME Synthesis by CO<sub>2</sub> Hydrogenation. *Appl. Catal., B* **2015**, *176*–*177*, 522–531.

(205) Sun, K.; Lu, W.; Wang, M.; Xu, X. Low-temperature Synthesis of DME from CO<sub>2</sub>/H<sub>2</sub> over Pd-modified CuO–ZnO–Al<sub>2</sub>O<sub>3</sub>–ZrO<sub>2</sub>/HZSM-5 Catalysts. *Catal. Commun.* **2004**, *5*, 367–370.

(206) Zhang, Y.; Li, D.; Zhang, Y.; Cao, Y.; Zhang, S.; Wang, K.; Ding, F.; Wu, J. V-modified CuO–ZnO–ZrO<sub>2</sub>/HZSM-5 Catalyst for Efficient Direct Synthesis of DME from CO<sub>2</sub> Hydrogenation. *Catal. Commun.* **2014**, *55*, 49–52.

(207) Qi, G.-X.; Fei, J.-H.; Zheng, X.-M.; Hou, Z.-Y. DME Synthesis from Carbon Dioxide and Hydrogen over Cu–Mo/HZSM-5. *Catal. Lett.* **2001**, *72*, 121–124.

(208) Li, Q.; Xin, C.; Lian, P. The Synthesis and Application of CuO–ZnO/HZSM-5 Catalyst With Core-shell Structure. *Pet. Sci. Technol.* **2012**, *30*, 2187–2195.



- (209) Liu, R.; Tian, H.; Yang, A.; Zha, F.; Ding, J.; Chang, Y. Preparation of HZSM-5 Membrane Packed CuO–ZnO–Al<sub>2</sub>O<sub>3</sub> Nanoparticles for Catalysing Carbon Dioxide Hydrogenation to Dimethyl Ether. *Appl. Surf. Sci.* **2015**, *345*, 1–9.
- (210) Wang, J.; Zeng, C. Al<sub>2</sub>O<sub>3</sub> Effect on the Catalytic Activity of Cu–ZnO–Al<sub>2</sub>O<sub>3</sub>–SiO<sub>2</sub> Catalysts for Dimethyl Ether Synthesis from CO<sub>2</sub> Hydrogenation. *J. Nat. Gas Chem.* **2005**, *14*, 156–162.
- (211) Bonura, G.; Cordaro, M.; Cannilla, C.; Mezzapica, A.; Spadaro, L.; Arena, F.; Frusteri, F. Catalytic Behaviour of a Bifunctional System for the One Step Synthesis of DME by CO<sub>2</sub> Hydrogenation. *Catal. Today* **2014**, *228*, 51–57.
- (212) Gascon, J.; van Ommen, J. R.; Moulijn, J. A.; Kapteijn, F. Structuring Catalyst and Reactor - an Inviting Avenue to Process Intensification. *Catal. Sci. Technol.* **2015**, *5*, 807–817.
- (213) Chinchin, G. C.; Denny, P. J.; Jennings, J. R.; Spencer, M. S.; Waugh, K. C. Synthesis of Methanol- Part 1. Catalysts and Kinetics. *Appl. Catal.* **1988**, *36*, 1–65.
- (214) Chorkendorff, I.; Niemantsverdriet, J. W. Methanol Synthesis. In *Concepts of modern catalysis and kinetics*; Wiley-VCH: Weinheim, 2003; Section 8.3.1, pp. 311–323.
- (215) Yang, Y.; Mims, C. A.; Mei, D. H.; Peden, C. H. F.; Campbell, C. T. Mechanistic Studies of Methanol Synthesis over Cu from CO/CO<sub>2</sub>/H<sub>2</sub>/H<sub>2</sub>O Mixtures: The Source of C in Methanol and the Role of Water. *J. Catal.* **2013**, *298*, 10–17.
- (216) Nakamura, J.; Uchijima, T.; Kanai, Y.; Fujitani, T. The Role of ZnO in Cu/ZnO Methanol Synthesis Catalysts. *Catal. Today* **1996**, *28*, 223–230.
- (217) Ostrovskii, V. E. Mechanisms of Methanol Synthesis from Hydrogen and Carbon Oxides at Cu–Zn-Containing Catalysts in the Context of some Fundamental Problems of Heterogeneous Catalysis. *Catal. Today* **2002**, *77*, 141–160.
- (218) Choi, Y.; Futagami, K.; Fujitani, T.; Nakamura, J. The role of ZnO in Cu/ZnO Methanol Synthesis Catalysts —morphology Effect or Active Site Model? *Appl. Catal., A* **2001**, *208*, 163–167.
- (219) Arena, F.; Mezzatesta, G.; Zafarana, G.; Trunfio, G.; Frusteri, F.; Spadaro, L. How Oxide Carriers Control the Catalytic Functionality of the Cu–ZnO System in the Hydrogenation of CO<sub>2</sub> to Methanol. *Catal. Today* **2013**, *210*, 39–46.
- (220) Kunkes, E. L.; Studt, F.; Abild-Pedersen, F.; Schlögl, R.; Behrens, M. Hydrogenation of CO<sub>2</sub> to Methanol and CO on Cu/ZnO/Al<sub>2</sub>O<sub>3</sub>: Is there a Common Intermediate or not? *J. Catal.* **2015**, *328*, 43–48.
- (221) Behrens, M.; Studt, F.; Kasatkin, I.; Kühl, S.; Hävecker, M.; Abild-Pedersen, F.; Zander, S.; Girsdiess, F.; Kurr, P.; Knief, B.-L.; Tovar, M.; Fischer, R. W.; Nørskov, J. K.; Schlögl, R. The Active Site of Methanol Synthesis over Cu/ZnO/Al<sub>2</sub>O<sub>3</sub> Industrial Catalysts. *Science* **2012**, *336*, 893–897.
- (222) Kuld, S.; Conradsen, C.; Moses, P. G.; Chorkendorff, I.; Sehested, J. Quantification of Zinc Atoms in a Surface Alloy on Copper in an Industrial-Type Methanol Synthesis Catalyst. *Angew. Chem., Int. Ed.* **2014**, *53*, 5941–5945.
- (223) Zander, S.; Kunkes, E. L.; Schuster, M. E.; Schumann, J.; Weinberg, G.; Teschner, D.; Jacobsen, N.; Schlögl, R.; Behrens, M. The Role of the Oxide Component in the Development of Copper Composite Catalysts for Methanol Synthesis. *Angew. Chem., Int. Ed.* **2013**, *52* (25), 6536–6540.
- (224) Klier, K. Methanol Synthesis. *Adv. Catal.* **1982**, *31*, 243–313.
- (225) Bems, B.; Schur, M.; Dassenoy, A.; Junkes, H.; Herein, D.; Schlögl, R. Relations between Synthesis and Microstructural Properties of Copper/zinc Hydroxycarbonates. *Chem. - Eur. J.* **2003**, *9*, 2039–2052.
- (226) Lunkenbein, T.; Schumann, J.; Behrens, M.; Schlögl, R.; Willinger, M. G. Formation of a ZnO Overlayer in Industrial Cu/ZnO/Al<sub>2</sub>O<sub>3</sub> Catalysts Induced by Strong Metal–Support Interactions. *Angew. Chem., Int. Ed.* **2015**, *54*, 4544–4548.
- (227) Arena, F.; Italiano, G.; Barbera, K.; Bonura, G.; Spadaro, L.; Frusteri, F. Basic Evidences for Methanol-Synthesis Catalyst Design. *Catal. Today* **2009**, *143*, 80–85.
- (228) Arena, F.; Italiano, G.; Barbera, K.; Bordiga, S.; Bonura, G.; Spadaro, L.; Frusteri, F. Solid-state Interactions, Adsorption Sites and Functionality of Cu–ZnO/ZrO<sub>2</sub> Catalysts in the CO<sub>2</sub> Hydrogenation to CH<sub>3</sub>OH. *Appl. Catal., A* **2008**, *350*, 16–23.
- (229) Grabow, L. C.; Mavrikakis, M. Mechanism of Methanol Synthesis on Cu through CO<sub>2</sub> and CO Hydrogenation. *ACS Catal.* **2011**, *1*, 365–384.
- (230) Eren, B.; Weatherup, R. S.; Liakakos, N.; Somorjai, G. A.; Salmeron, M. Dissociative Carbon Dioxide Adsorption and Morphological Changes on Cu(100) and Cu(111) at Ambient Pressures. *J. Am. Chem. Soc.* **2016**, *138*, 8207–8211.
- (231) Wachs, I. E.; Madix, R. J. The Selective Oxidation of CH<sub>3</sub>OH to H<sub>2</sub>CO on a copper(110) Catalyst. *J. Catal.* **1978**, *53*, 208–227.
- (232) Yang, Y.; Evans, J.; Rodriguez, J. A.; White, M. G.; Liu, P. Fundamental Studies of Methanol Synthesis from CO(2) Hydrogenation on Cu(111), Cu Clusters, and Cu/ZnO(0001). *Phys. Chem. Chem. Phys.* **2010**, *12*, 9909–9917.
- (233) Kim, Y.; Trung, T. S. B.; Yang, S.; Kim, S.; Lee, H. Mechanism of the Surface Hydrogen Induced Conversion of CO<sub>2</sub> to Methanol at Cu(111) Step Sites. *ACS Catal.* **2016**, *6*, 1037–1044.
- (234) Tabatabaei, J.; Sakakini, B. H.; Waugh, K. C. On the mechanism of Methanol Synthesis and the Water-gas Shift Reaction on ZnO. *Catal. Lett.* **2006**, *110*, 77–84.
- (235) Kattel, S.; Ramírez, P. J.; Chen, J. G.; Rodriguez, J. A.; Liu, P. Active Sites for CO<sub>2</sub> Hydrogenation to Methanol on Cu/ZnO Catalysts. *Science* **2017**, *355* (6331), 1296–1299.
- (236) Larmier, K.; Liao, W.-C.; Tada, S.; Lam, E.; Verel, R.; Bansode, A.; Urakawa, A.; Comas-Vives, A.; Copéret, C. CO<sub>2</sub>-to-Methanol Hydrogenation on Zirconia-Supported Copper Nanoparticles: Reaction Intermediates and the Role of the Metal-Support Interface. *Angew. Chem., Int. Ed.* **2017**, *56*, 2318–2323.
- (237) Zhao, Y.-F.; Yang, Y.; Mims, C.; Peden, C. H. F.; Li, J.; Mei, D. Insight into Methanol Synthesis from CO<sub>2</sub> Hydrogenation on Cu(111): Complex Reaction Network and the Effects of H<sub>2</sub>O. *J. Catal.* **2011**, *281*, 199–211.
- (238) Yang, Y.; Mims, C. A.; Disselkamp, R. S.; Kwak, J.-H.; Peden, C. H. F.; Campbell, C. T. (Non)formation of Methanol by Direct Hydrogenation of Formate on Copper Catalysts. *J. Phys. Chem. C* **2010**, *114*, 17205–17211.
- (239) Chinchin, G. C.; Denny, P. J.; Parker, D. G.; Spencer, M. S.; Whan, D. A. Mechanism of Methanol Synthesis from CO<sub>2</sub>/CO/H<sub>2</sub> Mixtures over Copper/zinc Oxide/alumina Catalysts: use of <sup>14</sup>C-labelled Reactants. *Appl. Catal.* **1987**, *30*, 333–338.
- (240) Chinchin, G. C.; Waugh, K. C. The Chemical State of Copper during Methanol Synthesis. *J. Catal.* **1986**, *97*, 280–283.
- (241) Carr, R. T.; Neurock, M.; Iglesia, E. Catalytic Consequences of Acid Strength in the Conversion of Methanol to Dimethyl Ether. *J. Catal.* **2011**, *278*, 78–93.
- (242) Moses, P. G.; Nørskov, J. K. Methanol to Dimethyl Ether over ZSM-22: A Periodic Density Functional Theory Study. *ACS Catal.* **2013**, *3*, 735–745.
- (243) Shah, R.; Gale, J. D.; Payne, M. C. In Situ Study of Reactive Intermediates of Methanol in Zeolites from First Principles Calculations. *J. Phys. Chem. B* **1997**, *101*, 4787–4797.
- (244) Blaszkowski, S. R.; van Santen, R. A. The Mechanism of Dimethyl Ether Formation from Methanol Catalyzed by Zeolitic Protons. *J. Am. Chem. Soc.* **1996**, *118*, 5152–5153.
- (245) Blaszkowski, S. R.; van Santen, R. A. Theoretical Study of the Mechanism of Surface Methoxy and Dimethyl Ether Formation from Methanol Catalyzed by Zeolitic Protons. *J. Phys. Chem. B* **1997**, *101*, 2292–2305.
- (246) Schiffino, R. S.; Merrill, R. P. A Mechanistic Study of the Methanol Dehydration Reaction on Gamma-alumina Catalyst. *J. Phys. Chem.* **1993**, *97*, 6425–6435.
- (247) Ghorbanpour, A.; Rimer, J. D.; Grabow, L. C. Computational Assessment of the Dominant Factors Governing the Mechanism of Methanol Dehydration over H-ZSM-5 with Heterogeneous Aluminum Distribution. *ACS Catal.* **2016**, *6*, 2287–2298.
- (248) Centi, G.; Perathoner, S. Opportunities and Prospects in the Chemical Recycling of Carbon Dioxide to Fuels. *Catal. Today* **2009**, *148*, 191–205.



- (249) Bartholomew, C. H.; Farrauto, R. J. Hydrogen Production and Synthesis Gas Reactions. In *Fundamentals of Industrial Catalytic Processes*; John Wiley & Sons, Inc.: 2005; pp 339–486.
- (250) Olah, G. A.; Goepfert, A.; Prakash, S. *Beyond Oil and Gas: The Methanol economy*, 2nd ed.; Wiley-VCH Verlag GmbH & Co. KGaA: Weinheim, 2009.
- (251) Joo, O.-S.; Jung, K.-D.; Moon, I.; Rozovskii, A. Y.; Lin, G. I.; Han, S.-H.; Uhm, S.-J. Carbon Dioxide Hydrogenation To Form Methanol via a Reverse-Water-Gas-Shift Reaction (the CAMERE Process). *Ind. Eng. Chem. Res.* **1999**, *38*, 1808–1812.
- (252) von der Assen, N. V.; Lafuente, A. M. L.; Peters, M.; Bardow, A. Environmental Assessment of CO<sub>2</sub> Capture and Utilisation. In *Carbon Dioxide Utilisation*; Styring, P., Quadrelli, E. A., Armstrong, K., Eds.; Elsevier: Amsterdam, 2015; Chapter 4, pp 45–56.
- (253) Aresta, M.; Caroppo, A.; Dibenedetto, A.; Narracci, M. Life Cycle Assessment (LCA) Applied to the Synthesis of Methanol. Comparison of the use of Syngas with the use of CO<sub>2</sub> and Dihydrogen Produced from Renewables. In *Environmental Challenges and Greenhouse Gas Control for Fossil Fuel Utilization in the 21st Century*; Maroto-Valer, M. M., Song, C., Soong, Y., Eds.; Springer US: Boston, MA, 2002; pp 331–347.
- (254) von der Assen, N.; Jung, J.; Bardow, A. Life-cycle Assessment of Carbon Dioxide Capture and Utilization: Avoiding the Pitfalls. *Energy Environ. Sci.* **2013**, *6*, 2721–2734.
- (255) Koroneos, C.; Dompros, A.; Roumbas, G.; Moussiopoulos, N. Life Cycle Assessment of Hydrogen Fuel Production Processes. *Int. J. Hydrogen Energy* **2004**, *29*, 1443–1450.
- (256) Keith, D. W.; Ha-Duong, M.; Stolaroff, J. K. Climate Strategy with CO<sub>2</sub> Capture from the Air. *Clim. Change* **2006**, *74*, 17–45.
- (257) Spath, P. L.; Mann, M. K. *Life Cycle Assessment of Renewable Hydrogen Production via Wind/Electrolysis*; National Renewable Energy Laboratory: 2004.
- (258) Spath, P. L.; Mann, M. K. *Life Cycle Assessment of Hydrogen Production via Natural Gas Steam Reforming*; National Renewable Energy Laboratory: 2001.
- (259) Ecoinvent Life Cycle Inventory Database, Ecoinvent V 3.3, 2016; <http://www.ecoinvent.org/> (accessed 15 June 2017).
- (260) Tidona, B.; Urakawa, A.; Rudolf von Rohr, P. High Pressure Plant for Heterogeneous Catalytic CO<sub>2</sub> Hydrogenation Reactions in a Continuous Flow Microreactor. *Chem. Eng. Process.* **2013**, *65*, 53–57.
- (261) Alperowicz, N. Mitsui seeks Partners for CO<sub>2</sub>-based Methanol Plant. *Chem. Week* **2010**, 172 (5), 18.
- (262) Sanz-Pérez, E. S.; Murdock, C. R.; Didas, S. A.; Jones, C. W. Direct Capture of CO<sub>2</sub> from Ambient Air. *Chem. Rev.* **2016**, *116*, 11840–11876.
- (263) Schlögl, R. *Chemical Energy Storage*; De Gruyter: 2012.
- (264) Singh, A. K.; Singh, S.; Kumar, A. Hydrogen Energy Future with Formic Acid: a Renewable Chemical Hydrogen Storage System. *Catal. Sci. Technol.* **2016**, *6*, 12–40.
- (265) Manyar, H. G.; Paun, C.; Pilus, R.; Rooney, D. W.; Thompson, J. M.; Hardacre, C. Highly Selective and Efficient Hydrogenation of Carboxylic Acids to Alcohols using Titania supported Pt Catalysts. *Chem. Commun.* **2010**, 46, 6279–6281.
- (266) Falorni, M.; Porcheddu, A.; Taddei, M. Mild Reduction of Carboxylic Acids to Alcohols using Cyanuric Chloride and Sodium Borohydride. *Tetrahedron Lett.* **1999**, *40*, 4395–4396.
- (267) Liu, J.; Zeng, X.; Cheng, M.; Yun, J.; Li, Q.; Jing, Z.; Jin, F. Reduction of Formic Acid to Methanol under Hydrothermal Conditions in the Presence of Cu and Zn. *Bioresour. Technol.* **2012**, *114*, 658–662.
- (268) Yao, H.; Xu, Z.; Cheng, M.; Yun, J.; Jing, Z.; Jin, F. Catalytic Conversion of Formic Acid to Methanol With Cu and Al under Hydrothermal Conditions. *BioResources* **2012**, *7*, 972–983.
- (269) Korstanje, T. J.; Ivar van der Vlugt, J.; Elsevier, C. J.; de Bruin, B. Hydrogenation of Carboxylic Acids with a Homogeneous Cobalt Catalyst. *Science* **2015**, *350*, 298–302.
- (270) Alberico, E.; Nielsen, M. Towards a Methanol Economy based on Homogeneous Catalysis: Methanol to H<sub>2</sub> and CO<sub>2</sub> to Methanol. *Chem. Commun.* **2015**, 51, 6714–6725.
- (271) Wesselbaum, S.; Moha, V.; Meuresch, M.; Brosinski, S.; Thenert, K. M.; Kothe, J.; Stein, T. v.; Englert, U.; Hoelscher, M.; Klankermayer, J.; Leitner, W. Hydrogenation of Carbon Dioxide to Methanol using a Homogeneous Ruthenium-Triphos Catalyst: from Mechanistic Investigations to Multiphase Catalysis. *Chemical Science* **2015**, *6*, 693–704.
- (272) Schneidewind, J.; Adam, R.; Baumann, W.; Jackstell, R.; Beller, M. Low-Temperature Hydrogenation of Carbon Dioxide to Methanol with a Homogeneous Cobalt Catalyst. *Angew. Chem., Int. Ed.* **2017**, *56*, 1890–1893.
- (273) Struis, R. P. W. J.; Stucki, S. Verification of the Membrane Reactor Concept for the Methanol Synthesis. *Appl. Catal., A* **2001**, *216*, 117–129.
- (274) Van der Ham, L. G. J.; Van den Berg, H.; Benneker, A.; Simmelink, G.; Timmer, J.; Van Weerden, S. Hydrogenation of Carbon Dioxide for Methanol Production. *Chem. Eng. Trans.* **2012**, *29*, 181.